RESEARCH ARTICLE

Six new *Phytophthora* species from ITS Clade 7a including two sexually functional heterothallic hybrid species detected in natural ecosystems in Taiwan

T. Jung[1,2*], M.H. Jung[1], B. Scanu[3], D. Seress[4], G.M. Kovács[4,5], C. Maia[1],
A. Pérez-Sierra[6], T.-T. Chang[7], A. Chandelier[8], K. Heungens[9], K. van Poucke[9],
P. Abad-Campos[10], M. Léon[10], S.O. Cacciola[11], J. Bakonyi[4]

Abstract   During a survey of *Phytophthora* diversity in natural ecosystems in Taiwan six new species were detected. Multigene phylogeny based on the nuclear ITS, ß-tubulin and *HSP90* and the mitochondrial *cox1* and *NADH1* gene sequences demonstrated that they belong to ITS Clade 7a with *P. europaea*, *P. uniformis*, *P. rubi* and *P. cambivora* being their closest relatives. All six new species differed from each other and from related species by a unique combination of morphological characters, the breeding system, cardinal temperatures and growth rates. Four homothallic species, *P. attenuata*, *P. flexuosa*, *P. formosa* and *P. intricata*, were isolated from rhizosphere soil of healthy forests of *Fagus hayatae*, *Quercus glandulifera*, *Q. tarokoensis*, *Castanopsis carlesii*, *Chamaecyparis formosensis* and *Araucaria cunninghamii*. Two heterothallic species, *P. ×heterohybrida* and *P. ×incrassata*, were exclusively detected in three forest streams. All *P. ×incrassata* isolates belonged to the A2 mating type while isolates of *P. ×heterohybrida* represented both mating types with oospore abortion rates according to Mendelian ratios (4–33 %). Multiple heterozygous positions in their ITS, ß-tubulin and *HSP90* gene sequences indicate that *P. ×heterohybrida*, *P. ×incrassata* and *P. cambivora* are interspecific hybrids. Consequently, *P. cambivora* is redescribed as *P. ×cambivora* without nomenclatural act. Pathogenicity trials on seedlings of *Castanea sativa*, *Fagus sylvatica* and *Q. suber* indicate that all six new species might pose a potential threat to European forests.

Article info   Received: 19 June 2016; Accepted: 5 September 2016; Published: 21 October 2016.

INTRODUCTION

The causal agents of several devastating *Phytophthora* epidemics in Europe, Australia and North America, including *P. cinnamomi* (Shearer & Tippett 1989, Erwin & Ribeiro 1996, Hardham 2005, Jung et al. 2013a), *P. lateralis* (Hansen et al. 2000), *P. plurivora* (Jung & Burgess 2009, Jung et al. 2013b) and *P. ramorum* (Rizzo et al. 2002, Brasier & Webber 2010) have a supposed origin in Southeast Asia (Ko et al. 1978, Arentz & Simpson 1986, Chang et al. 1996, Jung & Burgess 2009, Brasier et al. 2010, 2012, Vettraino et al. 2011, Hansen et al. 2012, Jung et al. 2016b). An increasing body of circumstantial evidence, including occurrence of highly pathogenic *Phytophthora* spp. in healthy native forests, presence of both mating types of heterothallic *Phytophthora* species, high intraspecific genetic variability and high aggressiveness to introduced crop species, is pointing at natural and semi-natural ecosystems in Southeast Asia as a hotspot of *Phytophthora* diversity from phylogenetic Clades 2, 5, 7, 8 and 9 (Ko et al. 1978, 2006, Ho 1990, Erwin & Ribeiro 1996, Ho & Lu 1997, Drenth & Guest 2004, Zeng et al. 2009, Ann et al. 2010, Brasier et al. 2010, Vettraino et al. 2011, Huai et al. 2013, Jung et al. 2016a). Therefore, in previously unstudied natural ecosystems of Southeast Asia a high diversity of unknown *Phytophthora* species might be expected which as a result of their co-evolution with a highly diverse flora are a potential threat to forests, natural ecosystems or crops in other continents.

In March and August 2013, in the frame of a collaborative research project between the University of Algarve and the Taiwanese Forestry Research Centre, a survey of *Phytophthora* diversity was performed in each of 25 natural and semi-natural forest stands and rivers in temperate montane and subtropical to tropical lowland regions of Taiwan during which 10 described species and 17 previously unknown taxa of *Phytophthora* were detected (Jung et al. 2016a). Preliminary analysis of sequence data from the rDNA internal transcribed spacer regions (ITS) and part of the mitochondrial *cox1* gene showed that six new species belong to *Phytophthora* major Clade 7 (Jung et al. 2016a) which is currently divided into two subclades. Subclade a (in the following Clade 7a) contains the six new species from Taiwan and eight described species including several important

[1]   Laboratory of Molecular Biotechnology and Phytopathology, Center for Mediterranean Bioresources and Food (MeditBio), University of Algarve, Campus de Gambelas, 8005-130 Faro, Portugal;
    corresponding author e-mail: trjung@ualg.pt and dr.t.jung@t-online.de.
[2]   Phytophthora Research and Consultancy, Am Rain 9, 83131 Nussdorf, Germany.
[3]   Dipartimento di Agraria, Sezione di Patologia vegetale ed Entomologia (SPaVE), Università degli Studi di Sassari, Viale Italia 39, 07100 Sassari, Italy.
[4]   Plant Protection Institute, Centre for Agricultural Research, Hungarian Academy of Sciences, Budapest, Hungary.
[5]   Department of Plant Anatomy, Institute of Biology, Eötvös Loránd University, Budapest, Hungary.
[6]   Forest Research, Alice Holt Lodge, Farnham, Surrey, United Kingdom.
[7]   Forest Protection Division, Taiwan Forestry Research Institute, Taipei, Taiwan.
[8]   Life Sciences Department, Walloon Agricultural Research Centre, 5030 Gembloux, Belgium.
[9]   Plant Sciences Research – Crop Protection, Institute for Agricultural and Fisheries Research (ILVO), Burg. Van Gansberghelaan 96, 9820 Merelbeke, Belgium.
[10]   Instituto Agroforestal Mediterráneo, Universitat Politècnica de València, Valencia, Spain.
[11]   Department of Agriculture, Food and Environment, University of Catania, 95123 Catania, Italy.

plant pathogens like the multivorous *P. cambivora* and the host-specific *P. fragariae*, *P. rubi*, *P. uniformis*, *P.* x*alni* and *P.* x*multiformis*. Subclade b consists of nine taxa including the wide-host range pathogens *P. cinnamomi*, *P. niederhauserii* and *P. parvispora* and host-specific crop pathogens like *P. cajani*, *P. melonis*, *P. sojae* and *P. vignae* (Martin et al. 2014). The presence of several heterozygous positions in their ITS sequences suggested that two of the six new Clade 7 species from Taiwan, informally designated as *P.* x*incrassata* nom. prov. and *P.* x*heterohybrida* nom. prov., might be interspecific hybrids (Jung et al. 2016a). Interspecific hybridisations are a major evolutionary force in the genus *Phytophthora* facilitating adaptation to new environments and expansion of host ranges (Brasier et al. 2004, Man in' t Veld et al. 2012, Bertier et al. 2013, Burgess 2015). In Clade 7a an interspecific hybridisation between unknown parental species formed *P.* x*multiformis* which then hybridized with *P. uniformis* creating the host-specific pathogen *P.* x*alni* (Brasier et al. 2004, Ioos et al. 2006, Husson et al. 2015). This latter hybrid is significantly more widespread and aggressive to *Alnus* spp. than its parents causing epidemic mortality of *Alnus* trees along rivers and in plantings across Europe (Brasier & Kirk 2001, Jung & Blaschke 2004, Jung et al. 2013b). In Australia and South Africa, a high proportion of *Phytophthora* isolates recovered from river systems belonged to sexually sterile Clade 6 hybrids and it was hypothesized that, similar to their parental species (Jung et al. 2011), they are successfully adapted to a lifestyle as litter decomposers and opportunistic pathogens (Nagel et al. 2013, Burgess 2015).

In this study, morphological and physiological characteristics were used in combination with DNA sequence data from the ITS and part of the nuclear heat shock protein 90 and β-tubulin, and the mitochondrial *cox1* and *NADH1* genes to:

1. characterise the six new species within Clade 7a from Taiwan, and compare them to isolates of all known species from Clade 7a;
2. assess their potential hybrid status; and
3. describe them as *P. attenuata* sp. nov., *P. flexuosa* sp. nov., *P. formosa* sp. nov., *P. intricata* sp. nov., *P.* x*heterohybrida* sp. nov. and *P.* x*incrassata* sp. nov.

In addition, their pathogenicity to *Castanea sativa*, *Fagus sylvatica* and *Quercus suber* was tested in a soil infestation trial to assess the potential threat of these new species to European forests. Finally, *P. cambivora* is re-described as *P.* x*cambivora* without nomenclatural act.

MATERIAL AND METHODS

Phytophthora isolates

Details of all isolates used in the phylogenetic, morphological and physiological studies and in the pathogenicity test are given in Table 1. Sampling and isolation methods from forest soil and river systems in Taiwan were described in Jung et al. (2016a). The isolates of *P. attenuata* sp. nov., *P. formosa* sp. nov., *P. flexuosa* sp. nov. and *P. intricata* sp. nov. came from rhizosphere soil of mature trees of *Fagus hayatae*, *Castanopsis carlesii*, *Chamaecyparis formosensis* and *Araucaria cunninghamii* in five healthy forest stands and from young trees of *Quercus glandulifera* and *Q. tarokoensis* in an arboretum established in a natural *Castanopsis-Machilus* forest (Table 1). Noteworthy, *P. attenuata* was exclusively isolated from *Castanopsis carlesii* and *Chamaecyparis formosensis* in two mature mixed forest stands, both located above 2000 m altitude in Sheipa National-park (Jung et al. 2016a). All isolates of *P.* x*incrassata* sp. nov. and *P.* x*heterohybrida* sp. nov. were recovered from three rivers in the Fushan region (Table 1) using baiting rafts (Jung et al. 2016a). In addition, isolates of *P. cambivora* from various host

species in Germany, Italy, Portugal, Spain, Slovakia and Chile, and *P.* x*alni* from Germany (Table 1) were obtained in 2013 and 2014 for comparative studies using standard isolation methods (Jung et al. 1996, Jung 2009). For all isolates, single hyphal tip cultures were produced under the stereomicroscope from the margins of fresh cultures on V8-juice agar (V8A; 16 g agar, 3 g CaCO$_3$, 100 mL Campbell's V8 juice, 900 mL distilled water). Further isolates of described Clade 7a species were selected from the culture collections of the authors and sourced from other culture collections (Table 1). Stock cultures were maintained on carrot juice agar (CA; 16 g agar, 3 g CaCO$_3$, 100 mL carrot juice, 900 mL distilled water; Scanu et al. 2014) at 10 °C in the dark. All isolates of the six new *Phytophthora* spp. are preserved in the culture collection maintained at the University of Algarve. Ex-type and isotype cultures were deposited at the Centraalbureau voor Schimmelcultures (CBS; Utrecht, Netherlands) (Table 1).

DNA isolation, amplification and sequencing

For all *Phytophthora* isolates obtained in this study mycelial DNA was extracted from pure cultures grown in pea-broth medium (Erwin & Ribeiro 1996). Pea-broth cultures were kept for 7–10 d at 25 °C without shaking. Mycelium was harvested by filtration through filter paper, washed with sterile deionized water, then freeze-dried and ground to a fine powder in liquid nitrogen. Total DNA was extracted using the DNeasy Plant Mini kit (QIAGEN GmbH, Hilden, Germany) or the E.Z.N.A.® Fungal DNA Mini Kit (OMEGA Bio-tek, Norcross, GA) following the manufacturer's instructions and checked for quality and quantity by spectrophotometry. DNA was stored at –20 °C until further use. For 36 isolates of the six new Clade 7a species, 48 isolates of the known Clade 7a species *P. cambivora*, *P. europaea*, *P. fragariae*, *P. rubi*, *P. uliginosa*, *P. uniformis*, *P.* x*alni* and *P.* x*multiformis*, and the ex-type isolate of *P. cinnamomi* and one isolate of *P. niederhauserii* from Clade 7b, three nuclear and two mitochondrial loci were amplified and sequenced (Table 1). The internal transcribed spacer (ITS1-5.8S-ITS2) region of the nuclear ribosomal DNA was amplified using the primer-pair ITS1/ITS4 (White et al. 1990) and the PCR reaction mixture and cycling conditions described by Nagy et al. (2003) with an annealing temperature of 57 °C for 30 s. Partial heat shock protein 90 (*HSP90*) gene was amplified with the primer-pair HSP90F1int/HSP90R1 as described previously (Blair et al. 2008). Segments of the β-tubulin (*Btub*) and the mitochondrial genes cytochrome c oxidase subunit 1 (*cox1*) and NADH dehydrogenase subunit 1 (*NADH1*) were amplified with primer-pairs TUBUF2/TUBUR1, COXF4N/COXR4N and NADHF1/NADHR1, respectively, using the PCR reaction mixture and cycling conditions as described earlier (Kroon et al. 2004). Products of Thermo Fisher Scientific Inc. (Waltham, MA, USA) and Bio-Rad C1000™ or Applied Biosystems® 2720 Thermal Cyclers were used for the PCR reactions. Amplicons were purified and sequenced in both directions using the primers of the PCR reactions by Macrogen Inc. (Amsterdam, The Netherlands) and LGC Genomics GmbH (Berlin, Germany). Electropherograms were quality checked and forward and reverse reads were compiled using Pregap4 v. 1.5 and Gap v. 4.10 of the Staden sofware package (Staden et al. 2000). Heterozygous sites observed were labelled according to the IUPAC coding system. All sequences derived in this study were deposited in GenBank and accession numbers are given in Table 1.

Phylogenetic analysis

The sequences gained in this work were complemented with sequences deposited in GenBank. *Phytophthora cinnamomi* (CBS 144.22) and *P. niederhauserii* (CBS 124086), both from Clade 7b, were used as outgroups. The 86-isolate datasets of

Table 1 Details of isolates from *Phytophthora* major Clade 7 considered in the phylogenetic, flow cytometry, morphological, growth-temperature and pathogenicity studies.

Phytophthora species (mating type)	Isolate numbers[a]		Host	Origin		GenBank accession numbers				
	International collections	Local collections		Location; year	Collector; reference	ITS	cox1	Btub	NADH1	HSP90
P. attenuata[bcde] ex-type	CBS 141199	TW129	*Castanopsis carlesii*	Taiwan; 2013	T. Jung; Jung et al. 2016a	KU517154	KU517148	KU899277	KU899519	KU899434
P. attenuata[bcd]	CBS 141200	TW118	*Chamaecyparis formosensis*	Taiwan; 2013	T. Jung; this study	KU899196	KU899351	KU899274	KU899516	KU899431
P. attenuata[bcd]		TW119	*C. formosensis*	Taiwan; 2013	T. Jung; this study	KU899197	KU899352	KU899275	KU899517	KU899432
P. attenuata[bcd]		TW130	*C. carlesii*	Taiwan; 2013	T. Jung; this study	KU899200	KU899355	KU899279	KU899521	KU899436
P. attenuata[bcd]		TW128	*C. carlesii*	Taiwan; 2013	T. Jung; this study	KU899198	KU899353	KU899276	KU899518	KU899433
P. attenuata[c]		TW423	*C. formosensis*	Taiwan; 2013	T. Jung; this study	KX237557	n.a.	n.a.	n.a.	n.a.
P. cinnamomi[b] ex-type (A2)	CBS 144.22 IMI 022938 WPC P2110 PD_01681 ATCC 1407	Pc 110	*Cinnamomum burmannii*	Indonesia (Sumatra); 1922	Rands; Scanu et al. 2014	KU899160	KU899315	KU899233	KU899475	KU899390
P. cinnamomi[c] (A1)		TW12	*Cinnamomum micranthum*	Taiwan; 2013	T. Jung; this study	n.a.	n.a.	n.a.	n.a.	n.a.
P. cinnamomi[c] (A2)		MP74	n.a.	Australia (WA); n.a.	CALM[c]; Hüberii 1995	n.a.	n.a.	n.a.	n.a.	n.a.
P. europaea[bcd] ex-type	CBS 109049 WPC P10324 PD_00082	EUR 2	*Quercus robur*	France; 1998	T. Jung; Jung et al. 2002	HQ261556	KU681022	EU079482	KU899469	EU079485
P. europaea[bcd]	CBS 109051	EUR 3; 2AE2	*Quercus* sp.	France; 1998	E.M. Hansen; Jung et al. 2002	KU899157	KU899312	KU899229	KU899470	KU899384
P. europaea[cd]	CBS 109053	EUR 1	*Q. robur*	Germany; 1995	T. Jung; Jung et al. 2002	n.a.	n.a.	n.a.	n.a.	n.a.
P. europaea[c]		EUR 4	*Quercus* sp.	France; 1998	E.M. Hansen; Jung et al. 2002	n.a.	n.a.	n.a.	n.a.	n.a.
P. europaea[c]	CBS 109052	EUR 5	*Quercus* sp.	France; 1998	E.M. Hansen; Jung et al. 2002	n.a.	n.a.	n.a.	n.a.	n.a.
P. europaea[c]	CBS 109050	EUR 6	*Quercus* sp.	France; 1998	E.M. Hansen; Jung et al. 2002	n.a.	n.a.	n.a.	n.a.	n.a.
P. flexuosa[bcde] ex-type	CBS 141201	TW78	*Fagus hayatae*	Taiwan; 2013	T. Jung; Jung et al. 2016a	KU517152	KU517146	KU899302	KU899544	KU899459
P. flexuosa[bcd]	CBS 141202	TW108	*F. hayatae*	Taiwan; 2013	T. Jung; this study	KU899193	KU899348	KU899271	KU899513	KU899428
P. flexuosa[bcd]		TW79	*F. hayatae*	Taiwan; 2013	T. Jung; this study	KU899220	KU899375	KU899303	KU899545	KU899460
P. formosa[bcde] ex-type	CBS 141203	TW107	*A. cunninghamii*	Taiwan; 2013	T. Jung; Jung et al. 2016a	KU517153	KU517147	KU899270	KU899512	KU899427
P. formosa[bcd]		TW105	*Araucaria cunninghamii*	Taiwan; 2013	T. Jung; this study	KU899191	KU899346	KU899268	KU899510	KU899425
P. formosa[bc]		TW106	*A. cunninghamii*	Taiwan; 2013	T. Jung; this study	KU899192	KU899347	KU899269	KU899511	KU899426
P. formosa[bcd]		TW109	*A. cunninghamii*	Taiwan; 2013	T. Jung; this study	KU899194	KU899349	KU899272	KU899514	KU899429
P. formosa[bcd]		TW13	*Quercus glandulifera*	Taiwan; 2013	T. Jung; this study	KU899199	KU899354	KU899278	KU899520	KU899435
P. formosa[bcd]	CBS 141204	TW14	*Q. glandulifera*	Taiwan; 2013	T. Jung; this study	KU899201	KU899356	KU899280	KU899522	KU899437
P. formosa[bc]		TW110	River baiting	Taiwan; 2013	T. Jung; this study	KU899195	KU899350	KU899273	KU899515	KU899430
P. fragariae[bcd] ex-type	CBS 209.46 WPC P6231 IMI 181417		*Fragaria*	UK; 1946	C.J. Hickman; n.a.	HQ643230	n.a.	n.a.	n.a.	n.a.
P. fragariae[bcd]	–	BBA 11/94; K018	*Fragaria xananassa*	Germany; 1994	JKI; n.a.	KU899153	KU899308	KU899225	KU899465	KU899380
P. fragariae[bc]	–	BBA L1	*F. xananassa*	Germany; 1983	JKI; n.a.	KU899156	KU899311	KU899228	KU899468	KU899383
P. fragariae[bd]	WPC P6362	FVF 7; SCRP245	*F. xananassa*	UK; 1945	C.J. Hickman; n.a.	KU899190	KU899345	KU899267	KU899509	KU899424
P. fragariae[b]	WPC P1435 PD_00388 ATCC 36057		*F. xananassa*	UK; 1969	n.a.	HQ261564	KU681021	EU079744	KU899548	EU079747
P. intricata[bcde] ex-type	CBS 141211	TW259	*Quercus tarokoensis*	Taiwan; 2013	T. Jung; Jung et al. 2016a	KU517155	KU517149	KU899284	KU899526	KU899441

Species	Culture collection(s)	Isolate(s)	Host	Country; year	Collector; reference					
P. intricata[bcd]		TW16	*Q. tarokoensis*	Taiwan; 2013	T. Jung; this study	KU899202	KU899281	KU899357	KU899523	KU899438
P. intricata[bcd]	CBS 141210	TW7	*Q. tarokoensis*	Taiwan; 2013	T. Jung; this study	KU899219	KU899301	KU899374	KU899543	KU899458
P. intricata[bcd]		TW257	*Q. tarokoensis*	Taiwan; 2013	T. Jung; this study	KU899203	KU899282	KU899358	KU899524	KU899439
P. intricata[bcd]		TW258	*Q. tarokoensis*	Taiwan; 2013	T. Jung; this study	KU899204	KU899283	KU899359	KU899525	KU899440
P. intricata[bcd]		TW263	*Q. tarokoensis*	Taiwan; 2013	T. Jung; this study	KU899205	KU899285	KU899360	KU899527	KU899442
P. niederhauserii[b]	CBS 124086		*Chamaecyparis lawsoniana*	Hungary; 2007	A. Józsa; Józsa et al. 2010	GU230789	GU477613	GU477617	GU477619	KU899389
P. rubi[bcd] ex-type	CBS 967.95 WPC P16899 IMI 355974 ATCC 90442	FVR 11; SCRP333; R49	*Rubus idaeus*	UK; 1985	D. Kennedy; Man in 't Veld 2007	AF139370	DQ674736	KU899234	KU899476	KU899391
P. rubi[bc]		CH-106	*R. idaeus*	Sweden; n.a.	C. Olsson; n.a.	KU899180	KU899256	KU899335	KU899498	KU899413
P. rubi[bcd]		5005038	*R. idaeus*	Netherlands; 2010	K. Rosendahl; n.a.	KU899182	KU899258	KU899337	KU899500	KU899415
P. rubi[bcd]		9A9; CC947	n.a.	UK; n.a.	n.a.	KU899181	KU899257	KU899336	KU899499	KU899414
P. rubi[b]		BBA 390	*R. idaeus*	Germany; 1990	JKI; n.a.	KU899154	KU899226	KU899309	KU899466	KU899381
P. rubi[b]		BBA 93	*R. idaeus*	Germany; n.a.	JKI; n.a.	KU899155	KU899227	KU899310	KU899467	KU899382
P. rubi[bcd]	CBS 109892 WPC P15596	FVR 67; SCRP324; P823	*R. idaeus*	UK; 1991	D. Kennedy; Brasier et al. 1999	HQ643341	AY564064	AY564179	AY564006	KU899385
P. rubi[bcd]		PHRM 09	*R. idaeus*	Croatia; 2009	Z. Tomic; n.a.	KU899183	KU899259	KU899338	KU899501	KU899416
P. rubi[bcd]		230 553	*R. idaeus*	Norway; 2006	M.-L. Herrero; n.a.	n.a.	n.a.	n.a.	n.a.	n.a.
P. uliginosa[bcd] ex-type	CBS 109054 WPC P10413 PD_00157	ULI 1	*Q. robur*	Poland; 1998	T. Jung; Jung et al. 2002	AF449495	EU080012	KU681023	KU899471	EU080014
P. uliginosa[cd]	CBS 109055 WPC P10328 PD_00012	ULI 2	*Quercus petraea*	Germany; 1998	T. Jung; Jung et al. 2002	HQ261722	EU079693	n.a.		EU079696
P. uliginosa[c]		ULI13	*Q. robur*	Germany; 1998	T. Jung; Jung et al. 2002	n.a.	n.a.	n.a.	n.a.	n.a.
P. uniformis ex-type	IMI 392315 WPC P16206 PD_02131	P875	*Alnus glutinosa*	Sweden; 1997	C. Olsson; Brasier et al. 2004	GU259293	n.a.	n.a.	n.a.	n.a.
P. uniformis[bcd]	WPC P10565 PD_00098	155c; PAU 98	*A. glutinosa*	Hungary; 1999	Z.Á. Nagy; Ioos et al. 2006	KU899221	KU899304	KU899376	KU899546	KU899461
P. uniformis[bcd]		250001	*A. glutinosa*	Norway; 2012	G.M. Strømeng; n.a.	KU899175	KU899251	KU899330	KU899493	KU899408
P. uniformis[bcd]		ALN 58	*A. glutinosa*	Germany; 1998	T. Jung; Jung & Blaschke 2004	KU899173	KU899249	KU899328	KU899491	KU899406
P. uniformis[bcd]		ALN 222	*A. glutinosa*	Germany; 2001	T. Jung; Jung & Blaschke 2004	KU899174	KU899250	KU899329	KU899492	KU899407
P. uniformis[b]		PAU 558	*A. glutinosa*	Belgium; 2009	P. Aguayo; Aguayo et al. 2013	KU899186	KU899263	KU899341	KU899505	KU899420
P. uniformis[bc]		PAU 60	*A. glutinosa*	France; 1999	J.C. Streito; Ioos et al. 2006	KU899187	KU899264	KU899342	KU899506	KU899421
P. uniformis[bd]		P876	*A. glutinosa*	Sweden; 1997	C. Olsson; Brasier et al. 2004	KU681016	KU681019	KU681019	KU899502	KU899417
P. uniformis[bcd]		P887	*A. glutinosa*	Sweden; 1997	C. Olsson; Brasier et al. 1999	n.a.	n.a.	n.a.	n.a.	n.a.
P. ×alni[b] ex-type	IMI 392314 WPC P16203 PD_02130	P772	*A. glutinosa*	UK; 1994	G. Mac Askill; Brasier et al. 2004	KU681013	KU681017	KU681017	KU899480	KU899395
P. ×alni[bcd]		ALN 268	*Alnus incana*	Germany; 2001	T. Jung; Jung & Blaschke 2004	KU899169	KU899245	KU899324	KU899487	KU899402
P. ×alni[bcd]		ALN 45	*A. glutinosa*	Germany; 1999	T. Jung; Jung & Blaschke 2004	KU899167	KU899243	KU899322	KU899485	KU899400
P. ×alni[bcd]	WPC P10568 PD_00050	Héviz9; PAA 93	*A. glutinosa*	Hungary; 1999	Z.Á. Nagy; Ioos et al. 2006	KU899222	KU899305	KU899377	KU899547	KU899462
P. ×alni[bcd]		MAL5	*A. glutinosa*	Spain; 2009	T. Jung, Solla et al. 2010	KU899166	KU899242	KU899321	KU899484	KU899399
P. ×alni[bcd]		Reis 2	*A. glutinosa*	Germany; 2014	T. Jung; this study	KU899168	KU899244	KU899323	KU899486	KU899401
P. ×alni[bcd]	WPC P10569	H-5/02	*A. glutinosa*	Hungary; 2002	J. Bakonyi; Bakonyi et al. 2006	FJ801457	n.a.	n.a.	n.a.	n.a.

Table 1 (cont.)

Phytophthora species (mating type)	Isolate numbers[a]		Host	Origin		GenBank accession numbers				
	International collections	Local collections		Location; year	Collector; reference	ITS	cox1	Btub	NADH1	HSP90
P. ×alni[cd]		2303	*A. incana*	Belgium; 2002	A. Chandelier; De Merlier et al. 2005	n.a.	n.a.	n.a.	n.a.	n.a.
P. ×alni[c]		ALN 402	*A. glutinosa*	Germany; 2003	C. Clemenz; n.a.	n.a.	n.a.	n.a.	n.a.	n.a.
P. ×alni[bcd]		PHAKO 12	*A. glutinosa*	Croatia; 2012	Z. Tomic; n.a.	KU899172	KU899327	KU899248	KU899490	KU899405
P. ×cambivora[bcdf] (A2), neo-type	CBS 141218	IT 5-3	*Quercus pubescens*	Italy (Sicily); 2013	T. Jung; this study	KU899179	KU899334	KU899255	KU899497	KU899412
P. ×cambivora[c] (A2)		IT 5-3 L2	*Q. pubescens*	Italy (Sicily); 2013	T. Jung; this study	n.a.	n.a.	n.a.	n.a.	n.a.
P. ×cambivora (A1)[bcf]		4044.1	*Chrysolepis chrysophylla*	USA, 2001	A. Saavedra; Saavedra et al. 2007	KU899151	KU899306	KU899223	KU899463	KU899378
P. ×cambivora (A2)[bcf]		4050.1	*C. chrysophylla*	USA, 2001	A. Saavedra; Saavedra et al. 2007	KU899152	KU899307	KU899224	KU899464	KU899379
P. ×cambivora (A1)[bcf]		4031.O1	*C. chrysophylla*	USA, 2001	A. Saavedra; Saavedra et al. 2007	n.a.	n.a.	n.a.	n.a.	n.a.
P. ×cambivora (n.a.)[f]		4044.7	*C. chrysophylla*	USA; 2001	A. Saavedra; Saavedra et al. 2007	n.a.	n.a.	n.a.	n.a.	n.a.
P. ×cambivora (A2)[bcf]	CBS 114087 WPC P0592 PD_00043 ATCC 46719		*Abies procera*	USA; n.a.	Loring/Smithson; Saavedra et al. 2007	KU681015	KU681020	KU899232	KU899474	KU899388
P. ×cambivora (A1)[bcdf]		DE 1	*Fagus sylvatica*	Germany; 2013	T. Jung; this study	KU899176	KU899331	KU899252	KU899494	KU899409
P. ×cambivora (A1)[bcf]	IMI 229178 WPC P1432 PD_01225 ATCC 38811		*M. pumila*	Japan; 1978	T. Suzui; Suzui & Hoshino 1979	KU899163	KU899318	KU899237	KU899479	KU899394
P. ×cambivora (A2)[bcdf]	CBS 114086 WPC P1431 PD_00003 ATCC 36228	S107	*Malus sylvestris*	Australia; 1977	D.M.Halsall; Halsall & Forrester 1977	KU899159	KU899314	KU899231	KU899473	KU899387
P. ×cambivora (A1)[f]		W1846	Forest soil	Australia; 2013	n.a.	n.a.	n.a.	n.a.	n.a.	n.a.
P. ×cambivora (A2)[bcdf]		ES 1	*A. glutinosa*	Spain; 2012	T. Jung; this study	KU899177	KU899332	KU899253	KU899495	KU899410
P. ×cambivora (A2)[bcef]		IT 6-3	*F. sylvatica*	Italy (Sicily); 2013	T. Jung; this study	KU899164	KU899319	KU899240	KU899482	KU899397
P. ×cambivora (A2)[bcdf]		IT 6-4	*F. sylvatica*	Italy (Sicily); 2013	T. Jung; this study	KU899165	KU899320	KU899241	KU899483	KU899398
P. ×cambivora (A2)[bcdf]		SK 9	*F. sylvatica*	Slovakia; 2013	T. Jung; this study	KU899178	KU899333	KU899254	KU899496	KU899411
P. ×cambivora (n.a.)[g]		FR 1	*Quercus rubra*	France; 2013	T. Jung; this study	n.a.	n.a.	n.a.	n.a.	n.a.
P. ×cambivora (A2)[cf]		PT 1-1	*Castanea sativa*	Portugal; 2014	T. Jung; this study	n.a.	n.a.	n.a.	n.a.	n.a.
P. ×cambivora (A2)[cf]		PT 3-1	*C. sativa*	Portugal; 2014	T. Jung; this study	n.a.	n.a.	n.a.	n.a.	n.a.
P. ×cambivora (A2)[cf]		PT 7-3	*C. sativa*	Portugal; 2014	T. Jung; this study	n.a.	n.a.	n.a.	n.a.	n.a.
P. ×cambivora (A2)[cf]		CL 1	*F. sylvatica*	Chile; 2014	T. Jung; this study	KU899161	KU899316	KU899235	KU899477	KU899392
P. ×cambivora (A2)[cf]		CL 5	*F. sylvatica*	Chile; 2014	T. Jung; this study	KU899162	KU899317	KU899236	KU899478	KU899393
P. ×cambivora (A1)[cf]		3399H	*F. sylvatica*	Belgium; 2005	A. Chandelier; n.a.	n.a.	n.a.	n.a.	n.a.	n.a.
P. ×cambivora (A2)[cf]		3401H	*F. sylvatica*	Belgium; 2005	A. Chandelier; n.a.	n.a.	n.a.	n.a.	n.a.	n.a.
P. ×cambivora (A2)[cf]		4557H	*F. sylvatica*	Belgium; 2014	A. Chandelier; n.a.	n.a.	n.a.	n.a.	n.a.	n.a.
P. ×cambivora (A1)[cf]		Resi 75	*F. sylvatica*	Belgium; 2014	A. Chandelier; n.a.	n.a.	n.a.	n.a.	n.a.	n.a.
P. sp. *×cambivora*-like (A1)[bcf]	CBS 111329		*Malus pumila* var. *dulcissima*	S-Korea; 1996	H-J. Jee; Jee et al. 1997	KU899158	KU899313	KU899230	KU899472	KU899386
P. ×heterohybrida[bcdf] (A2), ex-type	CBS 141207	TW30	Baiting; tributary of Ha-pen River	Taiwan; 2013	T. Jung; Jung et al. 2016a	KU517151	KU517145	KU899290	KU899532	KU899447
P. ×heterohybrida[bcdef] (A2)		TW28	Baiting; tributary of Ha-pen River	Taiwan; 2013	T. Jung; this study	KU925908	n.a.	n.a.	n.a.	n.a.

Species	Culture collection[a]	Isolate[a]	Host/substrate	Location; year	Source	GenBank accessions				
P. ×*heterohybrida*[bcdf] (A1/A2)		TW29	Baiting; tributary of Ha-pen River	Taiwan; 2013	T. Jung; this study	KU899207	KU899362	KU899288	KU899530	KU899445
P. ×*heterohybrida*[bcdf] (A2)		TW31	Baiting; tributary of Ha-pen River	Taiwan; 2013	T. Jung; this study	KU899209	KU899364	KU899291	KU899533	KU899448
P. ×*heterohybrida*[bcdf] (A1)		TW32	Baiting; tributary of Ha-pen River	Taiwan; 2013	T. Jung; this study	KU899210	KU899365	KU899292	KU899534	KU899449
P. ×*heterohybrida*[df] (A1)		TW33	Baiting; tributary of Ha-pen River	Taiwan; 2013	T. Jung; this study	KX237558	n.a.	n.a.	n.a.	n.a.
P. ×*heterohybrida*[df] (A1)		TW34	Baiting; tributary of Ha-pen River	Taiwan; 2013	T. Jung; this study	KX237559	n.a.	n.a.	n.a.	n.a.
P. ×*heterohybrida*[bcdf] (A1)		TW35	Baiting; tributary of Ha-pen River	Taiwan; 2013	T. Jung; this study	KU925909	n.a.	n.a.	n.a.	n.a.
P. ×*heterohybrida*[bcd] (A2)	CBS 141205	TW38	Baiting; tributary of Ha-pen River	Taiwan; 2013	T. Jung; this study	KU899214	KU899369	KU899296	KU899538	KU899453
P. ×*heterohybrida*[df] (A2)		TW39	Baiting; tributary of Ha-pen River	Taiwan; 2013	T. Jung; this study	KX237560	n.a.	n.a.	n.a.	n.a.
P. ×*heterohybrida*[cdf] (A1)		TW40	Baiting; tributary of Ha-pen River	Taiwan; 2013	T. Jung; this study	KX237561	n.a.	n.a.	n.a.	n.a.
P. ×*heterohybrida*[df] (A1)	CBS 141206	TW46	Baiting; Ha-pen River	Taiwan; 2013	T. Jung; this study	KU925910	n.a.	n.a.	n.a.	n.a.
P. ×*heterohybrida*[cdf] (A1)		TW47	Baiting; Ha-pen River	Taiwan; 2013	T. Jung; this study	KX237562	n.a.	n.a.	n.a.	n.a.
P. ×*heterohybrida*[df] (A1)		TW48	Baiting; Ha-pen River	Taiwan; 2013	T. Jung; this study	KU925911	n.a.	n.a.	n.a.	n.a.
P. ×*heterohybrida*[c] (A1)		TW49	Baiting; Ha-pen River	Taiwan; 2013	T. Jung; this study	KX355327	n.a.	n.a.	n.a.	n.a.
P. ×*heterohybrida*[c] (A1)		TW50	Baiting; Ha-pen River	Taiwan; 2013	T. Jung; this study	KX355328	n.a.	n.a.	n.a.	n.a.
P. ×*heterohybrida*[bcdf] (A2)		TW51	Baiting; Cukeng River	Taiwan; 2013	T. Jung; this study	KU899216	KU899371	KU899298	KU899540	KU899455
P. ×*heterohybrida*[bcd] (A2)		TW56	Baiting; Cukeng River	Taiwan; 2013	T. Jung; this study	KU899217	KU899372	KU899299	KU899541	KU899456
P. ×*heterohybrida*[bc] (A2)		TW57	Baiting; Cukeng River	Taiwan; 2013	T. Jung; this study	KU899218	KU899373	KU899300	KU899542	KU899457
P. ×*heterohybrida*[cdf] (A2)		TW59	Baiting; Cukeng River	Taiwan; 2013	T. Jung; this study	KX237563	n.a.	n.a.	n.a.	n.a.
P. ×*heterohybrida*[c] (A2)		TW60	Baiting; Cukeng River	Taiwan; 2013	T. Jung; this study	KX355329	n.a.	n.a.	n.a.	n.a.
P. ×*heterohybrida*[c] (A2)		TW61	Baiting; Cukeng River	Taiwan; 2013	T. Jung; this study	KX355330	n.a.	n.a.	n.a.	n.a.
P. ×*incrassata*[bcdf] (A2), ex-type	CBS 141209	TW269	Baiting; tributary of Ha-pen River	Taiwan; 2013	T. Jung; Jung et al. 2016a	KU517156	KU517150	KU899286	KU899528	KU899443
P. ×*incrassata*[bcdf] (A2)		TW43	Baiting; tributary of Ha-pen River	Taiwan; 2013	T. Jung; this study	KU899215	KU899370	KU899297	KU899539	KU899454
P. ×*incrassata*[bcdf] (A2)	CBS 141208	TW283	Baiting; tributary of Ha-pen River	Taiwan; 2013	T. Jung; this study	KU899206	KU899361	KU899287	KU899529	KU899444
P. ×*incrassata*[bcdf] (A2)		TW299	Baiting; tributary of Ha-pen River	Taiwan; 2013	T. Jung; this study	KU899208	KU899363	KU899289	KU899531	KU899446
P. ×*incrassata*[bcdf] (A2)		TW344	Baiting; tributary of Ha-pen River	Taiwan; 2013	T. Jung; this study	KU899211	KU899366	KU899293	KU899535	KU899450
P. ×*incrassata*[bcdef] (A2)		TW347	Baiting; tributary of Ha-pen River	Taiwan; 2013	T. Jung; this study	KU899212	KU899367	KU899294	KU899536	KU899451
P. ×*incrassata*[bcdf] (A2)		TW350	Baiting; tributary of Ha-pen River	Taiwan; 2013	T. Jung; this study	KU899213	KU899368	KU899295	KU899537	KU899452
P. ×*multiformis*[b] ex-type	IMI 392316 WPC P16202 PD_01913	P770	*A. glutinosa*	Netherlands; 1994	H. van Kesteren, Brasier et al. 2004	AF139368	KU681018	KU899239	KU899481	KU899396
P. ×*multiformis*[bc]		PAM 396	*A. glutinosa*	France; 2007	T. Scordia; Husson et al. 2015	KU899184	KU899339	KU899261	KU899503	KU899418
P. ×*multiformis*[b]		PAM 859	*Alnus incana*	France; 2008	C. Husson; Husson et al. 2015	KU899185	KU899340	KU899262	KU899504	KU899419
P. ×*multiformis*[bcd]		PHAPI 12	*A. glutinosa*	Croatia; 2012	Z. Tomic; n.a.	KU899171	KU899326	KU899247	KU899489	KU899404
P. ×*multiformis*[cd]		PHAKA 12	*A. glutinosa*	Croatia; 2012	Z. Tomic; n.a.	n.a.	n.a.	n.a.	n.a.	n.a.
P. ×*multiformis*[cd]		P889; ALN 1	*A. incana*	Germany; 1995	T. Jung; Brasier et al. 2004	n.a.	n.a.	n.a.	n.a.	n.a.
P. ×*multiformis*[c]	IMI 392321	PH055	*A. glutinosa*	Italy; 2010	B. Scanu; this study	KX083686	n.a.	n.a.	n.a.	n.a.
P. sp. ×*multiformis*-like[bcd]		4971496	*A. glutinosa*	Netherlands; 2011	K. Rosendahl & W. Man in 't Veld; n.a.	KU899170	KU899325	KU899246	KU899488	KU899403

n.a. = not available.

[a] Abbreviations of isolates and culture collections: ATCC = American Type Culture Collection, Manassas, USA; CBS = Centraalbureau voor Schimmelcultures, Utrecht, Netherlands; IMI = CABI Bioscience, UK; PD = Phytophthora Database (http://www.phytophthoradb.org); WPC = World Phytophthora Collection, University of California Riverside, USA; other isolate names and numbers are as given by the collectors and on GenBank, respectively.

[b] Isolates used in the phylogenetic studies.

[c] Isolates used in the morphological studies.

[d] Isolates used in the temperature-growth studies.

[e] Isolates used in the soil infestation trial.

[f] Isolates used in the flow cytometry analysis.

[g] Isolate only used for sporangial measurements.

[h] CALM = Department of Conservation and Land Management, Como, Western Australia.

each of the five loci were used for all phylogenetic analyses. Sequences of each locus were aligned using the online MAFFT v. 7 (http://mafft.cbrc.jp/alignment/server/) (Katoh & Standley 2013) by the auto option. Although the robustness of phylogenetic analyses can be increased with the use of the indel positions coded (Nagy et al. 2012) none of the loci showed indel patterns usable for such coding.

First, the datasets of the five loci were analysed separately. Maximum likelihood (ML) phylogenetic analyses of the datasets were carried out with RAxML (Stamatakis 2014) in the raxmlGUI (Silvestro & Michalak 2012) implementation with the GTRGAMMA model. Bootstrap analysis with 1 000 replicates was used to test the support of the branches. There were no well-supported striking differences of the topologies of the clades on the trees. Only the positions of some isolates showed minor differences in some loci (see results).

Multi-locus phylogenetic Bayesian Inference (BI) analysis was performed with MrBayes v. 3.1.2 (Huelsenbeck & Ronquist 2001, Ronquist & Huelsenbeck 2003) using ITS, *Btub*, *HSP90*, *cox1* and *NADH1* sequences divided into five partitions with GTR+G model applied for those nucleotide partitions. Four Markov chains were run for 10 000 000 generations with three heated chains (temperature = 0.2) and one cold chain. Trees were sampled every 1 000 steps after removing the first 6 000 generations as burn in. The convergence of the MCMC Bayesian phylogenetic inferences was checked by AWTY online (Nylander et al. 2008). A maximum likelihood (ML) phylogenetic analyses of the multi-locus dataset was carried out with RAxML in the raxmlGUI implementation as described above. Bootstrap analysis with 1 000 replicates was used to test the support of the branches. Phylogenetic trees were visualized in MEGA v. 6 (Tamura et al. 2013) and edited in figure editor programs. All datasets and trees deriving from BI and ML analyses are available from TreeBASE (19249; http://purl.org/phylo/treebase/phylows/study/TB2:S19249).

Nuclear genome size determination

Nuclear genome size of selected isolates of *P.* x*cambivora*, *P.* x*heterohybrida* and *P.* x*incrassata* was assessed using laser flow cytometry. *Phytophthora* isolates were grown in clarified V8-broth for three to seven days at 20 °C. The mycelium was washed thoroughly with deionized water and blotted dry on a Whatman N°1 filter. Nuclei were prepared and stained using the CyStain PI Absolute P kit (Sysmex Partec GmbH, Görlitz, Germany). About 1 mg mycelium was chopped simultaneously with 0.5 cm^2 of young *Raphanus sativus* cv Saxa leaf tissue in 500 µL extraction buffer using a razor blade. The samples were filtered through a 10 µm CellTrics® filter to remove cellular debris. Nuclei were stained using 2 mL of staining solution and incubated overnight at 4 °C. Stained nuclei were analysed using a Partec PAS III flow cytometer (Sysmex Partec GmbH, Görlitz, Germany) equipped with a 488 nm Argon laser. Histograms were rendered and analysed using Flomax software (Sysmex Partec GmbH, Görlitz, Germany). The genome size of each sample was calculated by multiplying the genome size of the internal standard (*Raphanus*; 1086 Mbp) with the ratio of the fluorescence peaks of the sample and the internal standard. Nuclei of all isolates were measured on two days, each time in triplicate.

Morphology of asexual and sexual structures

Morphological features of sporangia, oogonia, oospores, antheridia, hyphal swellings and aggregations of all isolates of the six new species and selected isolates of all described species from Clade 7a (Table 1, 7) were compared with each other.

To induce the formation of sporangia, two 12–15 mm square discs were cut from the growing edge of a 3–7-d-old V8A colony,

and flooded in a 90 mm diam Petri dish with non-sterile soil extract (50 g of filtered oak forest soil in 1 000 mL of distilled water, filtered after 24 h) just above the surface of the aerial mycelium (Jung et al. 1996). The Petri dishes were incubated at 20 °C and natural daylight and the soil extract changed after c. 6 h. Shape, type of apex, caducity and special features of sporangia and the formation of hyphal swellings and aggregations were recorded after 24–48 h. For each isolate 50 sporangia were measured at x400 using a compound microscope (Zeiss Imager.Z2), a digital camera (Zeiss Axiocam ICc3) and a biometric software (Zeiss AxioVision).

The formation of gametangia (oogonia and antheridia) and their characteristic features were examined on V8A after 10 and 21 d growth at 20 °C in the dark. Self-sterile isolates of *P.* x*heterohybrida* and *P.* x*incrassata* were paired on V8A with known A1 and A2 mating type tester strains of *P. cinnamomi* (A1: TW12; A2: MP74) and *P.* x*cambivora* (A1: DE 1; A2: SK 9) and examined after 4 wk incubation at 20 °C in order to determine their mating type (Jung et al. 2011). Isolates of *P.* x*heterohybrida* were then paired with each of two isolates of *P.* x*heterohybrida* from the opposite mating type used as tester strains (A1: TW35, TW47; A2: TW28, TW57). For *P.* x*cambivora* 16 A2 isolates from North and South America, Europe, Asia and Australia (Table 1) were paired with the A1 isolate DE 1 from Germany. In addition, each of the other five A1 isolates (Table 1) was paired with one or two selected A2 isolates, so that gametangia from in total 24 mating combinations were examined. For each isolate of homothallic species and for each successful mating combination of *P.* x*heterohybrida*, *P.* x*incrassata* and *P.* x*cambivora* each 50 oogonia, oospores and antheridia chosen at random were measured under a compound microscope at x400 as described before. The oospore wall index was calculated according to Dick (1990).

Colony morphology, growth rates and cardinal temperatures

Colony growth patterns of all new and known Clade 7a species were described from 7-d-old cultures grown at 20 °C in the dark on V8A, malt-extract agar (MEA; Oxoid Ltd., UK) and potato-dextrose agar (PDA; Oxoid Ltd., UK). Colony morphologies were described according to patterns observed previously (Erwin & Ribeiro 1996, Jung et al. 2002, 2011, Brasier et al. 2004).

For temperature-growth relationships, representative isolates of all new and described *Phytophthora* species from Clade 7a (Table 1) were sub-cultured onto 90 mm V8A plates and incubated for 24 h at 20 °C to stimulate onset of growth (Jung et al. 2002). Then three replicate plates per isolate were transferred to 5, 10, 15, 20, 25, 30 and 35 °C. Radial growth was recorded before colonies reached the margin of the Petridishes, which was between 4 and 15 d, along two lines intersecting the centre of the inoculum at right angles and the mean growth rates (mm/d) were calculated. Plates showing no growth at 35 °C were returned to 20 °C to determine isolate viability.

Soil infestation trials

For assessing whether the six new *Phytophthora* species might pose a potential threat to European forests their pathogenicity to *Castanea sativa*, *Quercus suber* and *Fagus sylvatica*, important forest trees in Mediterranean and temperate regions of Europe, was tested using a soil infestation method (Jung et al. 1996, 2002). One isolate from each new species and as a comparison one isolate of *P.* x*cambivora* (IT 6-3), a serious pathogen of *C. sativa* and *F. sylvatica*, from a *F. sylvatica* forest in Sicily were included (Table 1). Inocula consisted of 4-wk-old cultures of the respective *Phytophthora* isolate grown at 20 °C in 500 mL Erlenmeyer flasks on an autoclaved mixture of 250 cm^3 of vermiculite and 20 cm^3 of millet seeds thoroughly

moistened with 175 mL of V8-juice broth (200 mL/L juice, 800 mL/L distilled water amended with 3 g/L CaCO$_3$). Before use, the colonized medium was rinsed with distilled water to remove excess nutrients. Fifteen plants of *C. sativa* growing in 50×35×27 cm boxes and 10 plants each of *F. sylvatica* and *Q. suber* growing in 35×25×17 cm boxes were infested per *Phytophthora* isolate. Being aware that growing all plants of a host-isolate combination in a single box does not fulfil the requirement of true replicates this trial design was chosen for reasons of space capacity and uniform inoculum distribution. The plants, raised from seeds in an autoclaved mixture of peat, vermiculite and sand (1:1:1 v:v:v), were c. 3 months old when the soil was infested. Tubes initially inserted as placeholders in the soil between the individual seeds were removed and the holes were filled with the inoculum (c. 40 cm^3 of inoculum per plant). Controls received only rinsed non-infested vermiculite/millet seed/V8-juice mixture at the same rate. The plants of *C. sativa*, *Q. suber* and *F. sylvatica* were incubated for 3, 5 and 10 mo, respectively, in a greenhouse at 20–25 °C (short-term maximum 30 °C) and 65 % relative humidity and were flooded every 3 wk for 72 h. At the end of each trial, for each seedling the proportion of healthy and dead roots was estimated visually after spreading the roots uniformly on trays etched with 2×2 cm rectangles. Specific symptoms like root and collar rot lesions and chlorosis and wilting of foliage were recorded. Plants were dried for 72 h at 65 °C and the dry weight of small woody roots (diam 2–10 mm), fine roots (diam < 2 mm) and shoots were registered for each plant. Data were analysed using one-way ANOVA followed by Dunnett's multiple comparisons test using the programme package Prism 6 (Graphpad, San Diego, USA). Re-isolations of *Phytophthora* spp. from necrotic tissues were made using selective PARPNH agar (Jung 2009). At the last flooding cycle of each trial soils were baited using *Q. suber* leaves as baits in order to test whether the respective *Phytophthora* species was still active. After each flooding cycle, the water was collected and autoclaved. At the end of each trial and all analyses, infested substrates, boxes and the plants were sterilised.

RESULTS

Phylogenetic analysis

Including outgroups, the aligned datasets for the nuclear ITS, *Btub* and *HSP90* genes and the mitochondrial *cox1* and *NADH1* genes consisted of 843, 918, 840, 867 and 797 characters, respectively. The majority of mutations were single base pair mutations and within the five gene regions of the 84 Clade 7a isolates there were only short indels of 1–2 base pairs (bp) in ITS at positions 9, 10, 174 and 483, and a 3-character long indel in *HSP90* at positions 449–451, the latter being present only in the six isolates of *P. intricata*. There were no gaps in the *Btub*, *cox1* and *NADH1* alignments. Excluding outgroups, the individual aligned datasets of ITS, *Btub*, *HSP90*, *cox1* and *NADH1* contained 44 (5.3 %), 72 (7.8 %), 74 (8.8 %), 64 (7.4 %) and 40 (5.0 %) polymorphic characters, respectively (Table 2–6). The aligned multigene dataset of 84 isolates from all Clade 7a taxa contained 4 255 characters of which 294 (6.9 %) were variable.

The BI analysis provided more support for deeper branches. Support for terminal clades and their clustering was equivalent in both ML and BI analyses and the latter is presented here with both Bayesian Posterior Probability values and Maximum Likelihood bootstrap values included (Fig. 1, TreeBASE: 19249). The ML bootstrap best tree and the majority consensus rule tree derived from the BI analysis showed nearly identical topology amongst species, with the exception that the relative positions of *P. intricata* and *P. formosa* to each other were not well supported. Both BI and ML analyses resulted in the same

grouping of sequences: the multigene phylogenies revealed 15 discrete lineages within Clade 7a unambiguously corresponding to eight described species, *P. europaea*, *P. fragariae*, *P. rubi*, *P. uliginosa*, *P. uniformis*, *P. ×cambivora* (previously *P. cambivora*) and *P. ×alni* / *P. ×multiformis*; the six new species *P. attenuata*, *P. flexuosa*, *P. formosa*, *P. intricata*, *P. ×incrassata* and *P. ×heterohybrida*; *P.* sp. xcambivora-like (previously designated as *P. cambivora*) and a new putative hybrid between *P. ×multiformis* and *P. uniformis* designated here as *P. ×multiformis-like* (Fig. 1). *Phytophthora flexuosa* had nine unique polymorphisms across the five loci and formed a well-supported clade with *P. europaea* both being separated by 1 bp, 7 bp and 2 bp in ITS, *HSP90* and *Btub* (Table 2–4) and by 17 bp and 6 bp in *cox1* and *NADH1* (Table 5, 6). The *P. europaea-P. flexuosa* cluster diverged early and was basal to the other 13 lineages. *Phytophthora uliginosa* was quite distinct from all other lineages (Fig. 1) with differences across the five loci ranging from 60 bp (*P. flexuosa*) to 84–100 bp (*P. ×cambivora*). The seven isolates of *P. formosa* from the two populations in Lenhuachih and Fushan formed a well-supported distinct clade (Fig. 1). The species had 19 unique polymorphisms across the five loci (Table 2–6) and differed from other species at 55–59 (*P. uniformis*), 57–60 (*P. rubi*), 58–60 (*P. intricata*), 56–69 (*P. ×heterohybrida*) and 62–68 positions (*P. attenuata*). *Phytophthora formosa* had two haplotypes each in *cox1* and *NADH1* which differed from each other in one position (Table 5–6). *Phytophthora formosa* and *P. intricata* are the basal branches within a large well-supported clade but their relative position could not be resolved (Fig. 1). The six *P. intricata* isolates from *Q. tarokoensis* at Fushan were identical in all five gene regions and had 21 unique polymorphisms of which nine (43 %) were present in *HSP90* (Table 2–6). *Phytophthora attenuata* possessed 17 unique polymorphisms across the five loci (Table 2–6) and formed a monophyletic group with the well supported clade of *P. fragariae* and *P. rubi* (Fig. 1) being separated from those by 61–66 and 49–52 polymorphisms, respectively. The five isolates of *P. attenuata* formed two groups according to the two sampling sites in Sheipa Nationalpark (Fig. 1). They had identical *Btub* and *HSP90* sequences (Table 3–4) but differed from each other by 1, 1 and 2 bases in ITS, *NADH1* and *cox1* (Table 2, 5–6). *Phytophthora fragariae* and *P. rubi* unambiguously separated in the phylogenetic analyses (Fig. 1). Apart from a deletion at position 10 in *P. rubi* isolate CBS 109892 the two species had identical ITS sequences (Table 2) but differed across the other four gene regions by 37–41 bp (Table 3–6). In contrast to *P. fragariae* with three *HSP90* and two *NADH1* genotypes, seven of the eight isolates of *P. rubi* from six European countries were identical suggesting clonal spread (Fig. 1; Table 2–6). The clade of *P. attenuata*, *P. fragariae* and *P. rubi* formed a well-supported monophyletic group with *P. ×heterohybrida*, *P. ×incrassata* and the five lineages of the *P. ×cambivora-P. ×alni* cluster (Fig. 1). *Phytophthora ×heterohybrida* and *P. ×incrassata* formed a clade in sister-group position to the clade of *P. ×cambivora*, *P. uniformis*, *P. ×alni* and *P. ×multiformis* (Fig. 1). Although not clearly visible in the combined multigene tree (Fig. 1) the ITS, *Btub* and *HSP90* sequences of the eight tested isolates of *P. ×heterohybrida* belonged to two, three and four different genotypes (Table 2–4), respectively, and were characterised by the presence of 23 heterozygous sites in the nuclear genes and 22 unique polymorphisms (Table 2–4). In contrast, all seven isolates of *P. ×incrassata* had identical nuclear sequences with 31 heterozygous positions (Table 2–4). In addition, *P. ×incrassata* showed 19 unique polymorphisms across the three nuclear genes and *cox1* (Table 2–5). Despite of high intraspecific variability with nine, seven and eight different genotypes and in total 55 heterozygous positions in the ITS, *Btub* and *HSP90* sequences (Table 2–4), the 13 tested isolates of *P. ×cambivora* from eight countries and five continents formed a highly

Table 2 Polymorphic sites from aligned ITS sequence data of 833 bp length showing inter- and intraspecific variation of eight described and six new *Phytophthora* species and two new *Phytophthora* taxa from Clade 7a represented by 84 isolates. Polymorphisms unique to a species are highlighted in **bold**.

Phytophthora species, isolate	No. iso-lates	Geno-type
P. xalni, ALN268	1	G1
P. xalni	4[a]	G2
P. xalni, WPC P10568	1	G3
P. xalni, PHAKO 12	1	G4
P. xmultiformis + *P.* sp. xmulti-formis-like	5[b]	G5
P. uniformis	5[c]	G6
P. uniformis, P876	1	G7
P. uniformis, 250001	1	G8
P. sp. xcambivora-like CBS 111329	1	G9
P. xcambivora, 4044.1	1	G10
P. xcambivora, IMI 229178	1	G11
P. xcambivora, CBS 114086	1	G12
P. xcambivora, 4050.1	1	G13
P. xcambivora, DE 1	1	G14
P. xcambivora, CBS 114087	1	G15
P. xcambivora, ES 1	1	G16
P. xcambivora	4[d]	G17
P. xcambivora, CL1, CL5	2	G18
P. xheterohybrida	7[e]	G19
P. xheterohybrida, CBS 141205	1	G20
P. xincrassata	7[f]	G21
P. fragariae + *P. rubi*	11[g]	G22
P. rubi, CBS 109892	1	G23
P. attenuata	4[h]	G24
P. attenuata, CBS 141199	1	G25
P. formosa	7[i]	G26
P. intricata	6[j]	G27
P. uliginosa, CBS 109054	1	G28
P. europaea, CBS 109051	1	G29
P. europaea, CBS 109049	1	G30
P. flexuosa	3[k]	G31

[a] IMI 392314, ALN 45, MAL 5, Reis 2.
[b] IMI 392316, 4971496, PAM 396, PAM 859, PHAPI 12.
[c] WPC P10565, ALN 58, ALN 222, PAU 60, PAU 558.
[d] CBS 141218, IT 6-3, IT 6-4, SK 9.
[e] CBS 141207, TW29, TW31, TW32, TW51, TW56, TW57.
[f] CBS 141208, CBS 141209, TW43, TW299, TW344, TW347, TW350.
[g] BBA11/94, BBAL1, SCRP245, WPC P1435, BBA 93, BBA 390, CBS 96795, CH-106, 9A9, 5005038, PHRM 09.
[h] CBS 141200, TW119, TW128, TW130.
[i] CBS 141203, CBS 141204, TW13, TW105, TW106, TW109, TW110.
[j] CBS 141210, CBS 141211, TW16, TW257, TW258, TW263.
[k] CBS 141201, CBS 141202, TW79.

Table 3 Polymorphic sites from aligned partial HSP90 sequence data of 840 bp length showing inter- and intraspecific variation of 8 described and 6 new *Phytophthora* species and two new *Phytophthora* taxa from Clade 7a represented by 84 isolates. Polymorphisms unique to a species are highlighted in **bold**.

Phytophthora species, isolate	No. of isolates	Haplotype
P. xalni [a]	3	G1
P. xalni + *P. xmultiformis* + *P. sp. xmultiformis*-like [b]	6	G2
P. xmultiformis [c]	2	G3
P. xmultiformis, IMI 392316	1	G4
P. uniformis [d]	7	G5
P. sp. xcambivora-like, CBS 111329	1	G6
P. xcambivora, 4044.1	1	G7
P. xcambivora, DE 1	1	G8
P. xcambivora, IMI 229178	1	G9
P. xcambivora, CBS 114086	1	G10
P. xcambivora, CBS 114087	1	G11
P. xcambivora	6 [e]	G12
P. xcambivora, ES 1	1	G13
P. xcambivora, IT 6-3	1	G14
P. xheterohybrida	4 [f]	G15
P. xheterohybrida, TW51	1	G16
P. xheterohybrida, TW32	1	G17
P. xheterohybrida	2 [g]	G18
P. xincrassata	7 [h]	G19
P. fragariae, BBA11/94	1	G20
P. fragariae	2 [i]	G21
P. fragariae, WPC P1435	1	G22
P. rubi	8 [j]	G23
P. attenuata	5 [k]	G24
P. formosa	7 [l]	G25
P. intricata	6 [m]	G26
P. uliginosa, CBS 109054	1	G27
P. europaea	2 [n]	G28
P. flexuosa	3 [o]	G29

[a] WPC P10568, PHAKO 12, Reis 2.
[b] IMI392314, 4971496, ALN 45, ALN 268, MAL5, PHAPI 12.
[c] PAM 396, PAM 859.
[d] WPC P10565, 250001, ALN 58, ALN 222, P876, PAU 60, PAU 558.
[e] CBS 141218, 4050.1, CL1, CL5, IT 6-4, SK 9.
[f] CBS 141205, CBS 141207, TW29, TW31.
[g] TW56, TW57.
[h] CBS 141208, CBS 141209, TW43, TW299, TW344, TW347, TW350.
[i] BBA L1, SCRP245.
[j] CBS 109892, CBS 967.95, 5005038, 9A9, BBA 93, BBA 390, CH-106, PHRM 09.
[k] CBS 141199, CBS 141200, TW119, TW128, TW130.
[l] CBS 141203, CBS 141204, TW13, TW105, TW106, TW109, TW1110.
[m] CBS 141210, CBS 141211, TW16, TW257, TW258, TW263.
[n] CBS 109049, CBS 109051.
[o] CBS 141201, CBS 141202, TW79.

Table 4 Polymorphic sites from aligned partial ß-tubulin sequence data of 918 bp length showing inter- and intraspecific variation of eight described and six new *Phytophthora* species and two new *Phytophthora* taxa from Clade 7a represented by 84 isolates. Polymorphisms unique to a species are highlighted in **bold**.

No. of iso-lates	Haplo-type	Phytophthora species, isolate
1	G1	P. xalni, IMI 392314
1	G2	P. xalni, WPC P10568
1	G3	P. xalni, ALN 268
1	G4	P. xalni, Reis 2
1	G5	P. xalni, PHAKO 12
4	G6[a]	P. xalni + P. sp. xmultiformis-like
1	G7	P. xmultiformis, IMI 392316
2	G8[b]	P. xmultiformis
7	G9[c]	P. uniformis
1	G10	P. sp. xcambivora-like, CBS 111329
1	G11	P. xcambivora, 4044.1
1	G12	P. xcambivora, DE 1
1	G13	P. xcambivora, IMI 229178
1	G14	P. xcambivora, CBS 114086
1	G15	P. xcambivora, CBS 114087
1	G16	P. xcambivora, IT 6-3
7	G17[d]	P. xcambivora
6	G18[e]	P. xheterohybrida
1	G19	P. xheterohybrida, TW32
1	G20	P. xheterohybrida, TW51
7	G21[f]	P. xincrassata
4	G22[g]	P. fragariae
8	G23[h]	P. rubi
5	G24[i]	P. attenuata
7	G25[j]	P. formosa
6	G26[k]	P. intricata
1	G27	P. uliginosa, CBS 109054
2	G28[l]	P. europaea
3	G29[m]	P. flexuosa

[a] ALN 45, 4971496, MAL5, PHAPI 12.
[b] PAM 396, PAM 859.
[c] WPC P10565, 250001, ALN 58, ALN 222, P876, PAU 60, PAU 558.
[d] CBS 141218, 4050.1, CL1, CL5, ES 1, IT 6-4, SK 9.
[e] CBS 141205, CBS 141207, TW29, TW31, TW56, TW57.
[f] CBS 141208, CBS 141209, TW43, TW299, TW344, TW347, TW350.
[g] WPC P1435, BBA 11/94, BBA L1, SCRP245.
[h] CBS 967.95, CBS 109892, 9A9, 5005038, BBA 93, BBA 390, CH-106, PHRM 09.
[i] CBS 141199, CBS 141200, TW119, TW128, TW130.
[j] CBS 141203, CBS 141204, TW13, TW105, TW106, TW109, TW110.
[k] CBS 141210, CBS 141211, TW16, TW257, TW258, TW263.
[l] CBS 109049, CBS 109051.
[m] CBS 141201, CBS 141202, TW79.

Table 5 Polymorphic sites from aligned partial *cox1* sequence data of 867 bp length showing inter- and intraspecific variation of eight described and six new *Phytophthora* species and two new *Phytophthora* taxa from Clade 7a represented by 84 isolates. Polymorphisms unique to a species are highlighted in **bold**.

Phytophthora species, isolate	Haplo-type	No. of isolates
P. xalni + *P. xmultiformis*	H1 [a]	11
P. uniformis + *P.* sp. xmultiformis-like	H2 [b]	8
P. sp. xcambivora-like, CBS 111329	H3	1
P. xcambivora	H4 [c]	13
P. xheterohybrida	H5 [d]	8
P. xincrassata	H6 [e]	7
P. fragariae	H7 [f]	4
P. rubi	H8 [g]	8
P. attenuata	H9 [h]	2
P. attenuata	H10 [i]	3
P. formosa	H11 [j]	6
P. formosa, TW110	H12	1
P. intricata	H13 [k]	6
P. uliginosa, CBS 109054	H14	1
P. europaea	H15 [l]	2
P. flexuosa	H16 [m]	3

[a] IMI 392314, IMI 392316, WPC P10568, ALN 45, ALN 268, MAL5, PAM 396, PAM 859, PHAPI 12, PHAKO 12, Reis 2.
[b] WPC P10565, 250001, 4971496, ALN 58, ALN 222, P876, PAU 60, PAU 558.
[c] IMI 229178, CBS 114086, CBS 114087, CBS 114218, 4044.1, 4050.1, CL1, CL5, DE 1, ES 1, IT 6-3, IT 6-4, SK 9.
[d] CBS 141205, CBS 141207, TW29, TW31, TW32, TW51, TW56, TW57.
[e] CBS 141208, CBS 141209, TW43, TW299, TW344, TW347, TW350.
[f] WPC P1435, BBA 11/94, BBA L1, SCRP245.
[g] CBS 967.95, CBS 109892, BBA 93, BBA 390, CH-106, 9A9, 5005038, PHRM 09.
[h] CBS 141200, TW119.
[i] CBS 141199, TW128, TW130.
[j] CBS 141203, CBS 141204, TW13, TW105, TW106, TW258, TW263.
[k] CBS 141210, CBS 141211, TW16, TW257, TW258, TW263.
[l] CBS 109049, CBS 109051.
[m] CBS 141201, CBS 141202, TW79.

Table 6 Polymorphic sites from aligned partial *NADH1* sequence data of 797 bp length showing inter- and intraspecific variation of eight described and six new *Phytophthora* species and two new *Phytophthora* taxa from Clade 7a represented by 84 isolates. Polymorphisms unique to a species are highlighted in **bold**.

Phytophthora species, isolate	Haplo-type	No. of isolates
P. xalni + *P. xmultiformis*	H1 [a]	11
P. uniformis + *P.* sp. xmultiformis-like	H2 [b]	8
P. sp. xcambivora-like, CBS 111329	H3	1
P. xcambivora	H4 [c]	2
P. xcambivora + *P. xheterohybrida* + *P. xincrassata*	H5 [d]	26
P. fragariae	H6 [e]	2
P. fragariae	H7 [f]	2
P. rubi	H8 [g]	8
P. attenuata	H9 [h]	2
P. attenuata	H10 [i]	3
P. formosa	H11 [j]	4
P. formosa	H12 [k]	3
P. intricata	H13 [l]	6
P. uliginosa, CBS 109054	H14	1
P. europaea	H15 [m]	2
P. flexuosa	H16 [n]	3

[a] IMI 392314, IMI 392316, WPC P10568, ALN 45, ALN 268, MAL5, PAM 396, PAM 859, PHAPI 12, PHAKO 12, Reis 2.
[b] WPC P10565, 4971496, ALN 58, ALN 222, 250001, P876, PAU 60, PAU 558.
[c] CBS 114086, IMI 229178.
[d] CBS 114087, CBS 141205, CBS 141207, CBS 141208, CBS 141209, CBS 141218, 4044.1, 4050.1, CL1, CL5, IT 6-4, DE 1, ES 1, IT 6-3, SK 9, TW29, TW31, TW32, TW51, TW56, TW57, TW43, TW299, TW344, TW347, TW350.
[e] BBA 11/94, BBA L1.
[f] WPC P1435, SCRP245.
[g] CBS 967.95, CBS 109892, 5005038, 9A9, BBA 93, BBA 390, CH-106, PHRM 09.
[h] CBS 141200, TW119.
[i] CBS 141199, TW128, TW130.
[j] CBS 141203, CBS 141204, TW13, TW105.
[k] TW106, TW109, TW110.
[l] CBS 141210, CBS 141211, TW16, TW257, TW258, TW263.
[m] CBS 109049, CBS 109051.
[n] CBS 141201, CBS 141202, TW79.

Fig. 1 Fifty percent majority rule consensus phylogram derived from Bayesian inference analysis of five-locus (ITS, *Btub*, *HSP90*, *cox1* and *NADH1*) dataset of Clade7a. Bayesian posterior probabilities and ML bootstrap values (in %) are indicated above and below branches, respectively. *Phytophthora cinnamomi* and *P. niederhauserii* from Clade 7b were used as outgroup taxa (not shown). Scale bar indicates 0.5 expected changes per site per branch.
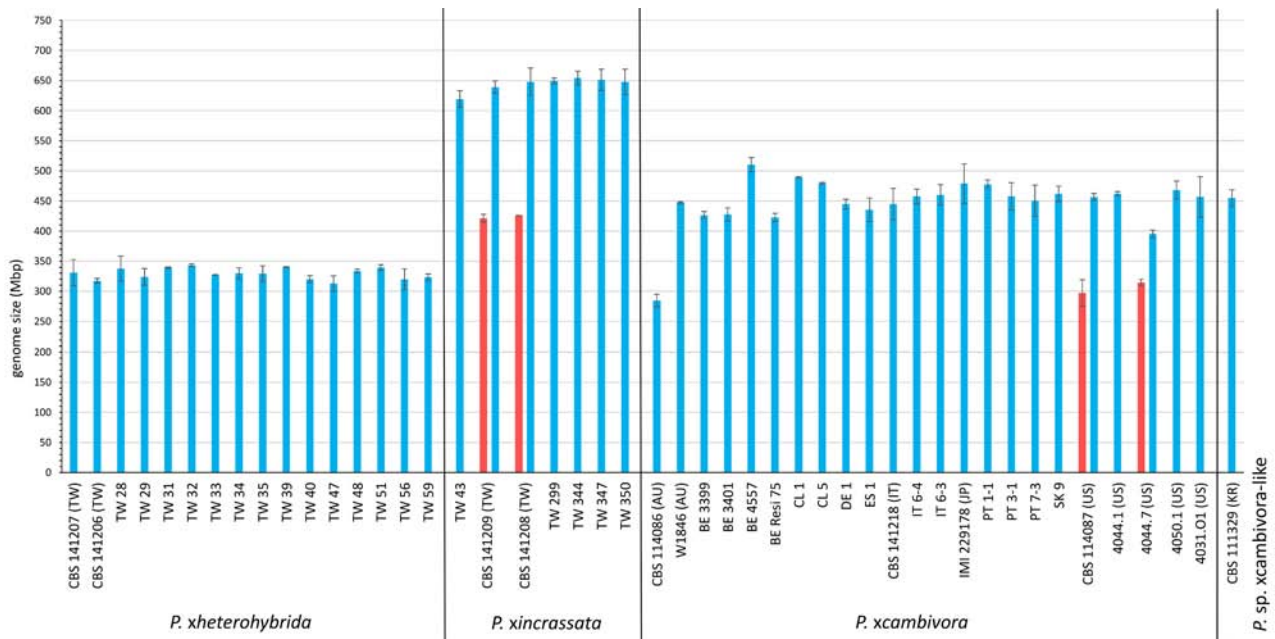
Fig. 2 Average holoploid genome size of *Phytophthora* x*heterohybrida*, *P.* x*incrassata*, *P.* x*cambivora* and *P.* sp. xcambivora-like determined using flow cytometry analysis. Primary nuclear populations are marked in blue, secondary nuclear populations are marked in red. Error bars indicate the standard deviation.

supported distinct lineage (Fig. 1). *Phytophthora* x*cambivora* was characterised by 40 unique polymorphisms across the three nuclear loci (Table 2–4). Interestingly, the *NADH1* sequences of all but two isolates (CBS 114086, IMI 229178) of *P.* x*cambivora* were identical to those of *P.* x*heterohybrida* and *P.* x*incrassata* (Table 6) although the *cox1* sequences of the three species were clearly different from each other with pairwise differences of seven characters for *P.* x*cambivora*/*P.* x*heterohybrida*, 13 characters for *P.* x*cambivora*/*P.* x*incrassata* and seven characters for *P.* x*heterohybrida*/*P.* x*incrassata* (Table 5). The closest relatives of *P.* x*cambivora* were *P.* x*alni*, *P.* x*multiformis* and isolate CBS 111329 from *Malus pumila* in South Korea (Fig. 1). Previously assigned to *P. cambivora*, this isolate formed a discrete lineage which was separated from *P.* x*cambivora* by 22–45 differences across the five gene regions tested (Table 2–6). This taxon, informally designated here as *P.* sp. xcambivora-like, is characterised by having 17 heterozygous positions across the three nuclear loci (Table 2–4) and nine unique polymorphisms across the five loci (Table 2–6). The multigene phylogeny could not resolve the tested isolates of *P.* x*alni* and their maternal parent *P.* x*multiformis* (Fig. 1) whereas *P.* x*uniformis*, the paternal parent of the *P.* x*alni* isolates, was in sister-group position in an unambiguously distinct clade. The nuclear gene sequences of *P.* x*alni* (ITS, *Btub* and *HSP90*) and *P.* x*multiformis* (*Btub* and *HSP90*) contained 30 and 18 heterozygous positions, respectively (Table 2–4). No heterozygous positions were found in the *cox1* and *NADH1* sequences of any Clade 7a species (Table 5–6). Noteworthy, isolate 4971496 from *A. glutinosa* in the Netherlands belonged to a discrete, previously unknown lineage (Fig. 1) which is designated here as *P.* sp. xmultiformis-like. While nuclear gene sequences (Table 2–4) identified this isolate as *P.* x*multiformis*, its *cox1* and *NADH1* sequences were identical to *P.* x*uniformis* (Table 5–6). Therefore, the phylogenetic position of this lineage within the clade formed by *P.* x*uniformis*, *P.* x*alni*, *P.* x*multiformis* and *P.* sp. xcambivora-like is not fully resolved (Fig. 1).

Nuclear genome size determination

The holoploid genome size of the 16 *P.* x*heterohybrida* isolates tested was homogeneous and ranged from 312.9 to 343.2 Mbp (av. 329.3 ± 9.1 Mbp) (Fig. 2). Also for *P.* x*incrassata* the genome size was similar for most of the seven isolates

ranging from 619.2 to 654.3 Mbp (av. 644.2 ± 12.0 Mbp). In *P.* x*incrassata* isolates CBS 141208 and CBS 141209, however, a secondary fluorescence peak was visible, representing a secondary population of smaller nuclei which have a genome size of 421.4 ± 6.5 and 426.0 ± 2.3 Mbp, respectively (Fig. 2). For *P.* x*incrassata* isolate CBS 141209, only in one measurement the smaller nuclei could be visualized (in triplicate).

The genome size of the *P.* x*cambivora* isolates was considerably more heterogeneous, ranging from 284.6 to 510.3 Mbp (av. 437.1 ± 56.0 Mbp). In *P.* x*cambivora* isolates CBS 114087 and 4044.7 also a secondary population of small nuclei with a genome size of 297.2 ± 22.1 and 314.6 ± 5.2 Mbp, respectively, was observed (Fig. 2).

The size of the secondary populations of small nuclei in some of the *P.* x*incrassata* and *P.* x*cambivora* isolates was always significantly smaller than that of the large nuclei (Fig. 2). In one measurement of isolate CBS 141209 it was even below the detection limit.

TAXONOMY

Morphological and physiological characters and measurements of the six new *Phytophthora* taxa and related species are given in the comprehensive Table 7.

Phytophthora attenuata T. Jung, M. Horta Jung, Scanu & Bakonyi, *sp. nov.* — MycoBank MB816566; Fig. 3

Etymology. Name refers to the tapering oogonial stalks (*attenuata* Lat = tapering).

Typus. Taiwan, Sheipa National Park, isolated from rhizosphere soil of a mature *Castanopsis carlesii* tree, *T. Jung*, 2013 (CBS H-22552 holotype, dried culture on V8A, Herbarium CBS-KNAW Fungal Biodiversity Centre, CBS 141199 = TW129, ex-type culture). ITS and *cox1* sequences GenBank KU517154 and KU517148, respectively.

Sporangia (Fig. 3a–h) — Sporangia of *P. attenuata* were not observed on solid agar but were produced abundantly in non-sterile soil extract. Sporangia were typically borne terminally on unbranched sporangiophores, less frequently in lax sympodia. Sporangia were non-caducous and nonpapillate (Fig. 3a–e), usually with a flat apex (Fig. 3a–c, e, g), sometimes

Table 7 Morphological characters and dimensions (μm), cardinal temperatures (°C) and temperature-growth relations (mm/d) on V8A of species in *Phytophthora* ITS Clade 7a. Most discriminating characters are highlighted in **bold**.

	P. attenuata	P. formosa	P. intricata	P. fragariae	P. rubi	P. flexuosa	P. europaea	P. uliginosa
No. of isolates	6[a]	6[a]	6[a]	2[a]	7[a]	3[a]	7[a]	3[a]
Sporangia	ovoid, obpyriform, (limoniform)	ovoid, ellipsoid, obpyriform, (limoniform)	ovoid, obpyriform, (limoniform, ellipsoid), **some bi- and trilobed**	ovoid, limoniform, obpyriform, ellipsoid	ovoid, ellipsoid, obpyriform, limoniform	ovoid, ellipsoid, (obpyriform, limoniform)	ovoid, obpyriform, ellipsoid, (subglobose), often pointed apex	**ellipsoid**, ovoid, peanut-shaped, (obpyriform, limoniform)
lxb mean	44.7 ± 11.7 × 29.4 ± 5.3	49.2 ± 8.1 × 32.6 ± 5.7	54.4 ± 8.0 × 34.2 ± 4.4	**65.9 ± 8.0 × 41.4 ± 4.0**	50.2 ± 12.7 × 29.3 ± 8.1	56.1 ± 7.4 × 36.7 ± 5.2	63.7 ± 16.9 × 44.6 ± 8.3	**67.0 ± 8.5 × 42.4 ± 6.4**
range of isolate means	34.5–60.3 × 24.7–35.4	43.7–59.6 × 29.3–40.4	51.0–58.9 × 32.1–37.5	**62.3–69.5 × 39.7–43.1**	35.6–61.9 × 33.9–39.4	53.3–58.6 × 33.9–39.4	50.0–78.9 × 36.7–51.2	**65.7–70.3 × 30.9–44.4**
total range	17.8–78.5 × 13.5–45.9	32.7–73.6 × 20.1–50.1	39.0–78.9 × 24.1–48.8	45.6–81.4 × 31.7–50.3	25.1–83 × 11.9–46.8	34.9–74.8 × 22.8–49.7	23.6–124.3 × 21.9–67.3	41.1–85.0 × 24.8–56.9
l/b ratio	1.50 ± 0.2	1.52 ± 0.17	1.60 ± 0.23	1.60 ± 0.25	1.75 ± 0.26	1.54 ± 0.18	1.42 ± 0.19	1.60 ± 0.19
caducity	–	–	–	–	–	–	–	–
exitpores	13.9 ± 2.7	13.5 ± 2.7	15.4 ± 2.3	16.1 ± 2.3	16.1 ± 4.6	19.7 ± 3.4	19.3 ± 4.7	15.4 ± 3.4
zoospore cysts	12.7 ± 2.6	14.3 ± 2.5	13.4 ± 1.9	12.5 ± 1.8	13.3 ± 1.9	13.3 ± 1.3	15.3 ± 2.0	11.9 ± 1.8
Breeding system	homothallic	homothallic	homothallic	homothallic	homothallic	homothallic	homothallic	homothallic
Oogonia								
mean diam	40.9 ± 4.8	38.5 ± 3.5	43.5 ± 5.1	**33.5 ± 4.2**	36.5 ± 5.1	36.8 ± 3.3	37.3 ± 5.4	46.2 ± 7.5
range of isolate means	36.8–45.2	37.2–40.7	41.5–46.0	31.4–35.6	33.0–39.1	36.0–38.3	34.4–39.9	17.9–65.5
total range	28.6–55.6	27.1–50.0	26.3–56.7	25–44.8	23.0–47.1	25.7–42.8	19.2–48.4	41.6–53.3
Thick-walled								–
tapering base	**77 % (46–96 %)**	52.3 % (38–82 %)	28.3 % (12–50 %)	**69 % (66–73 %)**	**13.9 % (4–33 %)**	47.9 % (32–58 %)	**60.0 % (52–81 %)**	–
intricate stalks	< 1 %	10 % (2–18 %)	**44.7 % (38–63 %)**	2.5 % (2–3 %)	2.5 % (0–8 %)			–
elongated	38 % (22–54 %)	**1.7 % (0–6 %)**	6.2 % (0–15 %)	**43 % (34–52 %)**	**9.5 % (2–25 %)**	19.7 % (4–36 %)	21.3 % (12–34 %)	–
excentric	15 % (2–40 %)	6.7 % (4–12 %)	9.4 % (4–23 %)	3.0 % (2–4 %)	8.6 % (0–18 %)	5.3 % (2–25 %)	4.0 % (0–8 %)	–
comma-shaped	2.3 % (0–3 %)	2.7 % (0–10 %)	–	3 %	–	< 1 % (0–1 %)	2.1 % (0–4 %)	–
ornamented	**18.3 % (1–43 %)**	**32 % (14–58 %)**	**1.6 % (0–2 %)**	–	–	**65.6 % (52–81 %)**	–	–
flexuose	5.7 % (0–22 %)				–	**25 % (20–28 %)**		–
Oospores								
plerotic oospores	100 %	> 99 % (99–100 %)	100 %	86 % (81–93 %)	**64.3 % (50–83 %)**	**> 99 % (99–100 %)**	**46.3 % (38–53 %)**	**30.0 % (12–46 %)**
mean diam	36.5 ± 3.5	34.6 ± 3.2	39.9 ± 4.6	28.2 ± 3.2	31.9 ± 4.5	32.2 ± 2.7	33.2 ± 5.3	41.3 ± 6.1
Total range	25.9–44.9	22.4–42.5	25.1–50.3	21.4–36.0	29.1–35.6	22.7–37.7	16.3–45.1	12.5–55.0
wall diam	2.9 ± 0.5	3.0 ± 0.5	3.6 ± 0.5	2.1 ± 0.4	2.0 ± 0.6	3.1 ± 0.5	2.5 ± 0.7	**4.2 ± 0.7**
oospore wall index	0.41 ± 0.05	0.43 ± 0.06	0.45 ± 0.05	0.38 ± 0.08	0.33 ± 0.08	**0.47 ± 0.06**	0.38 ± 0.06	**0.49 ± 0.07**
Abortion rate	11.0 % (2–18 %)	12.7 % (7–16 %)	8.1 % (4–16 %)	66 % (60–72 %)	65.8 % (45–82 %)	**1.7 % (1–2 %)**	**24.9 % (18–31 %)**	6.2 % (3–10 %)
Antheridia	**31.9 % amphigynous 33.7 %**	**96.7 % paragynous**	**100 % paragynous**	**30 % amphigynous**	**44.2 % amphigynous 4 %**	**100 % paragynous**	100 % paragynous	100 % paragynous
bicellular				–				
size	19.0 ± 3.3 × 15.3 ± 2.5	15.2 ± 2.9 × 11.8 ± 1.9	14.4 ± 2.5 × 11.4 ± 1.8	16.6 ± 6.3 × 12.7 ± 2.5	18.0 ± 3.8 × 13.9 ± 2.0	13.4 ± 2.1 × 10.0 ± 1.7	13.6 ± 2.6 × 10.8 ± 2.1	16.9 ± 3.1 × 13.3 ± 2.5
Hyphal swellings	–	–	in water; subglobose, limoniform; rare	**in water; subglobose, irregular, catenulate**	**in water; elongated, irregular, catenulate**	**coralloid**	–	**in water; subglobose, irregular, catenulate**
Maximum temperature	**30**	**30–< 35**	**30–< 35**	25–< 30	25–< 30	35	30–< 35	**25**
Optimum temperature	25	25	25	20	25	25	25	20
Growth rate at optimum	4.3 ± 0.26	5.1 ± 0.23	5.5 ± 0.27	1.9 ± 0.56	2.9 ± 0.91	4.7 ± 0.61	4.9 ± 0.53	1.2 ± 0.2
Growth rate at 20°C	3.9 ± 0.09	4.2 ± 0.08	5.0 ± 0.17	1.9 ± 0.56	2.7 ± 0.75	4.4 ± 0.56	4.4 ± 0.59	1.2 ± 0.2

Table 7 (cont.)

	P. ×incrassata	P. ×heterohybrida	P. ×cambivora	P. sp. ×cambivora-like	P. ×alni	P. ×multiformis	P. uniformis[o]	P. sp. ×multiformis-like
No. of isolates	7 [a,b]	21 [a]	23 [a]	1 [c]	9 [a]	6 [a]	6 [a]	1 [a]
Sporangia	ovoid, limoniform, ellipsoid, (pyriform)	ovoid, limoniform, obpyriform, (ellipsoid)	ovoid, obpyriform, ellipsoid, limoniform	ovoid, limoniform, ellipsoid, obpyriform	ovoid, obpyriform, (ellipsoid, limoniform)	ovoid, (limoniform, obpyriform, ellipsoid)	ovoid, obpyriform, (limoniform, ellipsoid)	ovoid
l×b mean	61.2 ± 8.5 × 43.7 ± 5.6	**75.3 × 13.2 × 45.7 ± 7.6**	68.3 ± 12.4 × 42.6 ± 7.0	66.2 ± 9.8 × 35.1 ± 6.2	54.2 ± 10.0 × 39.3 ± 5.2	50.9 ± 9.7 × 36.4 ± 4.7	58.2 ± 7.0 × 40.0 ± 3.9	51.8 ± 7.8 × 37.6 ± 4.7
range of isolate means	56.6–66.5 × 40.0–47.3	**64.0–82.8 × 38.9–50.1**	48.2–84.3 × 30.3–49	–	50.3–59.1 × 36.7–43.9	35.8–60.4 × 29.2–41.6	54.1–62.1 × 34.2–42.9	34.6–64.3 × 29.1–46.7
total range	36.9–88.2 × 28.5–56.6	29.7–123.8 × 21.4–77.3	35.1–120.9 × 22.7–62.9	47.4–86.9 × 23.5–50.3	31.5–78.8 × 25.9–53.8	28.3–80.3 × 22.1–49.2	36.8–78.3 × 24.1–57.4	
l/b ratio	1.40 ± 0.13	1.66 ± 0.23	1.61 ± 0.19	**1.90 ± 0.2**	1.38 ± 0.16	1.40 ± 0.18	1.47 ± 0.19	1.37 ± 0.1
caducity	–	**in all isolates; rare**	–	–	–	–	–	–
exit pores	15.0 ± 2.7	16.0 ± 2.6	17.1 ± 3.5	20.0 ± 2.4	15.3 ± 3.0	14.2 ± 3.1	15.5 ± 2.9	13.8 ± 1.6
zoospore cysts	14.4 ± 1.3	13.4 ± 1.4	13.7 ± 1.8	14.0 ± 2.1	14.3 ± 1.9	14.8 ± 3.6	14.3 ± 2.3	13.3 ± 0.8
Breeding system	**heterothallic**	**heterothallic**	**heterothallic**	**heterothallic**	homothallic	homothallic	homothallic	homothallic
Oogonia								
mean diam	45.2 ± 6.6	44.1 ± 6.7	46.5 ± 5.1	48.0 ± 4.5	48.7 ± 7.1	48.4 ± 5.6	47.6 ± 3.5	46.5 ± 5.8
range of isolate means	41.4–49.1	37.7–50.4	37.6–52.9	–	42.8–56.3	47.5–49.5	46.6–48.6	–
total range	31.8–63.6	25.2–61.2	30.4–61.8	36.8–57.3	25.6–69.5	30.8–58.1	36.3–58.4	31.9–56.3
thick-walled	77.9 % (50–100 %)	28.7 % (8–42 %)	**1.0 % (0–15 %)**	–	0.9 % (0–6 %)	2.0 % (0–8 %)	–	**12.0 %**
tapering base	39.7 (13–68 %)	89.1 % (72–100 %)	66.8 % (15–100 %)	43.5 % (30–57 %)	43.9 % (13–74 %)	53.9 % (30–66 %)	58.6 % (32–71 %)	62.0 %
twisted stalks	1 % (0–7 %)	–	–	–	–	–	–	–
elongated	**5.1 % (0–10 %)**	**73.2 % (44–98 %)**	**35.7 % (0–53 %)**	25 % (20–30 %)	5.5 % (0–16 %)	2.0 % (0–6 %)	3.5 % (0–14 %)	6.0 %
excentric	1.2 % (0–3 %)	3.2 % (0–8 %)	4.1 % (0–23 %)	–	4.7 % (0–10 %)	6.1 % (2–14 %)	**20.5 % (6–30 %)**	–
comma-shaped	7.6 % (0–23 %)	13.3 % (6–28 %)	8.3 % (0–17 %)	8.5 % (7–10 %)	14.2 % (0–33 %)	8.2 % (2–12 %)	1.2 % (0–3 %)	2.0 %
ornamented	**98.1 % (97–100 %)**	**97.9 % (94–100 %)**	**60.7 % (3–100 %)**	88 % (56–100 %)	**76.5 % (18–94 %)**	**74.9 % (29–96 %)**	4.2 % (0–10 %)	**94.0 %**
flexuose	–	1.2 % (0–4 %)	0.1 % (0–3 %)	–	1.6 % (0–5 %)	5.8 % (0–22 %)	–	–
Oospores								
plerotic oospores	**100 %**	97.2 % (90–100 %)	90.2 % (67–100 %)	98 % (96–100 %)	89.8 % (70–100 %)	80.6 % (43–98 %)	**57 % (52–62 %)**	96.0 %
mean diam	37.7 ± 4.7	36.8 ± 5.4	40.3 ± 4.5	41.3 ± 4.0	40.8 ± 6.1	39.8 ± 4.3	42.1 ± 3.1	38.2 ± 5.1
Total range	25.9–55.1	19.5–50.8	24.4–52.7	32.8–52.0	23.3–58.8	27.5–52.9	33.0–50.8	26.6–49.3
wall diam	3.1 ± 0.6	3.1 ± 0.6	3.1 ± 0.6	3.2 ± 0.7	3.1 ± 0.7	3.1 ± 0.6	3.2 ± 0.6	2.7 ± 0.4
oospore wall index	0.41 ± 0.06	0.43 ± 0.07	0.40 ± 0.06	0.39 ± 0.06	0.39 ± 0.07	0.40 ± 0.06	0.39 ± 0.06	0.37 ± 0.05
Abortion rate	47.4 % (30–61 %)	**17.3 % (4–33 %)**	**38.5 % (7–90 %)**	42.5 % (38–47 %)	**66.9 % (7–94 %)**	**54.0 % (32–64 %)**	**13 % (1–30 %)**	**69.0 %**
Antheridia	**100 % amphigynous**	**100 % amphigynous**	**97.9 % amphigynous**	**100 % amphigynous**	88.6 % amphigynous	**83.0 % amphigynous**	**100 % amphigynous**	**78.0 % amphigynous**
bicellular amphigynous	52.4 %	49.6 %	64.7 %	58.5 %	48.2 %	35.7 %	64.2 %	18.0 %
size	20.2 ± 3.4 × 16.4 ± 2.0	23.2 ± 4.3 × 18.0 ± 2.1	23.5 ± 5.0 × 17.9 ± 2.7	23.2 ± 4.7 × 17.8 ± 2.3	22.2 ± 5.0 × 16.9 ± 2.5	19.8 ± 4.2 × 15.7 ± 2.4	24.3 ± 4.3 × 17.7 ± 2.4	18.4 ± 2.2 × 15.9 ± 2.4
Hyphal swellings	**coralloid, catenulate**	**coralloid, catenulate**	**in water, subglobose; rare; only few isolates**	–	in water, subglobose in 1 isolate	–	in water; deltoid in 1 isolate	–
Maximum temperature	**35**	**30–<35**	**>35**	n.a.	35	35	35	35
Optimum temperature	**20**	25	25	n.a.	20	20	**25**	20
Growth rate at optimum	6.1 ± 0.18	6.9 ± 0.62	6.9 ± 0.08	n.a.	6.3 ± 1.26	6.5 ± 1.09	6.7 ± 0.17	5.8
Growth rate at 20°C	5.9 ± 0.5	5.4 ± 0.54	5.9 ± 0.23	n.a.	6.3 ± 1.26	6.5 ± 1.09	6.3 ± 0.19	5.8

[a] Numbers of isolates included in the growth tests: P. ×incrassata – 7; P. ×heterohybrida – 10; P. ×cambivora – 6; P. ×alni – 7; P. uniformis – 6; P. ×multiformis – 4; P. sp. ×multiformis-like – 1; P. ×cambivora – 6; P. fragariae – 2; P. rubi – 6; P. attenuata – 5; P. formosa – 5; P. intricata – 6; P. flexuosa – 3; P. europaea – 4; P. uliginosa – 3.

[b] Data for oogonia, oospores and antheridia are from pairings of the seven A2 isolates of P. ×incrassata with P. cinnamomi A1 isolate TW12.

[c] Data for oogonia, oospores and antheridia are from pairings of the only known A1 isolate of P. sp. ×cambivora-like CBS 111329 with P. ×cambivora A2 isolates SK 9 and CBS 114087.

– = character not observed.
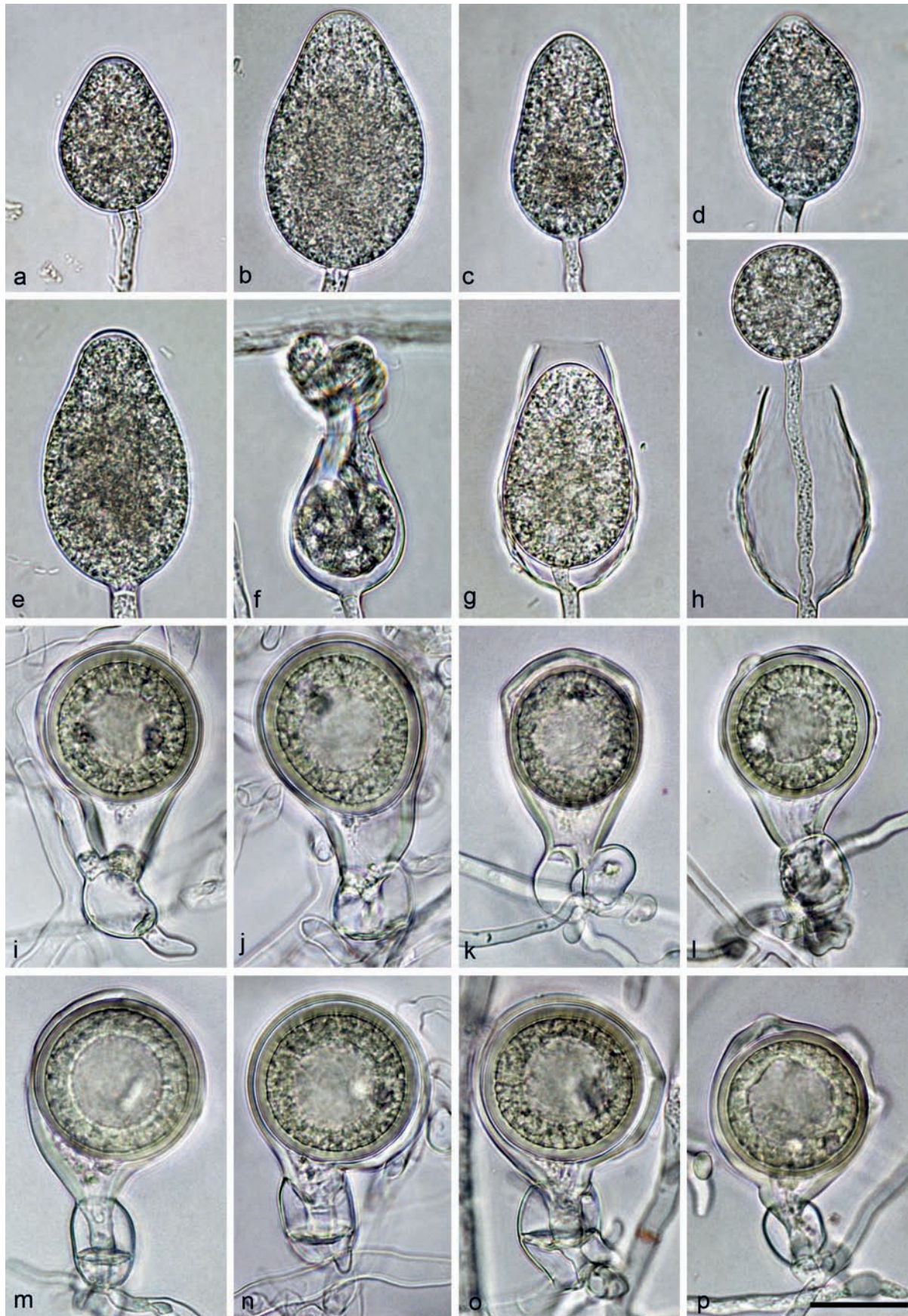
Fig. 3 Morphological structures of *Phytophthora attenuata*. — a–h. Nonpapillate sporangia formed on V8 agar (V8A) flooded with soil extract. a. Ovoid with flat apex; b. elongated ovoid with flat apex; c. obpyriform with external proliferation; d. limoniform with pointed apex; e. elongated ovoid with flat apex; f. ovoid sporangium releasing zoospores; g. empty elongated ovoid sporangium showing internal nested proliferation; h. empty elongated ovoid sporangium showing internal extended proliferation. — i–p. Mature oogonia containing thick-walled oospores with large ooplast, formed in single culture in V8A. i. Globose with long tapering base, binucleate oospore and paragynous antheridium with hyphal projection; j. elongated curved with long tapering base and amphigynous unicellular antheridium; k. elongated flexuose with tapering base and paragynous antheridium; l. globose with ornamented wall, tapering base, binucleate oospore and amphigynous unicellular antheridium; m–n. globose with tapering bases, binucleate oospores and amphigynous bicellular antheridia; o. slightly excentric, flexuose with amphigynous bicellular antheridium; p. globose with ornamented wall, binucleate oospore and amphigynous unicellular antheridium. — Scale bar = 25 μm, applies to a–p.

with a pointed apex (Fig. 3d). Sporangial shapes ranged from ovoid (73.2 %; Fig. 3a, f) to elongated ovoid (6.0 %; Fig. 3b, e), obpyriform (16.9 %; Fig. 3c), limoniform (2.8 %; Fig. 3d) or less frequently ellipsoid and subglobose (1.1 %). Sporangia proliferated internally in a nested (Fig. 3g) or in an extended (Fig. 3h) way or rarely externally. Zoospores of *P. attenuata* were discharged directly through an exit pore 8.4–21.3 µm wide (av. 13.9 ± 2.7 µm) (Fig. 3f). They were limoniform to reniform whilst motile, becoming spherical (av. diam = 12.7 ± 1.6 µm) on encystment. Sporangial dimensions of six isolates of *P. attenuata* averaged 44.7 ± 11.7 × 29.4 ± 5.3 µm (overall range 17.8–78.5 × 13.5–45.9 µm) with a range of isolate means of 34.5–60.3 × 24.7–35.4 µm. The length/breadth ratio averaged 1.50 ± 0.2 with a range of isolate means of 1.37–1.71. Small limoniform swellings were infrequently observed on sporangiophores.

Oogonia, oospores and antheridia (Fig. 3i–p) — Gametangia were readily produced in single culture by all isolates of *P. attenuata* on V8A within 1 wk. Oogonia were borne terminally or laterally, had either smooth (av. 76 %; Fig. 3i–j, m–n), flexuose (av. 5.7 %; Fig. 3k, o) or ornamented (av. 18.3 %; Fig. 3l, p) walls and tapering, often long bases (on av. 77 %; Fig. 3i–m, p). They were globose to subglobose (av. 47 %; Fig. 3i, l–n, p), elongated (on av. 38 %; Fig. 3j–k) or slightly excentric (av. 15 %; Fig. 3o). Oogonial diameters averaged 40.9 ± 4.8 µm (overall range 28.6–55.6 µm and range of isolate means 36.8–45.2 µm). Oospores had a mean diameter of 36.5 ± 3.5 µm (total range 25.9–44.9 µm), were always aplerotic, usually globose or rarely elongated (Fig. 3j) and contained a large ooplast (Fig. 3i–p). The oospores were relatively thick-walled (2.9 ± 0.5 µm), with a mean oospore wall index of 0.41 ± 0.05. Oogonial abortion rate was low (on av. 11.0 %; 2–18 %). The antheridia were paragynous (av. 68.1 %; Fig. 3i, k) or amphigynous (av. 31.9 %; of these 33.7 % 2-celled; Fig. 3j, l–p), averaging 19.0 ± 3.3 × 15.3 ± 2.5 µm, with shapes ranging from subglobose to cylindrical or irregular (Fig. 3i–p).

Colony morphology, growth rates and cardinal temperatures (Fig. 10, 12) — All six *P. attenuata* isolates formed similar colonies on the three different types of media (Fig. 10). Colonies on V8A were faintly striate with limited aerial mycelium, while colonies on MEA and PDA were uniform and woolly. All isolates had identical cardinal temperatures and similar growth rates at all temperatures. The temperature–growth relations on V8A are shown in Fig. 12. The maximum growth temperature was between 30 and 35 °C. All isolates were unable to grow at 35 °C, and isolates did not resume growth when plates incubated for 5 d at 35 °C were transferred to 20 °C. Of the six newly described species, *P. attenuata* showed the slowest growth with an average radial growth rate of 4.3 ± 0.3 mm/d at the optimum temperature of 25 °C.

Additional specimens. TAIWAN, Sheipa National Park, isolated from rhizosphere soil of mature *Chamaecyparis formosensis* trees, *T. Jung*, 2013; CBS 141200 = TW118; TW119; TW423; isolated from rhizosphere soil of mature *C. carlesii* trees, *T. Jung*, 2013; TW128; TW130.

Phytophthora formosa T. Jung, M. Horta Jung, Scanu & Bakonyi, *sp. nov.* — MycoBank MB816568; Fig. 4

Etymology. Name refers to the origin of all known isolates in Taiwan (*formosa* Lat = the beautiful one; previous name of Taiwan).

Typus. TAIWAN, Lenhuachih, isolated from rhizosphere soil of a mature *Araucaria cunninghamii* tree, *T. Jung*, 2013 (CBS H-22551 holotype, dried culture on V8A, Herbarium CBS-KNAW Fungal Biodiversity Centre, CBS 141203 = TW107, ex-type culture). ITS and *cox1* sequences GenBank KU517153 and KU517147, respectively.

Sporangia and hyphal swellings (Fig. 4a–h) — Sporangia of *P. formosa* were not observed on solid agar but were produced abundantly in non-sterile soil extract. Sporangia were borne terminally on unbranched sporangiophores. Sporangia were non-caducous, usually nonpapillate with a flat apex (Fig. 4a–e, g) or less frequently shallow semipapillate (4.3 %). Sporangial shapes ranged from ovoid (76 %; Fig. 4a–b, e–g) to elongated ovoid (4.3 %), ellipsoid (7.7 %; Fig. 4d), obpyriform (6.3 %; Fig. 4c), limoniform (3 %) to subglobose (1 %) or rarely pyriform, obturbinate or funnel-like (1.7 %). Sporangia usually proliferated internally in both a nested (Fig. 4g) and extended way (Fig. 4h). Zoospores were discharged through an exit pore 8.6–24.4 µm wide (av. 13.5 ± 2.7 µm) (Fig. 4f–h). They were limoniform to reniform whilst motile, becoming spherical (av. diam = 14.3 ± 2.5 µm) on encystment. Cysts usually germinated directly by forming a hypha but diplanetism was also observed in all isolates. Sporangial dimensions of nine isolates averaged 49.2 ± 8.1 × 32.6 ± 5.7 µm (overall range 32.7–73.6 × 20.1–50.1 µm) with a wide range of isolate means of 43.7–59.6 × 29.3–40.4 µm. The length/breadth ratio averaged 1.52 ± 0.17 with a range of isolate means of 1.47–1.63. Hyphal swellings were not observed.

Oogonia, oospores and antheridia (Fig. 4i–p) — All six isolates of *P. formosa* produced oogonia in single culture on V8A. Oogonia were borne terminally or laterally and had globose to subglobose (93.3 %; Fig. 4i–n, p) or slightly excentric (6.7 %; Fig. 4o) shapes, often with a tapering base (52.3 %; Fig. 4i–l, n–p). Elongated oogonia were rarer and ornamented oogonial walls were more common in *P. formosa* (1.7 % and 32 %) than in *P. attenuata* (38.1 % and 18.3 %). Oogonial diameters averaged 38.5 ± 3.5 µm (overall range 27.1–50.0 µm and range of isolate means 37.2–40.7 µm). Oospores were plerotic, globose and usually contained a large ooplast (Fig. 4i–m, o). They had a mean diameter of 34.6 ± 3.2 µm (total range 22.4–42.5 µm), thick walls (av. 3.0 ± 0.5 µm, total range 1.6–4.2 µm) and a mean oospore wall index of 0.43 ± 0.06. With 12.7 %, mean oogonial abortion rate was low. Antheridia were formed terminally or laterally (Fig. 4m) and were predominantly paragynous (96.7 %; Fig. 4i–m) or infrequently amphigynous unicellular or bicellular (3.3 %; Fig. 4n–p), averaging 15.2 ± 2.9 × 11.8 ± 1.9 µm, with shapes ranging from clavate, subglobose to cylindrical.

Colony morphology, growth rates and cardinal temperatures (Fig. 10, 12) — Colonies on V8A and PDA uniform and woolly, on MEA faintly dendroid with small-lobed margins (Fig. 10). Temperature-growth relations are shown in Fig. 12. All four isolates included in the growth test had similar growth rates. The maximum growth temperature was 30–35 °C. All isolates resumed growth when plates incubated for 5 d at 35 °C were transferred to 20 °C. The average radial growth rate at the optimum temperature of 25 °C was 5.1 ± 0.2 mm/d.

Additional specimens. TAIWAN, Lenhuachih, isolated from rhizosphere soil of mature *A. cunninghamii* trees, *T. Jung*, 2013; TW105; TW106; TW109; Fushan, isolated from rhizosphere soil of planted *Quercus glandulifera* trees. *T. Jung*, 2013; CBS 141204 = TW14; TW13; Fushan, baiting from a tributary of Hapen river, *T. Jung*, 2013; TW110.

Phytophthora intricata T. Jung, M. Horta Jung, Scanu & Bakonyi, *sp. nov.* — MycoBank MB816569; Fig. 5

Etymology. Name refers to the intricate, intertwining oogonial and antheridial stalks (*intricata* Lat = intricate or intertwining).

Typus. TAIWAN, Fushan, isolated from rhizosphere soil of a planted *Quercus tarokoensis* tree, *T. Jung*, 2013 (CBS H-22553 holotype, dried culture on V8A, Herbarium CBS-KNAW Fungal Biodiversity Centre, CBS 141211 = TW259, ex-type culture). ITS and *cox1* sequences GenBank KU517155 and KU517149, respectively.

Sporangia and hyphal swellings (Fig. 5a–h) — Sporangia of *P. intricata* were not formed on solid agar but were produced abundantly in non-sterile soil extract. Sporangia were non-caducous and nonpapillate with a flat apex (Fig. 5a–f). Sporangial shapes ranged from ovoid (51.9 %; Fig. 5a), elongated ovoid (14.2 %; Fig. 5b–c), obpyriform (23 %; Fig. 5d), limoniform (4.9 %), ellipsoid (3.8 %) to less frequently pyriform, subglobose,
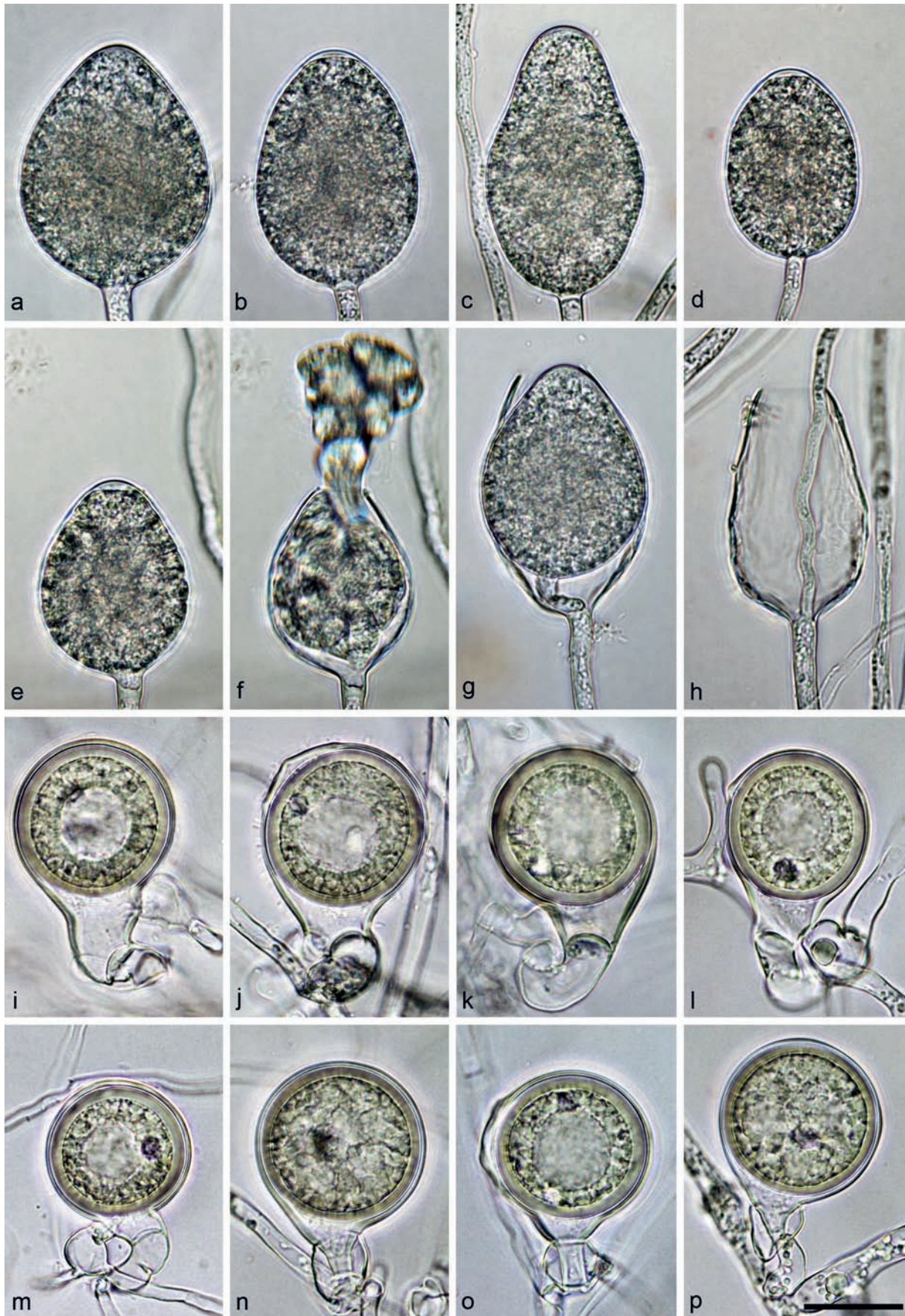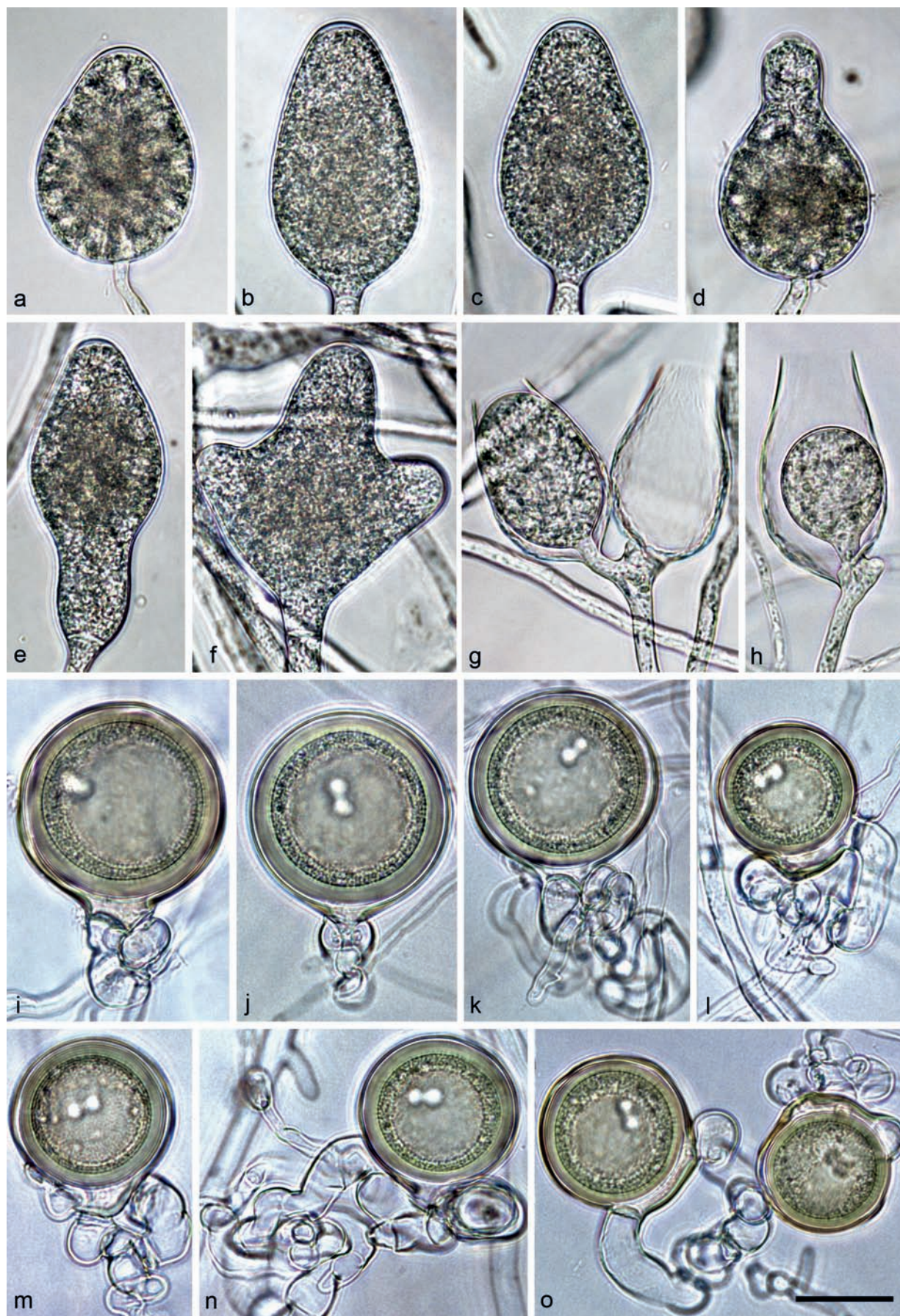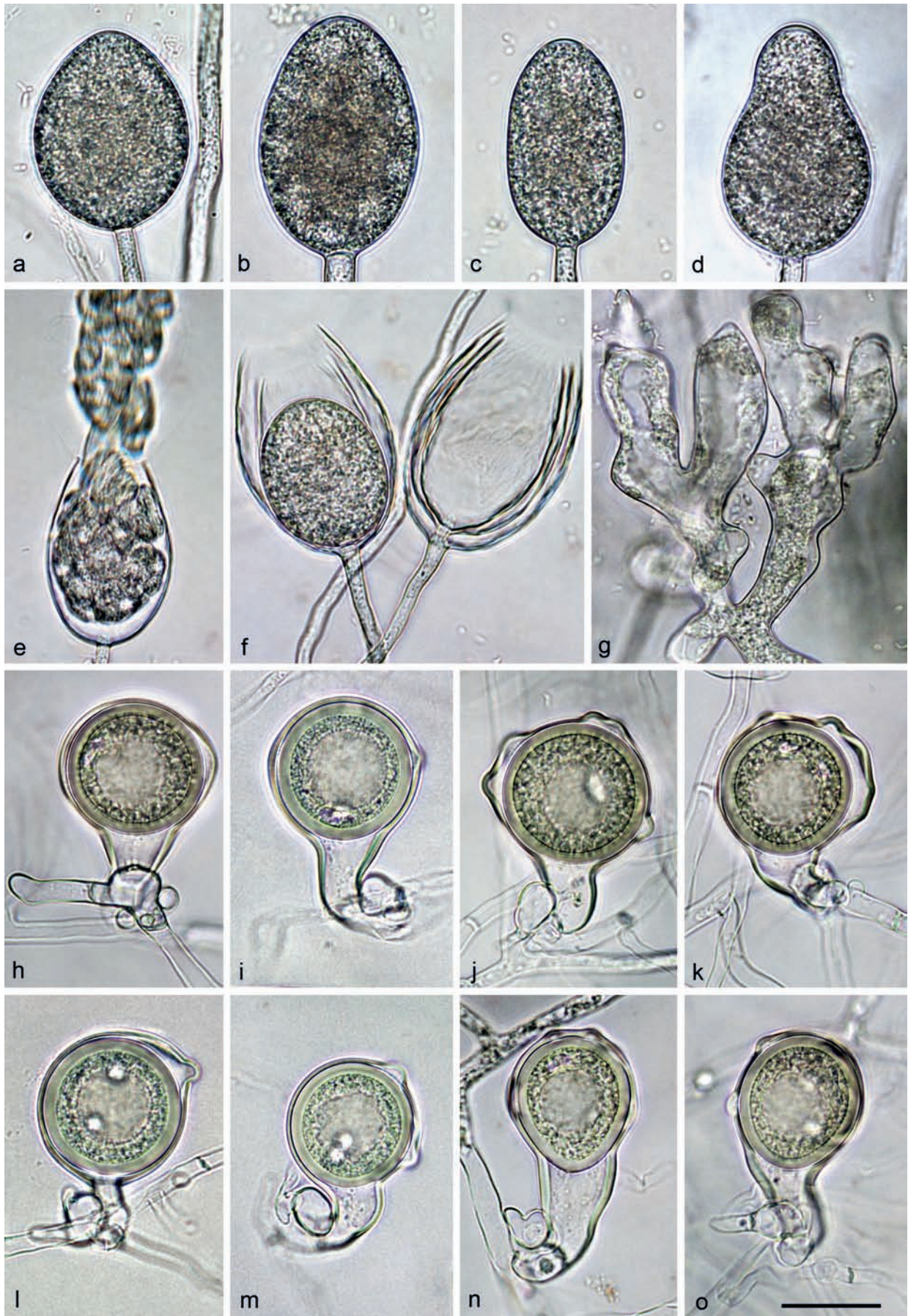
Fig. 4 Morphological structures of *Phytophthora formosa*. — a–h. Sporangia formed on V8 agar (V8A) flooded with soil extract. a. Nonpapillate, ovoid with pointed apex; b. semipapillate, ovoid with flat apex; c. nonpapillate obpyriform; d–e. semipapillate ellipsoid (d) and ovoid (e) with flat apex; f. same sporangium as in (e) releasing zoospores; g. empty elongated ovoid sporangium showing internal nested proliferation; h. empty elongated ovoid sporangium showing internal extended proliferation. — i–p. mature oogonia containing thick-walled plerotic oospores, formed in single culture in V8A. i. Globose with long tapering base, binucleate oospore and paragynous antheridium; j. subglobose, slightly ornamented with tapering base, binucleate oospore and paragynous antheridium; k. subglobose with tapering base, curved stalk and paragynous antheridium; l. subglobose with tapering base and paragynous antheridium; m. globose with paragynous antheridium; n. globose with tapering base and amphigynous bicellular antheridium; o. excentric, slightly ornamented with tapering base and amphigynous unicellular antheridium; p. subglobose with tapering base and amphigynous unicellular antheridium. — Scale bar = 25 μm, applies to a–p.

Fig. 5 Morphological structures of *Phytophthora intricata*. — a–h. Sporangia formed on V8 agar (V8A) flooded with soil extract. a–f. Nonpapillate with flat apex: a. ovoid; b–c. elongated ovoid; d. obpyriform; e. ampulliform; f. trilobed; g. sympodial branching of sporangiophore in a dichasium, with mother hypha ending in a short protuberance, and empty elongated ovoid sporangia, the left one showing internal nested proliferation; h. empty elongated ovoid sporangium showing internal extended proliferation and sympodial branching of sporangiophore in a monochasium with mother hypha ending in a short protuberance. — i–o. Mature smooth-walled oogonia formed in single culture in V8A, containing thick-walled plerotic, binucleate oospores with big ooplasts, with paragynous antheridia. i–k and m–n. Globose; l, o. slightly excentric with a widened base between the oogonial stalk and the point of antheridial attachment; k–o. twisted intertwining oogonial and antheridial stalks. — Scale bar = 25 µm, applies to a–o.

Fig. 6 Morphological structures of *Phytophthora flexuosa*. — a–f. Sporangia formed on V8 agar (V8A) flooded with soil extract. a–d. Nonpapillate with flat apex: a–b. ovoid; c. ellipsoid; d. obpyriform; e. elongated ovoid sporangium releasing zoospores; f. empty, elongated ovoid sporangia showing internal nested proliferation. — g. Swollen coralloid hyphae in V8A. — h–o. Mature oogonia formed in single culture in V8A, with thick-walled plerotic oospores and paragynous antheridia, with finger-like projections (h, l, n–o); h. slightly excentric with long, tapering funnel-like base; i. globose, slightly ornamented, with long, curved funnel-like base and binucleate oospore; j–k. flexuose ornamented, with tapering curved base; l. flexuose, slightly ornamented, non-tapering with thin base and binucleate oospore; m. ornamented, with tapering curved base and binucleate oospore; n. elongated, ornamented with long tapering base and elongated oospore; o. ornamented, with tapering curved base and binucleate oospore. — Scale bar = 25 µm, applies to a–o.

ampulliform, bilobed or trilobed (2.2 %; Fig. 5e–f). Mean sporangial dimensions of six isolates were 54.4 ± 8.0 × 34.2 ± 4.4 µm (overall range 39.0–78.9 × 24.1–48.8 µm) with a range of isolate means of 51.0–58.9 × 32.1–37.5 µm. The length/breadth ratio averaged 1.60 ± 0.23 with a range of isolate means of 1.44–1.76. Sporangia were borne terminally on unbranched sporangiophores or in lax sympodia. Sporangia proliferated internally in both a nested (Fig. 5g–h) and extended way. In addition, sporangiophores often branched in a monochasium or dichasium (Fig. 5g–h). Zoospores of *P. intricata* were discharged through an exit pore 11–22.5 µm wide (15.4 ± 2.3 µm). They were limoniform to reniform whilst motile, becoming spherical (av. diam = 13.4 ± 1.9 µm) on encystment. Cysts usually germinated directly but diplanetism was also observed in all isolates. Subglobose, angular or limoniform swellings on sporangiophores with an average diameter of 16.0 ± 2.3 µm were infrequently formed by most isolates.

Oogonia, oospores and antheridia (Fig. 5i–o) — All six isolates of *P. intricata* produced gametangia readily on V8A in single culture. Oogonia were borne terminally or laterally, had smooth walls and usually non-tapering bases (Fig. 5i–l, o). Oogonia were globose to subglobose (on av. 90.6 %; Fig. 5i–k, m–n) or slightly excentric with a widened base between the oogonial stalk and the point of antheridial attachment (av. 9.4 %; Fig. 5l, o). Oogonial diameters averaged 43.5 ± 5.1 µm with an overall range of 26.3–56.7 µm and isolate means ranging from 41.5–46.0 µm. Oospores had a mean diameter of 39.9 ± 4.6 µm (total range 25.1–50.3 µm), were always plerotic and contained two nuclei and a large ooplast (Fig. 5i–o). The oospores were thick-walled (3.6 ± 0.6 µm), with a mean oospore wall index of 0.45 ± 0.05. Oogonial abortion rate was low (av. 8.1 %; 4–16 %). Oogonial and antheridial stalks were often twisted and intertwining (44.7 %; Fig. 5k–o). The antheridia were exclusively paragynous, averaging 14.4 ± 2.5 × 11.4 ± 1.8 µm, with shapes ranging from subglobose to cylindrical (Fig. 5i–o).

Colony morphology, growth rates and cardinal temperatures (Fig. 10, 12) — All *P. intricata* isolates formed uniform woolly colonies on V8A, faintly stellate colonies with sparse aerial mycelium on MEA and rosacous colonies with limited aerial mycelium in the centre and submerged margins on PDA (Fig. 10). The temperature–growth relations on V8A are shown in Fig. 12. All isolates had similar growth rates at all temperatures. Minimum and maximum growth temperatures were below 5 °C and between 30 and 35 °C, respectively. All isolates resumed growth when plates incubated for 5 d at 35 °C were transferred to 20 °C. The average radial growth rate at the optimum temperature of 25 °C was 5.5 ± 0.3 mm/d.

Additional specimens. Taiwan, Fushan, isolated from rhizosphere soil of planted *Quercus tarokoensis* trees, *T. Jung*, 2013; CBS 141210 = TW7; TW16; TW257; TW258; TW263.

Phytophthora flexuosa T. Jung, M. Horta Jung, Scanu & Bakonyi, *sp. nov.* — MycoBank MB816571; Fig. 6

Etymology. Name refers to the flexuose oogonial walls (*flexuosa* Lat = flexuose, bulged).

Typus. Taiwan, Taiping Mountain, isolated from rhizosphere soil of a mature *Fagus hayatae* tree, *T. Jung*, 2013 (CBS H-22550 holotype, dried culture on V8A, Herbarium CBS-KNAW Fungal Biodiversity Centre, CBS 141201 = TW78, ex-type culture). ITS and *cox1* sequences GenBank KU517152 and KU517146, respectively.

Sporangia, hyphal swellings and chlamydospores (Fig. 6a–g) — Sporangia of *P. flexuosa* were not observed on solid agar but were produced abundantly in non-sterile soil extract. Sporangia were borne terminally on unbranched sporangiophores and proliferated internally in both a nested (Fig. 6f) and extended way. Due to the lack of external proliferation no sympodia were formed. Sporangia were non-caducous and nonpapillate (Fig. 6a–d). Sporangial shapes ranged from ovoid and elongated ovoid (80.4 %; Fig. 6a–b, e–f), ellipsoid (8.8 %; Fig. 6c) to obpyriform (6.9 %; Fig. 6d) and limoniform (3.9 %). Sporangial dimensions of *P. flexuosa* averaged 56.1 ± 7.4 × 36.7 ± 5.2 µm (overall range 34.9–74.8 × 22.8–49.7 µm) with rather similar isolate means (53.3–58.6 × 33.9–39.4 µm). The length/breadth ratio of the sporangia averaged 1.54 ± 0.18 with a range of isolate means of 1.49–1.60. Zoospores were discharged through a wide exit pore (av. 19.7 ± 3.4 µm; total range 10.1–25.0 µm; Fig. 6e–f). They were limoniform to reniform whilst motile, becoming spherical (av. diam = 13.3 ± 1.3 µm) on encystment. Cysts germinated either directly or indirectly by releasing a secondary zoospore (diplanetism). In both liquid culture and solid agar inflated, tubular to coralloid hyphal swellings were regularly formed (Fig. 6g).

Oogonia, oospores and antheridia (Fig. 6h–o) — The three isolates of *P. flexuosa* produced oogonia in single culture on V8A within 5 d. Oogonia were borne terminally or laterally and had globose to subglobose (32.4 %; Fig. 6h–i), flexuose (25 %; Fig. 6j–m) or elongated (42.6 %; Fig. 6n, o) shapes, often with long tapering to funnel-like (47.9 %; Fig. 6h–k, m–o) and curved bases (51.5 %; Fig. 6i, k, m). Oogonial walls were ornamented (65.6 %; Fig. 6i–o) or less frequently smooth (34.4 %; Fig. 6h). Oogonial diameters averaged 36.8 ± 3.3 µm (overall range 25.7–42.8 µm and range of isolate means 36.0–38.3 µm). Oospores were plerotic, globose or elongated and contained a large ooplast (Fig. 6h–o) and often two nuclei (70.6 %; Fig. 6i, l–m, o). They had a mean diameter of 32.2 ± 2.7 µm (total range 22.7–37.7 µm), thick walls (av. 3.1 ± 0.5 µm, total range 1.7–4.4 µm) and a mean oospore wall index of 0.47 ± 0.06. Mean oogonial abortion rate was very low (1.7 %). Antheridia were formed terminally or laterally (Fig. 6m) and were exclusively paragynous (Fig. 6h–o), averaging 13.4 ± 2.1 × 10.0 ± 1.7 µm, with shapes ranging from clavate, subglobose to cylindrical, often with finger-like hyphal projections (23.7 %).

Colony morphology, growth rates and cardinal temperatures (Fig. 10, 12) — All three *P. flexuosa* isolates examined formed uniform colonies, largely submerged with sparse to limited aerial mycelium on V8A and MEA, and domeshaped woolly on PDA (Fig. 10). On V8A, all isolates had similar growth rates at all temperatures. Minimum temperature was below 5 °C. All isolates showed slow growth at 35 °C (Fig. 12). The average radial growth rate at the optimum temperature of 25 °C was 4.7 ± 0.6 mm/d.

Additional specimens. Taiwan, Taiping Mountain, isolated from rhizosphere soil of mature *Fagus hayatae* trees, *T. Jung*, 2013; CBS 141202 = TW108; TW79.

Phytophthora ×heterohybrida T. Jung, M. Horta Jung, Scanu & Bakonyi, *sp. nov.* — MycoBank MB816572; Fig. 7

Etymology. Name refers to the heterothallic breeding system and the hybrid origin.

Typus. Taiwan, Fushan, isolated from a tributary of Hapen River, *T. Jung*, 2013 (CBS H-22549 holotype, dried culture on V8A, Herbarium CBS-KNAW Fungal Biodiversity Centre, CBS 141207 = TW30, ex-type culture). ITS and *cox1* sequences GenBank KU517151 and KU517145, respectively.

Sporangia and hyphal swellings (Fig. 7a–i) — Sporangia of *P. ×heterohybrida* were not produced on solid agar but formed abundantly in non-sterile soil extract. Sporangia were borne terminally on unbranched sporangiophores or in lax sympodia after external proliferation. All 15 isolates examined showed abundant internal proliferation both in a nested (Fig. 7h) and extended way and also formed secondary lateral sporangia. Sporangia were usually non-caducous (Fig. 7a–d, g–h) but a low proportion (< 1 %) of caducous sporangia without preformed
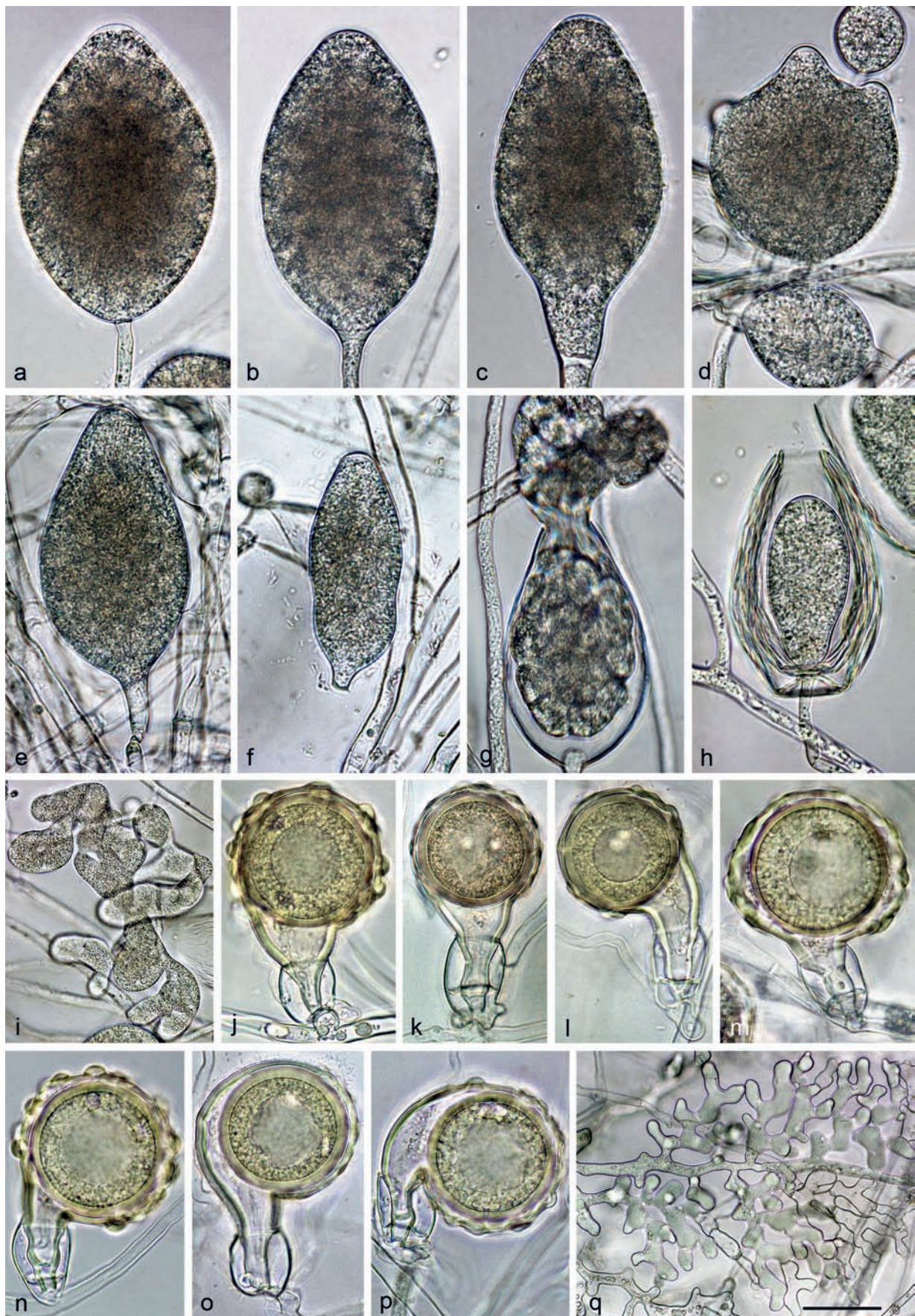
Fig. 7 Morphological structures of *Phytophthora* x*heterohybrida*. — a–f. Sporangia with flat apex formed on V8 agar (V8A) flooded with soil extract. a. Semi-papillate ovoid; b. nonpapillate, elongated ovoid; c. nonpapillate, elongated limoniform with tapering base; d. semipapillate with three apices; e. nonpapillate obpyriform, shedding from the sporangiophore; f. nonpapillate ampulliform, caducous; g. elongated ovoid, releasing zoospores; h. empty, elongated ovoid sporangium with internal nested proliferation; i. freshly released clump of multiple zoospores unable to separate completely. — j–p. Mature, ornamented golden-brown oogonia with long, tapering, often funnel-like bases, containing thick-walled, globose and binucleate oospores with large ooplasts, formed in intraspecific pairings between A1 and A2 isolates in V8A. j, o. Amphigynous unicellular antheridia; k–n, p. amphigynous bicellular antheridia; l. comma-shaped oogonium; m. excentric oogonium with thick, highly ornamented wall; n–p. comma-shaped oogonia; q. coralloid hyphae in V8A. — Scale bar = 25 μm for all except (q) where scale bar = 40 μm.

pedicels (Fig. 7e–f) were observed in most isolates. Sporangia were nonpapillate with a flat apex (Fig. 7b–c, e–f) or less frequently shallow semipapillate, sometimes with two or three apices (Fig. 7a, d). Sporangial shapes ranged from ovoid and elongated ovoid (62.8 %; Fig. 7a–b, g–h), limoniform (18.1 %; Fig. 7c), obpyriform (12.9 %; Fig. 7e) to ellipsoid (3.5 %) and, less frequently, pyriform, ampulliform, subglobose and obturbinate (2.5 %; Fig. 7d, f). Features such as a tapering base (Fig. 7c), a widening of the sporangiophore towards the sporangial base, lateral attachment of the sporangiophore and a curved or laterally displaced apex occurred infrequently. Sporangia of *P.* x*heterohybrida* were large averaging 75.3 ± 13.2 × 45.7 ± 7.6 µm with an overall range of 29.7–123.8 × 21.4–77.3 µm and isolate means of 64.0–82.8 × 38.9–50.1 µm. The length/breadth ratio of the sporangia averaged 1.66 ± 0.23 with a range of isolate means of 1.53–1.81. Zoospores were discharged through an exit pore 9.8–25.6 µm wide (av. 16.0 ± 2.6 µm) (Fig. 7g–h). They were limoniform to reniform whilst motile, becoming spherical (av. diam = 13.4 ± 1.4 µm) on encystment. Cysts germinated directly or indirectly (diplanetism). In all isolates a low proportion of sporangia released zoospores which were not able to separate completely resulting in the formation of bizarre, multinucleate and multiflagellate motile structures (Fig. 7i). In liquid culture, angular, subglobose or irregular-elongated hyphal swellings were infrequently formed on sporangiophores averaging 17.1 ± 4.4 µm. In solid agar, all isolates produced irregular coralloid hyphal swellings (Fig. 7q).

Oogonia, oospores and antheridia (Fig. 7j–p) — All 21 isolates of *P.* x*heterohybrida* tested were self-sterile. Mating tests with A1 and A2 tester strains of *P.* x*cambivora* and *P. cinnamomi* revealed that each 10 of the 21 isolates belonged to the A1 and A2 mating type, respectively, while one isolate, TW29, formed gametangia in pairings with both mating types (= A1/A2). In a second intraspecific mating test six A1 isolates of *P.* x*heterohybrida* were paired with the two A2 isolates TW28 and TW57, and five A2 isolates of *P.* x*heterohybrida* were paired with the two A1 isolates TW35 and TW47. The A1/A2 isolate TW29 was paired with all four tester strains. Oogonia were mostly elongated with long tapering, often funnel-like bases (89.1 %; Fig. 7j–l, n–p) or less frequently subglobose to excentric (10.9 %; Fig. 7m). Special features like curved stalks (5.0 %), comma-like bending (13.3 %; Fig. 7l, n–p) and thick oogonial walls (28.7 %; Fig. 7j, l–o) were common. Oogonial walls were usually ornamented (97.9 %) and turned golden-brown within 4 wk (Fig. 7j–p). Oogonial diameters averaged 44.1 ± 6.7 µm with a total range of 25.2–61.2 µm and isolate means of 37.7–50.4 µm. Most oogonia looked viable (mean abortion rate = 17.3 %), containing oospores with a large ooplast and often two nuclei (58.5 %; Fig. 7j–p). Oospores were usually plerotic (97.2 %; Fig. 7j–p) and averaged 36.8 ± 5.4 µm in diameter with thick oospore walls (av. diam 3.1 ± 0.6 µm) and a mean oospore wall index of 0.43 ± 0.07. The antheridia were exclusively amphigynous (Fig. 7j–p), 49.6 % of them bicellular, and measured 23.2 ± 4.3 × 18.0 ± 2.1 µm.

Colony morphology, growth rates and cardinal temperatures (Fig. 11, 12) — All nine isolates of *P.* x*heterohybrida* tested formed woolly colonies on all three agar media, faintly stellate on V8A, uniform on MEA and faintly petaloid with irregular margins on PDA (Fig. 11). On V8A all isolates had similar growth rates at all temperatures. Minimum and maximum growth temperatures were below 5 °C and between 30 and 35 °C, respectively. All isolates failed to resume growth when plates incubated for 5 d at 35 °C were transferred to 20 °C. *Phytophthora* x*heterohybrida* had a clear optimum of growth at 25 °C with an average radial growth rate of 6.9 ± 0.6 mm/d (Fig. 12).

Additional specimens. Taiwan, Fushan, isolated from a tributary of Hapen River, *T. Jung*, 2013; CBS 141205 = TW38; TW28; TW29; TW31; TW32; TW33; TW34; TW35; TW39; TW40; isolated from Hapen River, *T. Jung*, 2013; CBS 141206 = TW46; TW48; TW49; TW50; isolated from Cukeng River, *T. Jung*, 2013; TW51; TW56; TW57; TW59; TW60; TW61.

Phytophthora x*incrassata* T. Jung, M. Horta Jung, Scanu & Bakonyi, *sp. nov.* — MycoBank MB816573; Fig. 8

Etymology. Name refers to the thickened oogonial walls (*incrassata* Lat = thickened, dilated).

Typus. Taiwan, Fushan, isolated from a tributary of Hapen River, *T. Jung*, 2013 (CBS H-22554 holotype, dried culture on V8A, Herbarium CBS-KNAW Fungal Biodiversity Centre, CBS 141209 = TW269, ex-type culture). ITS and *cox1* sequences GenBank KU517156 and KU517150, respectively.

Sporangia, hyphal swellings and chlamydospores (Fig. 8a–j) — Sporangia of *P.* x*incrassata* were not observed on solid agar but were produced abundantly in non-sterile soil extract. Sporangia were borne terminally on unbranched sporangiophores, often in chains of internally proliferating sporangia in both a nested and extended way (Fig. 8i–j) or in lax sympodia after external proliferation. Sporangia were non-caducous with a flat apex (Fig. 8a–g), nonpapillate (Fig. 8a, f) or shallow semipapillate (Fig. 8b–e). Sporangial shapes were predominantly ovoid and elongated ovoid (85.2 %; Fig. 8a–c, g) and less frequently limoniform (6.4 %), ellipsoid (6.1 %; Fig. 8d–e) or pyriform (1.6 %; Fig. 8f), obovoid or subglobose (0.7 %). Sporangial dimensions of seven isolates of *P.* x*incrassata* averaged 61.2 ± 8.5 × 43.7 ± 5.6 µm with an overall range of 36.9–88.2 × 28.5–56.6 µm and isolate means of 56.6–66.5 × 40.0–47.3 µm. The length/breadth ratio of the sporangia averaged 1.40 ± 0.13 with a range of isolate means of 1.38–1.43. Zoospores were discharged through an exit pore 11.6–18.5 µm wide (av. 15.0 ± 2.7 µm) (Fig. 8h). They were limoniform to reniform whilst motile, becoming spherical (av. diam = 14.4 ± 1.3 µm) on encystment. Cysts usually germinated directly but diplanetism was observed in all isolates. In liquid culture subglobose to limoniform swellings were infrequently formed on sporangiophores (10.8–27.4 µm). In solid agar irregular coralloid hyphal swellings were abundantly formed (Fig. 8s).

Oogonia, oospores and antheridia (Fig. 8k–r) — All seven isolates of *P.* x*incrassata* were self-sterile and produced gametangia when paired with A1 strains of *P.* x*cambivora*, *P. cinnamomi* and *P.* x*heterohybrida*. In pairings with the *P.* x*heterohybrida* A1 isolate TW47, 98.7 % of oogonia had ornamented walls. Since *P. cinnamomi* exclusively produces smooth- and thin-walled oogonia all oogonia with ornamented walls and all smooth thick-walled oogonia produced in pairings between *P.* x*incrassata* isolates and the *P. cinnamomi* A1 isolate TW12 were attributed to *P.* x*incrassata*. Oogonia of *P.* x*incrassata* were globose to subglobose, usually with thick walls (77.9 %; av. 2.1 ± 0.5 µm; Fig. 8k–p), often with tapering short bases (39.7 %; Fig. 8k–l, p–r) and infrequently comma-shaped (7.6 %; Fig. 8n–o, r). Oogonial walls were almost exclusively ornamented (98.1 %), in most cases with only a few conspicuous, globose to subglobose warts (Fig. 8k–o). Diameters averaged 45.2 ± 6.6 µm with a total range of 31.8–63.6 and a range of isolate means of 41.4–49.1 µm. A relatively high proportion of oogonia aborted (47.4 %) either before or after forming an oospore wall (Fig. 8q–r). Oospores were plerotic and averaged 37.7 ± 4.7 in diameter with relatively thick oospore walls (3.1 ± 0.6 µm; 1.5–4.6 µm) and an oospore wall index of 0.41 ± 0.06. The antheridia were exclusively amphigynous (Fig. 8k–r), 52.4 % of them 2-celled, and measured 20.2 ± 3.4 × 16.4 ± 2.0 µm.

Colony morphology, growth rates and cardinal temperatures (Fig. 11, 12) — All seven isolates of *P.* x*incrassata* formed faintly striate woolly colonies on V8A, and uniform to faintly petaloid, woolly colonies MEA and PDA (Fig. 11). On V8A all isolates had similar growth rates at all temperatures. Minimum and
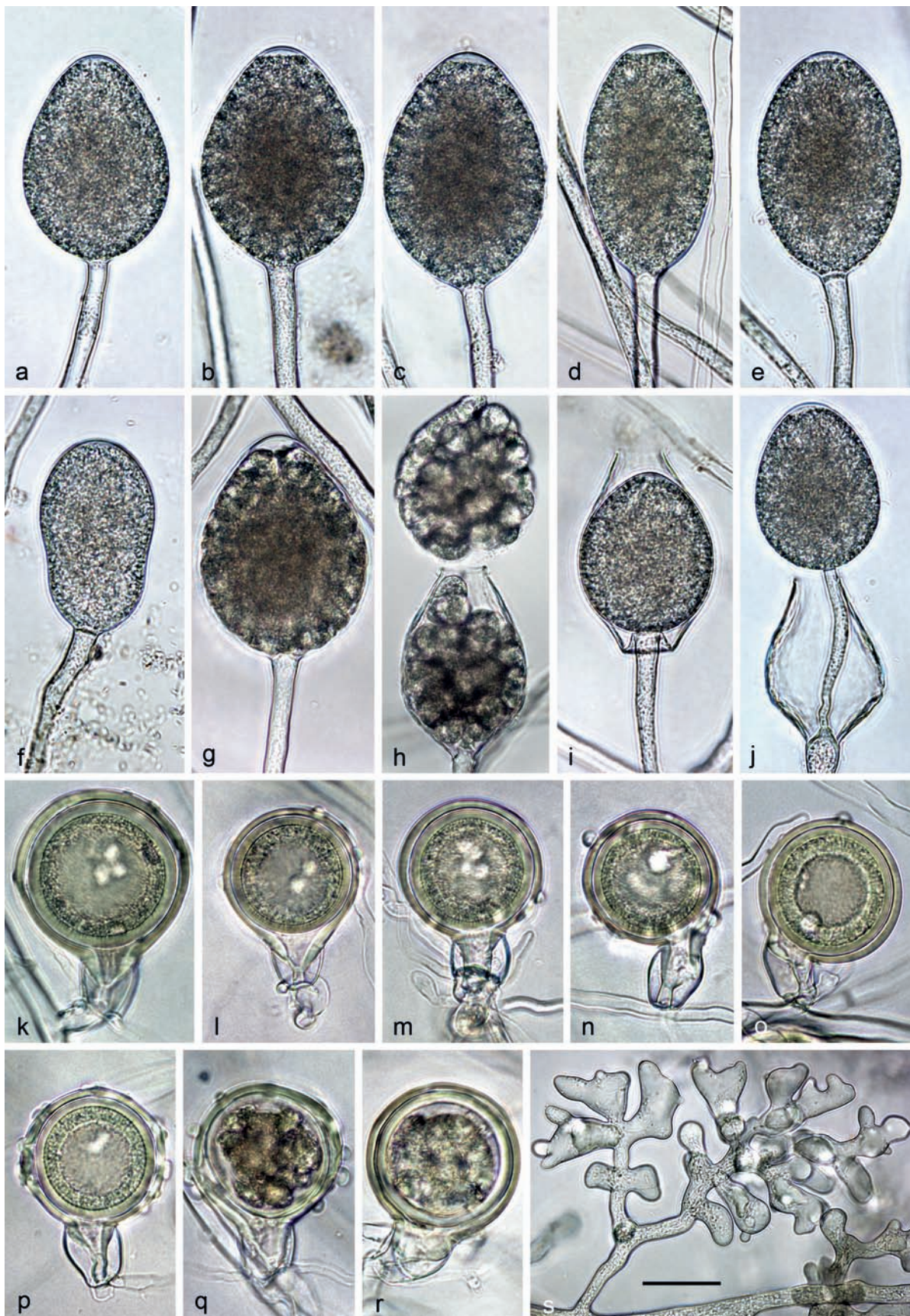
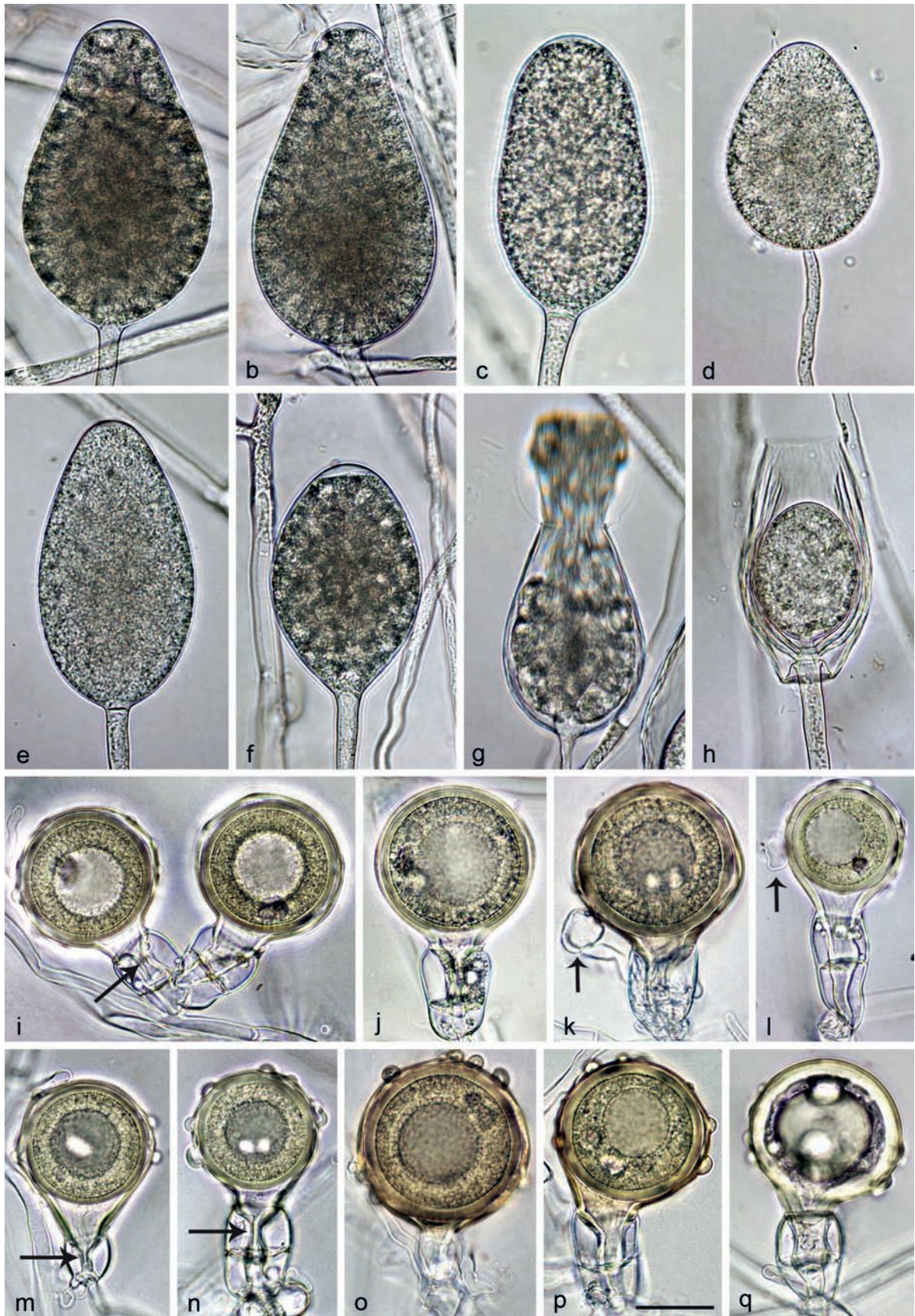**Fig. 8** Morphological structures of *Phytophthora* ×*incrassata*. — a–j. Sporangia with flat apex formed on V8 agar (V8A) flooded with soil extract. a. Nonpapillate ovoid; b–c. semipapillate ovoid; d–e. semipapillate ellipsoid; f. nonpapillate pyriform; g. ovoid, shortly before release of already differentiated zoospores; h. limoniform, releasing zoospores; i. empty elongated ovoid sporangium with internal nested proliferation; j. empty limoniform sporangium with internal extended proliferation. — k–p. Mature thick-walled oogonia containing thick-walled plerotic oospores with large ooplasts, formed in pairings with *P. cinnamomi* A1 isolate TW12 in V8A. k–o. Oogonial walls slightly ornamented with individual, globose protuberances; k–l. globose with short tapering base, multinucleate oospore and amphigynous unicellular antheridium; m. globose with multinucleate oospore and amphigynous bicellular antheridium; n. globose, comma-shaped with tapering base, binucleate oospore and amphigynous unicellular antheridium; o. globose, comma-shaped with amphigynous unicellular antheridium; p. globose with short tapering base, excessively ornamented oogonial wall, binucleate oospore and amphigynous unicellular antheridium; q. aborted, globose ornamented oogonium with short tapering base and amphigynous unicellular antheridium; r. aborted, comma-shaped smooth-walled oogonium with short tapering base and amphigynous bicellular antheridium; s. coralloid hyphae in V8A. — Scale bar = 25 μm, applies to a–s.

Fig. 9 Morphological structures of *Phytophthora* x*cambivora*. — a–f. Nonpapillate sporangia with flat apex formed on V8 agar (V8A) flooded with soil extract. a. Shallow semipapillate, elongated ovoid; b. shallow semipapillate, obpyriform; c. nonpapillate, ellipsoid; d. nonpapillate ovoid; e. nonpapillate, elongated ovoid; f. semipapillate, ellipsoid, before releasing zoospores; g. ovoid, releasing zoospores; h. empty, elongated ovoid sporangium with internal nested proliferation. — i–p. Mature, golden-brown oogonia with tapering bases, containing thick-walled globose oospores with large ooplasts, formed in intraspecific pairings between A1 and A2 isolates in V8A. i–j, l, n, p. Amphigynous bicellular antheridia; k, m, o. amphigynous unicellular antheridia; i. ornamented (on the left) and smooth-walled (on the right); oogonial base with conspicuous constriction (arrow); j. smooth-walled, with binucleate oospore; k. slightly ornamented wall; binucleate oospore and additional paragynous antheridium (arrow); l. slightly ornamented, thick oogonial wall, additional paragynous antheridium (arrow), long funnel-like base; m. slightly ornamented wall, funnel-like base with conspicuous constriction (arrow); n. ornamented oogonium with binucleate oospore; oogonial base with conspicuous constriction (arrow); o. ornamented oogonium with binucleate oospore; p. ornamented, slightly comma-shaped with binucleate oospore; q. ornamented, slightly comma-shaped, aborted oogonium. — Scale bar = 25 µm, applies to a–q.

maximum growth temperatures were below 5 °C and 35 °C, respectively. *Phytophthora* x*incrassata* had a broad optimum of growth with average radial growth rates of 6.1 ± 0.2 mm/d and 5.9 ± 0.5 mm/d at 20 °C and 25 °C, respectively (Fig. 12).

Additional specimens. TAIWAN, Fushan, isolated from a tributary of Hapen River, *T. Jung*, 2013; CBS 141208 = TW283; TW43; TW299; TW344; TW347; TW350.

The presence of numerous heterozygous positions in the ITS, *HSP90* and ß-tubulin sequences (Table 2−4) and nuclear genome sizes (Fig. 2) obtained in this study, and analyses of cloned *HSP90* and ß-tubulin sequences (J. Bakonyi, D. Seress, K. van Poucke, K. Heungens & T. Jung unpubl. results) demonstrated that all 23 isolates of *P. cambivora* examined from North and South America, Europe, Asia and Australia are allopolyploid interspecific hybrids. Consequently, *P. cambivora* is re-described below as *P.* x*cambivora* without nomenclatural act. Since the extype isolate of *P. cambivora* is lost and no isotypes are known a neotype of *P.* x*cambivora* is designated here.

Phytophthora x*cambivora* (Petri) Buisman, *pro sp.*, Meded. Phytopathol. Lab. "Willie Commelin Scholten" 11: 4, 7. 1927 — Fig. 9

Basionym. Blepharospora cambivora Petri, Atti Reale Accad. Naz. Lincei, Rendiconti Cl. Sci. Fis., ser. 5, 26: 298. 1917.

Etymology. Name refers to the ability of the species to infect and kill the cambium of woody plant species (*cambi-* and -*vora* Lat = cambium eating).

Neotypus. ITALY, Sicily, Mount Etna, isolated from a declining mature *Quercus pubescens* tree, *T. Jung*, 2013 (CBS H-22558 neotype designated here, MBT 371963, dried culture on V8A, Herbarium CBS-KNAW Fungal Biodiversity Centre), CBS 141218 = IT 5-3, ex-neotype culture). ITS and *cox1* sequences GenBank KU899179 and KU899334, respectively.

Sporangia, hyphal swellings and chlamydospores (Fig. 9a−h) — In all 23 isolates of *P.* x*cambivora* sporangia were not observed on solid agar but were produced abundantly in non-sterile soil extract. Sporangia were usually borne terminally on unbranched sporangiophores, often in chains of internally proliferating sporangia in both a nested (Fig. 9h) and extended way. External proliferation was only rarely observed. The formation of secondary lateral sporangia was common in most isolates. Sporangia were non-caducous, usually nonpapillate with a flat apex (Fig. 9d−e) often becoming semipapillate during maturation (Fig. 9a−b, f). Sporangia were ovoid and elongated ovoid (72.3 %; Fig. 9a, d−e, g), obpyriform (11.9 %; Fig. 9b), ellipsoid (8.1 %; Fig. 9c, f), limoniform (7.1 %) or pyriform, peanut-like or cylindrical (0.6 %). Widening of sporangiophores towards the sporangial base or sporangia with tapering bases or laterally displaced or slightly curved apices were observed in all isolates examined. Sporangial dimensions averaged 68.3 ± 12.4 × 42.6 ± 7.0 µm with an overall range of 35.1–120.9 × 22.7–62.9 µm and variable isolate means of 48.2–84.3 × 30.3–49 µm. The length/breadth ratio of the sporangia averaged 1.61 ± 0.19 with a range of isolate means of 1.33–1.82. Zoospores were discharged through an exit pore 9.2–26.8 µm wide (av. 17.1 ± 3.5 µm) (Fig. 9g−h). They were limoniform to reniform whilst motile, becoming spherical (av. diam = 13.7 ± 1.8 µm) on encystment. Cysts germinated both directly and indirectly (diplanetism). In liquid culture small (12.6 ± 2.1 µm), subglobose to globose hyphal swellings were rarely formed by some isolates.

Oogonia, oospores and antheridia (Fig. 9i−q) — All 22 isolates of *P.* x*cambivora* included in the mating tests were self-sterile and produced oogonia abundantly when paired on V8A with *P.* x*cambivora* isolates of the opposite mating type. Oogonia were globose, sometimes with short tapering bases, (av. 64.3 %; Fig. 9i−k, o) or elongated with long, tapering and often funnel-like bases (av. 35.7 %; Fig. 9l−n, p). On aver-

age 66.8 % of oogonial bases were tapering and 19.1 % had a conspicuous girdling constriction (Fig. 9i, m−n). Oogonial walls turned golden-brown within 4 weeks (Fig. 9k, o−p) and were ornamented (av. 60.7 %), usually with only a few globose projections, (Fig. 9i, l−q), or smooth (av. 39.3 %; Fig. 9i−k). The proportion of ornamented oogonia in the individual pairings ranged from 3−100 % (Table 7). Special features like curved bases (av. 3.6 %; Fig. 9i) and comma-like bending (av. 8.3 %; Fig. 9p) were observed in all isolates. Oogonial diameters averaged 46.5 ± 5.1 µm with a total range of 30.4−61.8 µm and a range of isolate means of 37.6−52.9 µm. Mean oogonial abortion (Fig. 9q) rate was 38.5 % but varied widely in the individual pairings (7−90 %; Table 7). Oospores contained large ooplasts and usually two or more nuclei (av. 83.7 %; Fig. 9j−k, n−p), were mostly plerotic (av. 90.2 %) and averaged 40.3 ± 4.5 µm in diameter (24.4−52.7 µm). They had thick walls (on av. 3.1 ± 0.6 µm) with a mean oospore wall index of 0.40 ± 0.06. The majority of antheridia was amphigynous (97.9 %), 64.7 % bicellular (Fig. 9i−l, n−p) and 35.3 % unicellular (Fig. 9m, o), but paragynous antheridia (av. 2.1 %) and additional paragynous antheridia (Fig. 9k−l) were found in all isolates.

Colony morphology, growth rates and cardinal temperatures (Fig. 11, 12) — All isolates of *P.* x*cambivora* formed uniform to faintly stellate colonies on all three agar media, woolly on V8A and PDA and with limited aerial mycelium on MEA (Fig. 11). On V8A all isolates had similar growth rates at all temperatures. Minimum and maximum growth temperatures were below 5 °C and above 35 °C, respectively (Fig. 12). Average radial growth rate at the optimum temperature of 25 °C was 6.9 ± 0.1 mm/d (Table 7; Fig. 12).

Additional specimens. AUSTRALIA, isolated from *Malus sylvestris*, *D.M. Halsall*, 1977; CBS 114086. − BELGIUM, isolated from declining mature *Fagus sylvatica* trees, *A. Chandelier*, 2005; 3399H; 3401H; isolated from declining mature *F. sylvatica* trees, *A. Chandelier*, 2014; 4557H; Resi75. − CHILE, Valdivia, isolated from declining mature *F. sylvatica* trees, *T. Jung*, 2014; CL1; CL5. − FRANCE, Saint-Laurent-du-Cros, isolated from *Quercus rubra* nursery stock, *T. Jung*, 2013; FR 1. − GERMANY, Schleswig-Holstein, isolated from a declining *F. sylvatica* tree, *T. Jung*, 2013; DE 1. − ITALY, Sicily, isolated from a declining mature *Q. pubescens* tree, *T. Jung*, 2013; IT 5-3 L2; isolated from declining mature *Fagus sylvatica* trees, *T. Jung*, 2013; IT 6-3; IT 6-4. − JAPAN, Hokkaido, isolated from *Malus pumila*, *T. Suzui*, 1978; IMI 229178. − PORTUGAL, Tras-os-Montes, isolated from declining mature *Castanea sativa* trees, *T. Jung*, 2014; PT 1-1; PT 3-1; PT 7-3. − SLOVAKIA, Bratislava, isolated from a declining mature *F. sylvatica* tree, *T. Jung*, 2013; SK 9. − SPAIN, Castilla Leon, isolated from a declining planted *Alnus glutinosa* tree, *T. Jung*, 2012; ES 1. − USA, Oregon, isolated from declining *Chrysolepis chrysophylla* trees, *A. Saavedra*, 2001; 4044.1; 4050.1; 4031.O1; isolated from a *Abies procera* tree, *Loring/Smithson*, date not available; CBS 114087.

Notes — The ITS, *Btub*, *HSP90*, *cox1* and *NADH1* sequences of *P. attenuata*, *P. formosa*, *P. flexuosa*, *P. intricata*, *P.* x*incrassata* and *P.* x*heterohybrida* differ from each other and from those of other Clade 7a species in 33−99 positions and contain 17, 19, 9, 21, 19 and 22 unique polymorphisms, respectively (Table 2−6). In addition, the six new species can easily be separated from each other and from other Clade 7a species by a combination of morphological and physiological characters of which the most discriminating are highlighted in **bold** in Table 7. Morphological and morphometric characters of *P. fragariae* in the present study were congruent with the redescription of the species by Ho & Jong (1988) except of the predominance of paragynous antheridia (Table 7). Morphology, apart from the on average smaller sizes of sporangia and oogonia, and temperature-growth relations of *P. rubi* in the present work were in accordance to the original description of *P. fragariae* var. *rubi* (Wilcox et al. 1993) which was later re-named as *P. rubi* (Man in' t Veld 2007). *Phytophthora attenuata* shares a common ancestor with *P. rubi* and *P. fragariae* but can be easily differentiated from these sister species by the production of ornamented oogonia and bicellular amphigynous antheridia,
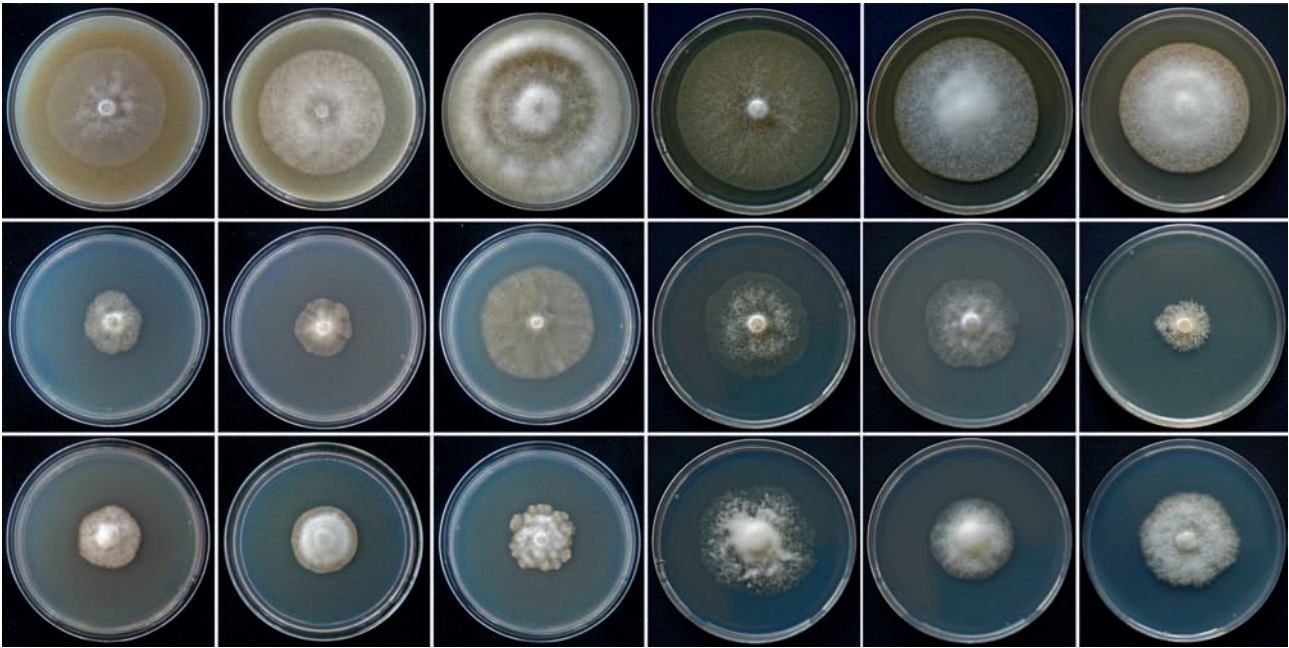
Fig. 10 Colony morphology of *Phytophthora attenuata*, *P. formosa*, *P. intricata*, *P. flexuosa*, *P. europaea* after 7 d growth and of *P. uliginosa* after 14 d growth (from left to right) at 20 °C on V8 agar, malt extract agar and potato-dextrose agar (from top to bottom).
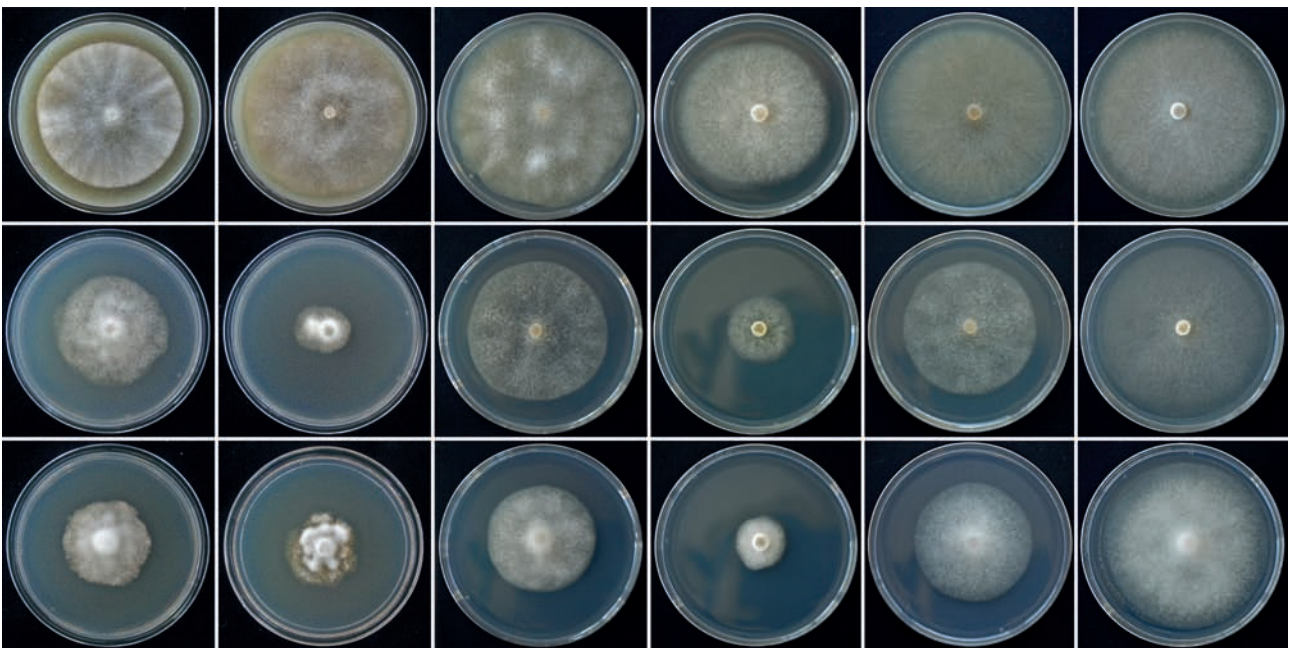

Fig. 11 Colony morphology of *Phytophthora* x*incrassata*, *P.* x*heterohybrida*, *P.* x*cambivora*, *P. uniformis*, *P.* x*alni* and *P.* x*multiformis* (from left to right) after 7 d growth at 20 °C on V8 agar, malt extract agar and potato-dextrose agar (from top to bottom).

the absence of hyphal swellings in water, much lower oogonial abortion rate, growth at 30 °C, faster growth between 5–30 °C, and different colony growth patterns on V8A, MEA and PDA (Table 7; Fig. 12). In addition, *P. attenuata* can be distinguished from *P. rubi* by having much higher frequency of oogonia with tapering bases. *Phytophthora intricata* can be separated from all other Clade 7a species by the frequent occurrence of intricate, intertwining oogonial and antheridial stalks and different colony growth patterns on V8A, MEA and PDA (Table 7; Fig. 10, 11). In addition, it is distinguished from its closest relative *P. formosa* by the absence of ornamented oogonia, on average bigger oogonia with thicker oospore walls; and from *P. uliginosa* by having smaller sporangia, higher optimum and maximum temperatures for growth and faster growth between 5–30 °C (Table 7; Fig. 10, 12). *Phytophthora formosa* is separated from *P. attenuata* by having much lower frequency of elongated oo-

gonia, higher frequency of ornamented oogonial walls, almost exclusive occurrence of paragynous antheridia, absence of bicellular amphigynous antheridia, and different colony morphologies on V8A, MEA and PDA (Table 7; Fig. 10). In addition, in accordance to its upper-montane origin *P. attenuata* shows much slower growth at 30 °C (Fig. 12). *Phytophthora flexuosa* is a sister species of *P. europaea* and can easily be distinguished from the latter by having different colony morphologies on V8A, MEA and PDA, much faster growth at 30 °C, the production of ornamented oogonia and flexuose oogonial shapes, almost exclusive occurrence of plerotic oospores with thicker walls, and lower frequency of oogonial abortion (Table 7; Fig. 10, 12). The sister species *P.* x*incrassata* and *P.* x*heterohybrida* can be differentiated by the production of larger and sometimes caducous sporangia, the high proportion of elongated oogonia and the more pronounced oogonial ornamentation in
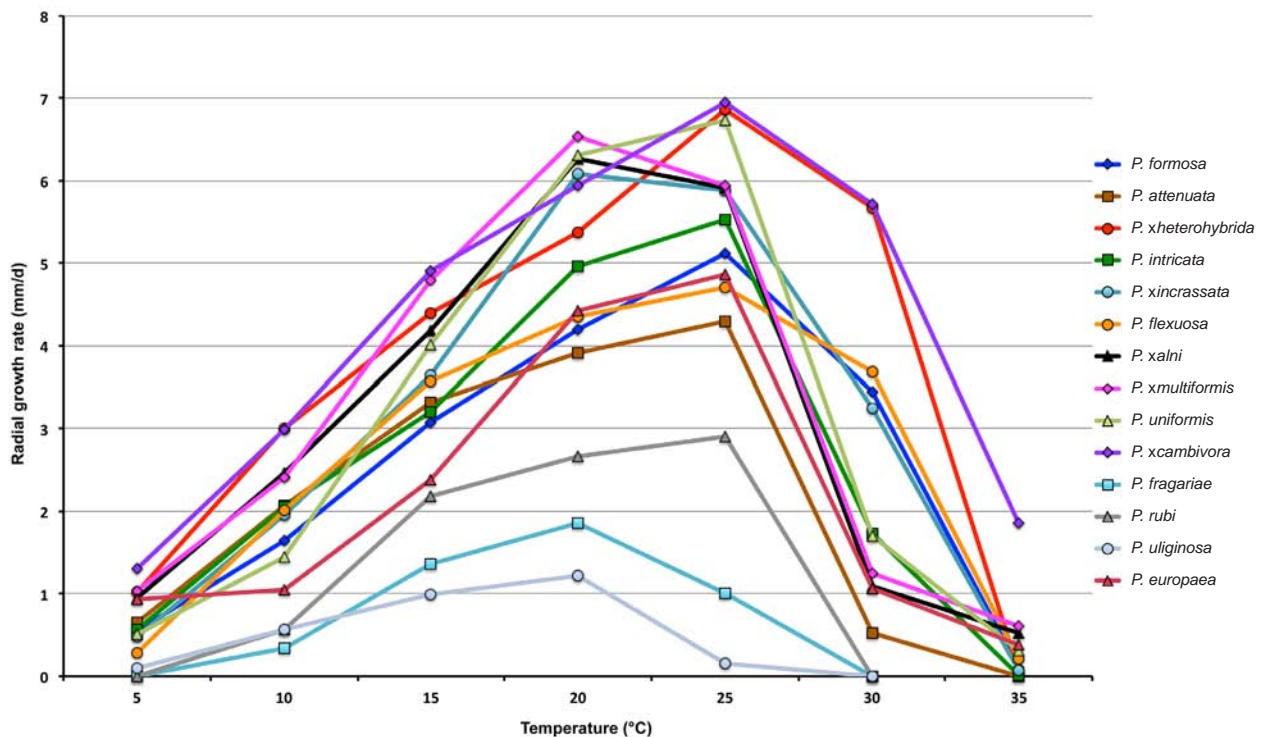
Fig. 12 Mean radial growth rates of *Phytophthora attenuata* (4 isolates), *P. formosa* (4 isolates), *P. intricata* (7 isolates), *P. flexuosa* (3 isolates), *P. europaea* (1 isolate), *P. x*incrassata* (7 isolates), *P. x*heterohybrida* (9 isolates), *P. x*cambivora* (6 isolates), *P. uliginosa* (2 isolates), *P. uniformis* (6 isolates), *P. x*alni* (8 isolates) and *P. x*multiformis* (4 isolates) on V8 agar at different temperatures.

*P. x*heterohybrida*, much higher frequency of thickwalled oogonia and higher oogonial abortion in *P. x*incrassata*, different colony morphologies on V8A, MEA and PDA and different optimum temperatures for growth (Table 7; Fig. 11, 12). Both species are separated from *P. x*cambivora* by the production of coralloid hyphal swellings, higher frequency of both thick-walled and ornamented oogonia, absence of paragynous antheridia and different colony morphologies on V8A, MEA and PDA (Table 7; Fig. 11, 12). In addition, *P. x*cambivora* shows considerable growth at 35 °C. Morphological and morphometric characters and temperature-growth relations of *P. x*alni* (previously *P. alni* ssp. *alni*), *P. x*multiformis* (previously *P. alni* ssp. *multiformis*) and *P. uniformis* (previously *P. alni* ssp. *uniformis*) and their differences to *P. x*cambivora* (previously *P. cambivora*) presented by Brasier et al. (2004) were largely confirmed by this study (Table 7). *Phytophthora x*incrassata* and *P. x*heterohybrida* are distinguished from *P. x*alni* and *P. x*multiformis* by their heterothallic breeding system, on average larger sporangia, higher frequency of both thick-walled and ornamented oogonia, absence of paragynous antheridia, different colony morphologies on V8A, MEA and PDA and failure to grow at 35 °C (Table 7; Fig. 11, 12). In addition, *P. x*heterohybrida* has a higher optimum temperature for growth than *P. x*alni* and *P. x*multiformis* and fails to grow at 35 °C (Table 7; Fig. 12).

Morphological features of *P. x*cambivora* were generally in accordance with Oudemans & Coffey (1991) who studied 12 isolates of *P. cambivora* from different countries including isolates IMI 229178 and CBS 114086 also examined in the present study, and with other studies on *P. cambivora* (summarised in Erwin & Ribeiro 1996). However, the finding of primary and additional secondary paragynous antheridia in most pairings, the occurrence of comma-like bent oogonial shapes, the relatively high frequencies of oogonial abortion and elongated oogonia with long tapering bases, and the girdling constriction of the tapering oogonial bases were previously not recorded for *P. cambivora*. In addition, the ability of all tested isolates to

grow at 35 °C was never reported for *P. cambivora*. With an average size of $68.3 \pm 12.4 \times 42.6 \pm 7.0$ µm and a total range of $35.1–120.9 \times 22.7–62.9$ µm the sporangia of 23 isolates of *P. x*cambivora* from four continents were markedly larger than those of the 12 *P. cambivora* isolates examined by Oudemans & Coffey (1991) with an average size of $50.4 \pm 10.9 \times 35.2 \pm 6.7$ µm, and more variable than in the description of *Blepharospora cambivora* by Petri (1918) with a total range of $60–75 \times 40–54$ µm. With a mean diameter of 46.5 ± 5.1 µm vs 40.5 ± 5.5 µm oogonia of *P. x*cambivora* in the present study were slightly larger than those of *P. cambivora* in the study of Oudemans & Coffey (1991). With a total range of $30.4–61.8$ µm vs $43–62$ µm oogonial diameters of *P. x*cambivora* were slightly more variable than reported for *P. cambivora* by Waterhouse & Waterston (1966). The only known isolate of *P.* sp. xcambivora-like from South Korea is distinguished from *P. x*cambivora* by $22–45$ bp differences across the ITS, *Btub*, *HSP90*, *cox1* and *NADH1* gene regions (Table 2–6), higher l/b ratio of sporangia and absence of primary paragynous antheridia (Table 7).

Soil infestation trials

At the end of the trials shoots and root systems of control plants of *C. sativa* (Fig. 13a, 14a–c), *F. sylvatica* (Fig 14d–f) and *Q. suber* were generally healthy and well developed. On *C. sativa*, *P. x*cambivora* was the most aggressive species causing within 3 months 73.3 % mortality, 96.6 % root rot and 59.8 % reduction of fine root weight compared to control plants (Fig. 14a–b). In addition, 80 % of plants showed extensive, often girdling collar rot. *Phytophthora x*incrassata* caused mortality (Fig. 13c), partly girdling collar rot infections (Fig. 13e) and necrotic root lesions or dieback of taproots (Fig. 13g) in 13.3 %, 66.7 % and 60 % of plants, respectively, and on average 77.6 % root rot and 45.5 % reduction of fine root weight (Fig. 14a–b). *Phytophthora x*heterohybrida* caused mortality (Fig. 13b), collar rot (Fig. 13f) and necrotic root lesions or dieback of taproots (Fig. 13h) in 6.7 %, 20.0 % and 80 % of plants, respectively, and on aver-

Fig. 13 *Castanea sativa* plants at the end of the soil infestation trial after 3 months growth in non-infested soil (a) and in soil infested by *Phytophthora* spp. (b−i). a. Healthy control plants; b. *Phytophthora* x*heterohybrida*: dead plant due to girdling collar rot (on the left), plants with small-sized leaves, dieback (centre) and chlorosis (on the right) caused by extensive fine root mortality; c. *P.* x*incrassata*: dead wilted plant due to girdling collar rot (on the left) and plants with stunted growth caused by extensive fine root mortality; d. *P. intricata*: plant with chlorotic and wilting leaves due to tap root dieback (on the left), relatively healthy plant (centre) and stunted plant with extensive destruction of the fine root system (on the left); e. girdling collar lesion caused by *P.* x*incrassata*; f. girdling collar lesion caused by *P.* x*heterohybrida*; g. extensive dieback of tap root with dark-brown necrotic lesion of inner bark (arrow) caused by *P.* x*incrassata*; h. girdling necrotic lesion of tap root caused by *P.* x*heterohybrida* with black outer bark and dark-brown inner bark (arrow); i. dieback of tap root (arrow) caused by *P. intricata*.
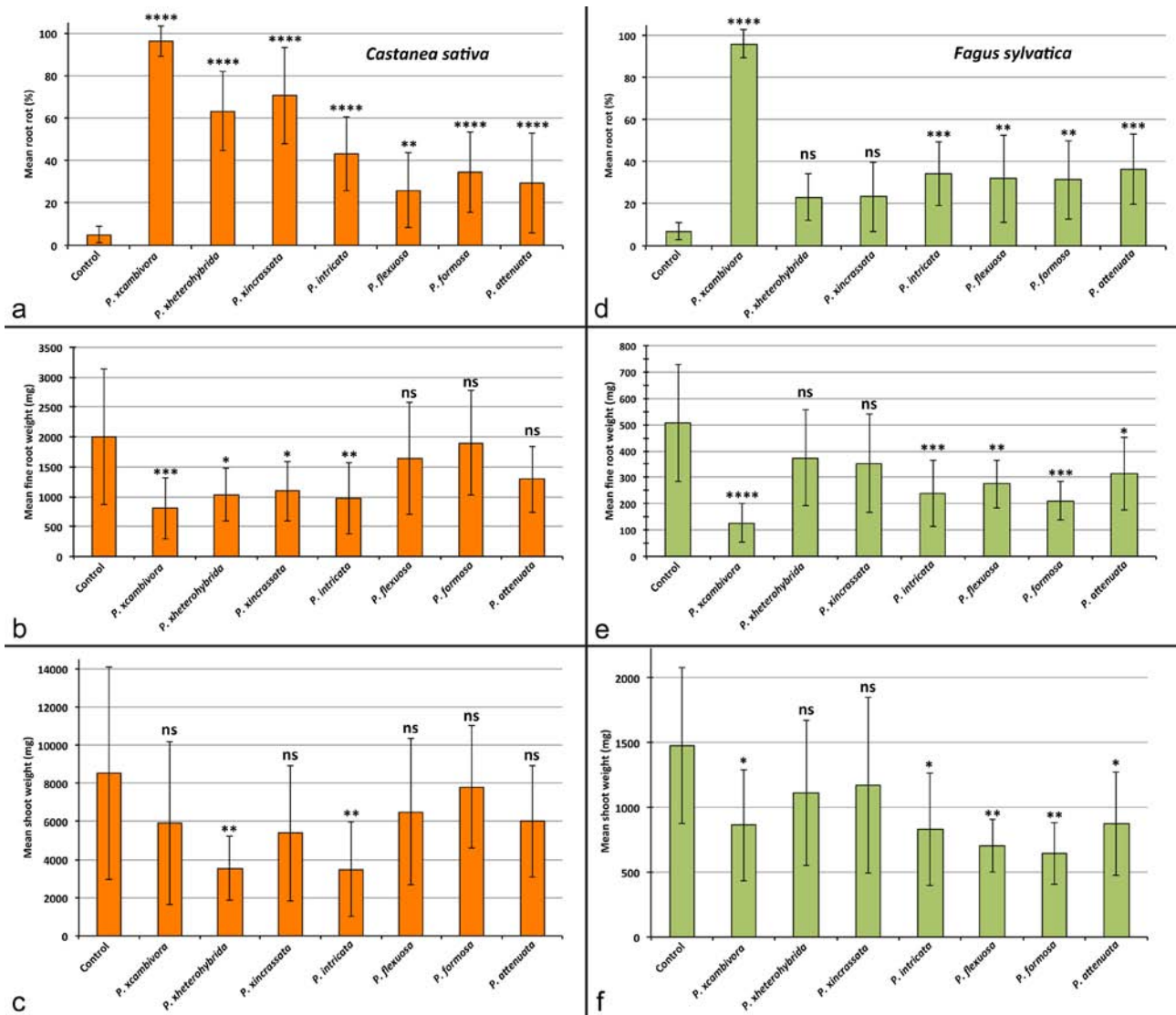
Fig. 14 Results of the soil infestation trials with *P.* ×*cambivora*, *P.* ×*heterohybrida*, *P.* ×*incrassata*, *P. intricata*, *P. flexuosa*, *P. formosa* and *P. attenuata*; mean root rot, mean fine root weight and mean shoot weight of *Castanea sativa* (a – c) after 3 mo and of *Fagus sylvatica* (d – f) after 5 mo. Bars show standard deviations; asterisks represent statistical significances (* = P < 0.05, ** = P < 0.01, *** = P < 0.001, **** = P < 0.0001), ns = not significant.

age 63.3 % root rot and 48.3 % reduction of fine root weight (Fig. 14a – b). Chestnut plants in soil infested by *P. intricata* showed 43.0 % root rot, 51.5 % reduction of fine root weight and necrotic root lesions or dieback of taproots (Fig. 13i) on 60 % of plants. Both *P.* ×*heterohybrida* and *P. intricata* caused small-sized chlorotic foliage (Fig. 13b, d) and a significantly reduced shoot weight (Fig. 14c). *Phytophthora attenuata*, *P. flexuosa* and *P. formosa* also caused significant root rot but the reductions of fine root weight and shoot weight were not significant (Fig. 14a – c).

Also on *F. sylvatica*, *P.* ×*cambivora* was the most aggressive of the seven *Phytophthora* species tested causing within 5 mo mortality in 20 % and collar rot in 50 % of the plants, and on average 96.0 % root rot and 74.8 % reduction of fine root weight compared to the control (Fig. 14d – e). *Phytophthora* ×*incrassata* and *P.* ×*heterohybrida* were less aggressive to *F. sylvatica* than to *C. sativa* and the differences in root rot, fine root weight and shoot weight to the control were not significant (Fig. 14d – f). In contrast, *P. intricata*, *P. flexuosa*, *P. formosa* and *P. attenuata* were pathogenic to *F. sylvatica* causing significant root rot and reductions of fine root weight and shoot weight compared to the control (Fig. 14d – f).

Of the three tree species tested, *Q. suber* was the least susceptible to the seven *Phytophthora* species tested. Although

the trial was running twice as long as with *F. sylvatica* and more than three times as long as with *C. sativa*, no plant was killed by any *Phytophthora* species after 10 months. All *Phytophthora* species proved to be fine root nibblers causing root rot ranging between 41.0 % (*P.* ×*heterohybrida*) and 64.5 % (*P. attenuata*) with the differences to the control being significant for all *Phytophthora* species (data not shown). However, reductions of fine root weight were not significant since infections were usually limited to non-suberised feeder roots (< 1 mm diam) whereas the non-infected suberised fine roots (1 – 2 mm diam) were still attached to the root system. All seven *Phytophthora* species had no significant effect on shoot weight.

DISCUSSION

In 2013, a survey of *Phytophthora* diversity in natural or semi-natural forests and rivers in Taiwan demonstrated the presence of ten described species and 17 previously unknown taxa of *Phytophthora* (Jung et al. 2016a). Based on differences in morphology, temperature-growth relations and sequence data of the nuclear ITS, *Btub* and *HSP90* and the mitochondrial *cox1* and *NADH1* gene loci, six new *Phytophthora* species from Clade 7a are described here as *P. attenuata*, *P. flexuosa*, *P. formosa*, *P. intricata*, *P.* ×*heterohybrida* and *P.* ×*incrassata*. In

addition, two new taxa are informally designated as *P.* sp. x*cambivora*-like and *P.* sp. x*multiformis*-like, thus doubling the number of known extant taxa in Clade 7a. All six species were isolated from rhizosphere soil or streams in healthy, natural or semi-natural forest stands. This apparent host-pathogen equilibrium, most likely resulting from long-term co-evolution, and the lack of similar DNA sequence data from other regions of the world suggest that the new species are indigenous to Taiwan suggesting Southeast Asia as a hotspot of diversity of Clade 7a. Interestingly, none of their known relatives from Clade 7a including *P. rubi*, *P. europaea*, *P. uliginosa* and the globally distributed forest pathogen *P.* x*cambivora* from Clade 7a were isolated in this or previous surveys of natural ecosystems in Taiwan (Ko et al. 1978, 2006, Brasier et al. 2010). Similarly, none of the closest known relatives of the eight new Clade 2 and Clade 9 taxa from Taiwanese ecosystems were found in Taiwan (Jung et al. 2016a). This suggests immigration of either the common ancestors of the new *Phytophthora* species and their closest relatives or of the closest relatives themselves to Taiwan most likely during the repeated temporary connections between Taiwan and mainland Asia in glacial periods followed by sympatric species radiation during periods of geographical separation in the interglacials (Chung-Fu 1994). The adaptive radiations within *Phytophthora* Clades 7a, 2 and 9 were most likely driven by the ecological diversity and high degree of plant species endemism of Taiwanese ecosystems (Chang-Fu & Chung-Fu 1994, Chang-Fu et al. 1994, Chung-Fu 1994) which caused introduced *Phytophthora* species to adapt to new ecological niches and coevolve with new host plants. Similarly, the sympatric radiations within Clade 6 in Australia with seven newly described species and six new informally designated taxa also occurred in a hotspot of biodiversity (Crous et al. 2011, 2012, 2014, Jung et al. 2011, Aghighi et al. 2012). The absence of both the close relatives of the new *Phytophthora* species from Clade 7a and their common ancestors in Taiwan is congruent with the central idea of the biogeographic island theory that species numbers remain in an equilibrium when new species arrive or emerge as old resident species are outcompeted and eventually driven to local extinction (Wilson 2001).

Apparently, in this evolutionary process interspecific hybridisations played an important role since *P.* x*heterohybrida*, *P.* x*incrassata* and seven of the eight new taxa from Clades 2 and 9 are putative hybrids (Jung et al. 2016a). In order to hybridise, the immigrating and resident *Phytophthora* species were most likely closely related and lacked efficient reproductive barriers due to relaxed selection resulting from geographical separation (Brasier 2012). Interspecific hybridisations are increasingly recognised as a driving evolutionary force in the genus *Phytophthora* facilitating adaptation to new environments and expansion of host ranges or host jumps due to accelerated pathogen evolution (Brasier et al. 1999, Brasier 2012, Burgess 2015). *Phytophthora* species in Clade 7a readily hybridise as demonstrated by *P.* x*alni* which originated most likely in a European nursery from a hybridisation between the two introduced species *P. uniformis* and *P.* x*multiformis*, the latter itself being an interspecific hybrid with unknown parents and geographical origin (Brasier et al. 2004, Ioos et al. 2006, Husson et al. 2015). Interestingly, isolate 4971496 from *A. glutinosa* in the Netherlands belongs to a discrete, previously unknown lineage which is designated here as *P.* sp. x*multiformis*-like. Both, nuclear gene sequences (Table 2–4) and phenotypic features like highly ornamented oogonial walls, high oospore abortion rate and production of both paragynous and amphigynous antheridia (Table 7) characterise this isolate as *P.* x*multiformis*. However, its *cox1* and *NADH1* sequences are identical to *P. uniformis* (Table 5–6). Similar to *P.* x*alni* this lineage most likely resulted from a hybridisation between *P.* x*multiformis* and *P. uniformis* but with reversed parental roles and *P. uniformis* acting as maternal

parent. *Phytophthora* x*alni* shows much higher aggressiveness to *Alnus glutinosa* than *P.* x*multiformis* and *P. uniformis* (Brasier & Kirk 2001) and is the main causal agent of the devastating epidemic mortality of riparian and planted *Alnus* trees in Europe (Brasier et al. 2004, Jung & Blaschke 2004, Jung et al. 2013b). Other well-known examples are the Clade 1 hybrid species *P.* x*pelgrandis* (*P. cactorum* x *P. nicotianae*) and *P.* x*serendipita* (*P. cactorum* x *P. hedraiandra*) which are currently outcompeting their parental species in European nurseries (Man in' t Veld et al. 2012); hybrids within the complex of host-specific vegetable pathogens in Clade 8b (Bertier et al. 2013); hybrids between *P. cryptogea* s.l., *P. erythroseptica* and *P. sansomeana* in Clade 8a from multiple horticultural crops in Australia, the USA, Europe and Iran (Safaiefarahani et al. 2016); and multiple sterile hybrid taxa in riparian ecosystems of South Africa and Western Australia and *P.* x*stagnum* in irrigation reservoirs in Virginia, all from Clade 6 and most likely adapted to a lifestyle as aquatic litter decomposers and opportunistic pathogens (Nagel et al. 2013, Yang et al. 2014, Burgess 2015). The nuclear ITS, *Btub* and *HSP90* gene sequences of *P.* x*heterohybrida*, *P.* x*incrassata* and *P. cambivora* contained in total 23, 31 and 55 heterozygous sites, respectively, clearly indicative of hybrid origin. In comparison, *P.* x*alni* and *P.* x*multiformis* had in total 30 and 18 heterozygous positions, respectively, across the three loci. Multiple ITS types in *P. cambivora* were also noted by Brasier et al. (1999). Analyses of nuclear genome sizes using flow cytometry in this study and analyses of cloned *HSP90* and ß-tubulin sequences (J. Bakonyi, D. Seress, K. van Poucke, K. Heungens & T. Jung unpubl. data) confirmed that *P.* x*heterohybrida*, *P.* x*incrassata* and *P. cambivora* are allopolyploid interspecific hybrids. Consequently, *P. cambivora* was re-described here as *P.* x*cambivora* without nomenclatural act. This globally distributed pathogen has been associated with root and collar rot diseases of many woody plant species (Erwin & Ribeiro 1996, Saavedra et al. 2007, Jung et al. 2013b). Since the ex-type of *P. cambivora* was lost and no isotypes are known, a neotype of *P.* x*cambivora* has been designated here to be used in future studies. In the multigene phylogeny *P.* x*cambivora* resided in a well-supported clade together with *P.* x*heterohybrida*, *P.* x*incrassata*, the other four hybrid taxa and *P. uniformis* as only non-hybrid species, suggesting a common ancestor.

The holoploid genome sizes of the nuclei of *P.* x*heterohybrida* (329.3 Mbp), *P.* x*incrassata* (644.2 Mbp) and *P.* x*cambivora* (437.1 Mbp) are significantly larger than that of most *Phytophthora* species with a known genome size, which is usually in the range of 112 to 224 Mbp (K. van Poucke & K. Heungens unpubl. data), with some exceptions in Clade 1 such as *P. infestans* (± 480 Mbp) due to a large number of repetitive sequences (Raffaele & Kamoun 2012, Pais et al. 2013, Wang et al. 2016). The genomes of *P.* x*multiformis* (0.453 pg = 443 Mbp) and *P.* x*alni* (0.384 pg = 376 Mbp) (Husson et al. 2015), which are allopolyploid hybrids from the same Clade 7a, and some Clade 8b isolates (Bertier et al. 2013), which are either hybrids or polyploid, are similarly large. Hence, these large genome sizes strongly indicate that *P.* x*heterohybrida*, *P.* x*incrassata* and *P.* x*cambivora* are allopolyploid hybrids, like their close relatives *P.* x*alni* and *P.* x*multiformis*. This hypothesis is supported by results from sequence analyses of cloned ß-tubulin and *HSP90* sequences (J. Bakonyi, D. Seress, K. van Poucke, K. Heungens & T. Jung unpubl. data). The diversity in genome size among the *P.* x*heterohybrida* isolates is limited, which may be due to their coinciding geographic origin. The same is true for the *P.* x*incrassata* isolates. However, in two *P.* x*incrassata* isolates a secondary population of smaller nuclei was observed. Since the isolates had been hyphal tipped this can only be explained as heterokaryons, as described previously in *Phytophthora* isolates from Clade 8b (Bertier et al. 2013). Single spore cultures derived

from these heterokaryotic isolates were either homokaryotic or heterokaryotic (data not shown). Most likely, the small nuclei resulted from the degeneration of some allopolyploid hybrid nuclei, but further experiments are needed to confirm this. The diversity in nuclear genome size among the *P. x cambivora* isolates is striking, even between isolates originating from the same country and belonging to the same mating type. The majority of the isolates have holoploid genome sizes ranging from 395.5 to 510.3 Mbp. This is in agreement with the reported haploid genome size of 216.5 Mbp of *P. x cambivora* isolate CBS 114087 based on whole genome sequencing (http://www.ncbi.nlm.nih.gov/Traces/wgs/?page=1&term=phytophthora). Isolate CBS 114086 had a single population of small nuclei (284.6 Mbp), which is only 55.8 % of the size of the largest nuclei. Similar to *P. x incrassata*, two isolates of *P. x cambivora* had heterokaryotic mycelium. The genome size of the small nuclei was similar to each other (297.2 and 314.6 Mbp) and to the nuclei of isolate CBS 114086 (284.6 Mbp).

The lack of heterozygous nucleotides in their maternally inherited mitochondrial *cox1* and *NADH1* sequences strongly suggests that they originated from sexual hybridisation rather than somatic fusion, a feature common to all known *Phytophthora* hybrids (Ioos et al. 2006, Man in 't Veld et al. 2012, Bertier et al. 2013, Nagel et al. 2013, Burgess 2015, Husson et al. 2015). *Phytophthora x cambivora*, *P. x heterohybrida* and *P. x incrassata* share the same *NADH1* genotype and, hence, most likely the same maternal parent. Interestingly, although apparently being common enough to become involved in multiple hybridisation events, this parental species is still unknown. In contrast, the *cox1* genotypes of *P. x cambivora*, *P. x heterohybrida* and *P. x incrassata* differ from each other by 7–13 base pairs. Having identical *NADH1* but different *cox1* genotypes represents a unique mtDNA pattern which, to our knowledge, was previously not reported in any oomycete, fungal, plant or animal hybrid. At the moment, the most likely explanation is via paternal leakage which has been demonstrated as a feasible pathway by which mtDNA might become non-clonal (Eyre-Walker & Awadalla 2001). During sexual hybridisation of the common maternal parent of the three hybrid species with their different paternal parents paternal mitochondria from one or multiple antheridia (Fig. 9k–l) could have been transferred to an oospore. Although such paternal mitochondria are preferentially degraded they can sometimes survive due to a breakdown of mechanisms that routinely eliminate paternal mitochondria (Eyre-Walker & Awadalla 2001). Subsequent sexual recombination between maternal and paternal mitochondria and vegetative segregation (Birky & William 2001), in this case the random partitioning of sporangial cytoplasm during zoospore differentiation, could have resulted in zoospores that contained exclusively or mainly mitochondria with recombined maternal/paternal DNA.

In contrast to most described *Phytophthora* hybrids which are either homothallic with often high rates of oospore abortion (Brasier et al. 2004, Man in' t Veld et al. 2012, Bertier et al. 2013, Safaiefarahani et al. 2016) or sterile (Nagel et al. 2013, Burgess 2015, Safaiefarahani et al. 2016), *P. x heterohybrida*, *P. x incrassata* and *P. x cambivora* all have a functional heterothallic breeding system. The only heterothallic hybrid species described so far is *P. andina* which originated from a hybridisation between *P. infestans* and a closely related unknown *Phytophthora* taxon in the Andes (Oliva et al. 2010, Wang et al. 2016). Other known natural hybrids with a heterothallic mating system result from crossings between *P. cryptogea* and *P. pseudocryptogea*. Unfortunately, no data are available on the viability of their oospores (Safaiefarahani et al. 2016). For *P. x heterohybrida* a population of A1, A2 and A1/A2 isolates with very low abortion rates in all performed mating tests was found in three forest streams flowing through a diverse subtropical

Castanopsis-Machilus monsoon forest. Also for *P. x cambivora* both mating types are known and widely occur in North America, Europe, Asia and Australia. However, abortion rates in different pairings varied considerably and were on average higher than in *P. x heterohybrida*. Currently, only the A2 mating type of *P. x incrassata* is known and more isolation tests from rivers and forests in Taiwan are required to clarify whether the A1 mating type of this species exists.

Phytophthora x alni and *P. x multiformis* are recent hybrids in a nascent state, characterised by unusually high developmental instabilities and oospore abortion rates (Brasier et al. 1999, 2004, Delcan & Brasier 2001). In contrast, the functional herothallic breeding system and lack of developmental instabilities suggest that *P. x heterohybrida* and *P. x cambivora* already went through the process of stabilization and homogenization and, hence, are not of recent origin. For *P. x cambivora* this conclusion is also supported by the fact that the original description as *Blepharospora cambivora* was published one century ago (Petri 1917). Unfortunately, none of the original isolates are available for morphological and molecular analyses. Due to the lack of isolates from the A1 mating type, A2 isolates of *P. x incrassata* were paired with an A1 tester strain of *P. cinnamomi*. Since the ornamented *P. x incrassata* oogonia in this interspecific pairing most certainly resulted from selfing the observed oospore abortion rate of 47 % is not surprising and does not allow conclusions about the viability of the breeding system.

Many predominantly aquatic *Phytophthora* species have abandoned sexual reproduction thus favouring rapid abundant zoospore production over genetic adaptability and long-term survival (Brasier et al. 2003a, Jung et al. 2011). In river systems of Australia and South Africa sterile interspecific hybrids between different Clade 6 species are prevailing. Other *Phytophthora* species thriving in water or continuously wet soils like *P. gregata* have a homothallic breeding system with often high oospore abortion rates indicating ongoing evolution towards sterility (Jung et al. 2011). Also in *P. inundata*, the only known heterothallic *Phytophthora* species with a predominantly aquatic lifestyle, the breeding system is partially disrupted (Brasier et al. 2003b). In contrast, a functional heterothallic breeding system with its intrinsic tendency to outcrossing provides *Phytophthora* pathogens with the ability to rapidly adapt to new host genotypes and host species in ecosystems with high spatial and flora diversity (Jung et al. 2011, Brasier & Hansen 1992). Almost all known *Phytophthora* species possessing a functional (not silent or disrupted) heterothallic breeding system have wide host ranges either within a plant family like *P. infestans* or more often across family boundaries like *P. cinnamomi*, *P. cryptogea*, *P. nicotianae*, *P. palmivora*, *P. ramorum* or *P. x cambivora*. Consequently, their functional heterothallic breeding system suggests that *P. x heterohybrida* and *P. x incrassata* are not specifically adapted to an aquatic lifestyle although they were exclusively isolated from forest streams. Apart from infrequent findings of *P. x cambivora* and *P. europaea* in forest streams in Oregon and of *P. parvispora* in Australian and Taiwanese rivers (Reeser et al. 2011, Hüberli et al. 2013, Jung et al. 2016a), Clade 7 species are usually not part of the aquatic *Phytophthora* communities (Oh et al. 2013, Huai et al. 2013, Hüberli et al. 2013, Nagel et al. 2013, Shrestha et al. 2013). Most likely, *P. x heterohybrida* and *P. x incrassata* have evolved and still thrive in the highly diverse *Castanopsis-Machilus* forests covering the catchments of the three streams around Fushan in North-eastern Taiwan; but this has yet to be verified by further isolation tests. Similar to the recently described *P. constricta* from Clade 9 in Australia (Rea et al. 2011), all isolates of *P. x heterohybrida* produced a low proportion of caducous sporangia without preformed pedicels indicating ongoing evolution towards a partially aerial lifestyle. Therefore, canopy drip might have been the source of

P. x*heterohybrida* inoculum in the forest streams as reported for airborne *Phytophthora* species from Clade 3 in Western US forests (Hansen et al. 2012).

The four non-hybrid species *P. attenuata*, *P. flexuosa*, *P. formosa* and *P. intricata* were isolated from rhizosphere soil or streams in healthy, natural or semi-natural forest stands. Although these species were not associated with diseased trees in Taiwanese forests, they still could represent a potential threat to non-coevolved tree or crop species in other continents. *Phytophthora melonis*, another Clade 7 member, has been recently found associated with *Juniper* trees in a natural forest on Caprera Island in Italy without association to diseased trees (Scanu et al. 2015). However, in Japan, mainland China, Taiwan, Iran, Egypt, Turkey and India *P. melonis* causes severe disease symptoms on crop species from the *Cucurbitaceae* (Ho et al. 2007). *Phytophthora attenuata* is closely related to *P. fragariae* and *P. rubi*, both aggressive pathogens of strawberries and raspberries, respectively (Erwin & Ribeiro 1996, Man in 't Veld 2007) and included in the EPPO A2 list of pests recommended for regulation as quarantine pests in Europe. Therefore, the potential aggressiveness of *P. attenuata* and the closely related *P. formosa* and *P. intricata* to different crop species deserves further investigation. On the other hand, *P. flexuosa* may be a weak pathogen like its closest relative *P. europaea*, a species occurring in soils of European broadleaved forests where it is not associated with disease symptoms (Jung et al. 2002). The soil infestation trials of this work demonstrated pathogenicity of the six new species from Clade 7a to root systems and collar tissue of *C. sativa* and *F. sylvatica* with the two hybrid species *P.* x*incrassata* and *P.* x*heterohybrida* being highly aggressive to *C. sativa*. Since more than a billion plants-for-planting are imported annually from Asia to Europe (Ludovic Rigoux, Université Libre de Bruxelles, Belgium, pers. comm.) it might only be a matter of time before the six new Clade 7a species and other yet unknown *Phytophthora* species will be introduced, following the 59 exotic *Phytophthora* taxa already present in Europe (Jung et al. 2016b). Considering the growing intensity and complexity of the international nursery trade (Dehnen-Schmutz et al. 2010, Drew et al. 2010) rapid spread of such new arrivals across Europe can be expected as demonstrated by the almost ubiquitous infestations of European nurseries with 49 mostly exotic *Phytophthora* taxa (Jung et al. 2016b). The new Clade 7a species would potentially pose a twofold risk to European ecosystems, directly by infecting and killing non-adapted native European tree species and indirectly by hybridising with allopatric *Phytophthora* species from Clade 7a already present in Europe like *P. fragariae*, *P. rubi*, *P. europaea*, *P. uliginosa*, *P. uniformis*, *P.* x*cambivora*, *P.* x*alni* and *P.* x*multiformis*, with potentially catastrophic effects on host ranges, aggressiveness and disease epidemiology.

More *Phytophthora* surveys in previously unstudied natural ecosystems in Asia, Africa and South America will help to elucidate the true global diversity of the genus *Phytophthora* which has been estimated as 400 ± 200 extant species (Brasier 2009) and understand the factors driving diversity and adaptation including the frequency and the role of interspecific hybridisations and polyploidisations in natural ecosystems. Data on the true diversity of *Phytophthora* species and assessments of their potential threat to non-native ecosystems, using standardised methods of host range testing, are urgently needed to persuade decision makers like the EU standing committee of plant health, the European and North American Plant Protection Organizations EPPO and NAPPO, the Animal and Plant Health Inspection Service (APHIS) and the World Trade Organization (WTO) that plant health legislations needs to be changed from the outdated list-based species-by-species to a modern pathway regulation approach (Brasier 2008, Jung et al. 2016b) in order to prevent

further introductions of potentially harmful alien forest pests and pathogens (Santini et al. 2013).

REFERENCES

Aghighi S, Hardy GEStJ, Scott JK, et al. 2012. Phytophthora bilorbang sp. nov., a new species associated with the decline of Rubus anglocandicans (European blackberry) in Western Australia. European Journal of Forest Pathology 133: 841–855.

Aguayo J, Adams GC, Halkett F, et al. 2013. Strong genetic differentiation between North American and European populations of Phytophthora alni subsp. uniformis. Phytopathology 103: 190–199.

Ann PJ, Wong IT, Tsai JN. 2010. New records of Phytophthora diseases of aromatic crops in Taiwan. Plant Pathology Bulletin 19: 53–68.

Arentz F, Simpson JA. 1986. Distribution of Phytophthora cinnamomi in Papua New Guinea and notes on its origin. Transactions of the British Mycological Society 87: 289–295.

Bakonyi J, Nagy ZÁ, Érsek T. 2006. PCR-based DNA markers for identifying hybrids within Phytophthora alni. Journal of Phytopathology 154: 168–177.

Bertier L, Leus L, D'hondt L, et al. 2013. Host adaptation and speciation through hybridization and polyploidy in Phytophthora. PloS ONE 8: e85385.

Birky C, William J. 2001. The inheritance of genes in mitochondria and chloroplasts: Laws, mechanisms, and models. Annual Reviews of Genetics 35: 125–148.

Blair JE, Coffey MD, Park S-Y, et al. 2008. A multi-locus phylogeny for Phytophthora utilizing markers derived from complete genome sequences. Fungal Genetics and Biology 45: 266–277.

Brasier CM. 2008. The biosecurity threat to the UK and global environment from international trade in plants. Plant Pathology 57: 792–808.

Brasier CM. 2009. Phytophthora biodiversity: How many Phytophthora species are there? In: Goheen EM, Frankel SJ (eds), Phytophthoras in forests and natural ecosystems. USDA Forest Service General Technical Report PSW-GTR-221: 101–115. Albany, CA.

Brasier CM. 2012. Rapid evolution of introduced tree pathogens via episodic selection and horizontal gene transfer. In: Sniezko RA, Yanchuk AD, Kliejunas JT, et al. (tech. coords), Proceedings of the fourth international workshop on the genetics of host-parasite interactions in forestry: Disease and insect resistance in forest trees. USDA Forest Service General Technical Report PSW-GTR-240: 133–142. Albany, CA.

Brasier CM, Cooke DEL, Duncan JM. 1999. Origins of a new Phytophthora pathogen through interspecific hybridisation. Proceedings of the National Academy of Sciences, USA 96: 5878–5883.

Brasier CM, Cooke DEL, Duncan JM, et al. 2003a. Multiple new phenotypic taxa from trees and riparian ecosystems in Phytophthora gonapodyides–P. megasperma ITS Clade 6, which tend to be high-temperature tolerant and either inbreeding or sterile. Mycological Research 107: 277–290.

Brasier CM, Franceschini S, Vettraino AM, et al. 2012. Four phenotypically and phylogenetically distinct lineages in Phytophthora lateralis. Fungal Biology 116: 1232–1249.

Brasier CM, Hansen EM. 1992. Evolutionary biology of Phytophthora. Part II: Phylogeny, speciation, and population structure. Annual Review of Phytopathology 30: 173–200.

Brasier CM, Kirk SA. 2001. Comparative aggressiveness of standard and variant hybrid alder Phytophthoras, Phytophthora cambivora and other Phytophthora species on bark of Alnus, Quercus and other woody hosts. Plant Pathology 50: 218–229.

Brasier CM, Kirk SA, Delcan J, et al. 2004. Phytophthora alni sp. nov. and its variants: designation of emerging heteroploid hybrid pathogens spreading on Alnus trees. Mycological Research 108: 1172–1184.

Brasier CM, Sanchez-Hernandez E, Kirk SA. 2003b. Phytophthora inundata sp. nov., a part heterothallic pathogen of trees and shrubs in wet or flooded soils. Mycological Research 107: 477–484.

Brasier CM, Vettraino AM, Chang TT, et al. 2010. Phytophthora lateralis discovered in an old growth Chamaecyparis forest in Taiwan. Plant Pathology 59: 595–603.

Brasier CM, Webber J. 2010. Sudden larch death. Nature 466: 824–825.

Burgess TI. 2015. Molecular characterization of natural hybrids formed between five related indigenous Clade 6 Phytophthora species. PLoS ONE 10, 8: e0134225.

Chang TT, Wang WW, Wang WY. 1996. Use of random amplified polymorphic DNA markers for the detection of genetic variation in Phytophthora cinnamomi in Taiwan. Botanical Bulletin Academia Sinica 37: 165–171.

Chang-Fu H, Chung-Fu S. 1994. Introduction to the flora of Taiwan, 1: geography, geology, climate, and soils. In: Chang-Fu H, Tseng-Cieng H, Hsuan K, et al. (eds), Flora of Taiwan. 2nd edn. Editorial Committee of the Flora of Taiwan, Republic of China: Vol. 1: 1–3. Taipei, Republic of China (http://tai2.ntu.edu.tw/ebook/ebookpage.php?volume= 1&book=Fl.%20 Taiwan%202nd%20edit.&page=1).

Chang-Fu H, Chung-Fu S, Kuoh-Cheng Y. 1994. Introduction to the flora of Taiwan, 3: floristics, phytogeography, and vegetation. In: Chang-Fu H, Tseng-Cieng H, Hsuan K, et al. (eds), Flora of Taiwan. 2nd edn. Editorial Committee of the Flora of Taiwan, Republic of China: Vol. 1: 7–18. Taipei, Republic of China (http://tai2.ntu.edu.tw/ebook/ebookpage. php?volume=1&book=Fl.%20Taiwan%202nd%20edit.&page=7).

Chung-Fu S. 1994. Introduction to the flora of Taiwan, 2: geotectonic evolution, paleogeography, and the origin of the flora. In: Chang-Fu H, Tseng-Cieng H, Hsuan K, et al. (eds), Flora of Taiwan. 2nd edn. Editorial Committee of the Flora of Taiwan, Republic of China: Vol. 1: 3–7. Taipei, Republic of China (http://tai2.ntu.edu.tw/ebook/ebookpage.php?volume=1&book=Fl.%20 Taiwan%202nd%20edit.&page=3).

Crous PW, Groenewald JZ, Shivas RG, et al. 2011. Fungal Planet description sheets: 69–91. Persoonia 26: 108–156.

Crous PW, Summerell BA, Shivas RG, et al. 2012. Fungal Planet description sheets: 107–127. Persoonia 28: 138–182.

Crous PW, Wingfield MJ, Schumacher RK, et al. 2014. Fungal Planet description sheets: 281–319. Persoonia 33: 212–289.

De Merlier D, Chandelier A, Debruxelles N, et al. 2005. Characterization of alder Phytophthora isolates from Wallonia and development of SCAR primers for their specific detection. Journal of Phytopathology 153: 99–107.

Dehnen-Schmutz K, Holdenrieder O, Jeger MJ, et al. 2010. Structural change in the international horticultural industry: Some implications for plant health. Scientia Horticulturae 125: 1–15.

Delcan J, Brasier CM. 2001. Oospore viability and variation in zoospore and hyphal tip derivatives of the hybrid alder phytophthoras. Forest Pathology 31, 65–83.

Dick MW. 1990. Keys to Pythium. University of Reading Press, Reading, UK.

Drenth A, Guest DI (eds). 2004. Diversity and management of Phytophthora in Southeast Asia. ACIAR Monograph 114. Australian Centre for International Agricultural Research, Canberra.

Drew J, Anderson N, Andow D. 2010. Conundrums of a complex vector for invasive species control: a detailed examination of the horticultural industry. Biological Invasions 12: 2837–2851.

Erwin DC, Ribeiro OK. 1996. Phytophthora diseases worldwide. APS Press, St. Paul, Minnesota.

Eyre-Walker A, Awadalla P. 2001. Does human mtDNA recombine? Journal of Molecular Evolution 53: 430–435.

Halsall DM, Forrester RI. 1977. Effects of certain cations on the formation and infectivity of Phytophthora zoospores. 1. Effects of calcium, magnesium, potassium, and iron ions. Canadian Journal of Microbiology 23: 994–1001.

Hansen EM, Goheen DJ, Jules ES, et al. 2000. Managing Port-Orford-Cedar and the introduced pathogen Phytophthora lateralis. Plant Disease 84: 4–14.

Hansen EM, Reeser PW, Sutton W. 2012. Phytophthora beyond agriculture. Annual Review of Phytopathology 50: 359–378.

Hardham AR. 2005. Phytophthora cinnamomi. Molecular Plant Pathology 6: 589–604.

Ho HH. 1990. Taiwan Phytophthora. Botanical Bulletin Academia Sinica 31: 89–106.

Ho HH, Gallegly ME, Hong CX. 2007. Redescription of Phytophthora melonis. Mycotaxon 102: 339–345.

Ho HH, Jong SC. 1988. Phytophthora fragariae. Mycotaxon, 31: 305–322.

Ho HH, Lu JY. 1997. A synopsis of the occurrence and pathogenicity of Phytophthora species in mainland China. Mycopathologia 138: 143–161.

Huai WX, Tian G, Hansen EM, et al. 2013. Identification of Phytophthora species baited and isolated from forest soil and streams in northwestern Yunnan province, China. Forest Pathology 43: 87–103.

Hüberli D. 1995. Analysis of variability among isolates of Phytophthora cinnamomi Rands from Eucalyptus marginata Donn ex Sm. and E. calophylla R. Br. based on cultural characteristics, sporangia and gametangia morphology, and pathogenicity. Bachelor thesis, Murdoch University, Murdoch, Western Australia.

Hüberli D, Hardy GEStJ, White D, et al. 2013. Fishing for Phytophthora from Western Australia' s waterways: A distribution and diversity survey. Australasian Plant Pathology 42: 251–260.

Huelsenbeck JP, Ronquist F. 2001. MrBayes: Bayesian inference of phylogeny. Bioinformatics 17: 754–755.

Husson C, Aguayo J, Revellin C, et al. 2015. Evidence for homoploid speciation in Phytophthora alni supports taxonomic reclassification in this species complex. Fungal Genetics and Biology 77: 12–21.

Ioos R, Andrieux A, Marçais B, et al. 2006. Genetic characterization of the natural hybrid species Phytophthora alni as inferred from nuclear and mitochondrial DNA analyses. Fungal Genetics and Biology 43: 511–529.

Jee H-J, Cho W-D, Kim W-G. 1997. Phytophthora diseases of apple in Korea: 2. Occurrence of an unusual fruit rot caused by P. cactorum and P. cambivora. Korean Journal Plant Pathology 13: 145–151.

Józsa A, Bakonyi J, Belbahri L, et al. 2010. A new species of Phytophthora reported to cause root and collar rot of common boxwood, Nordmann fir and Port Orford cedar in Hungary. Plant Pathology 59: 1166–1167.

Jung T. 2009. Beech decline in Central Europe driven by the interaction between Phytophthora infections and climatic extremes. Forest Pathology 39: 73–94.

Jung T, Blaschke H, Neumann P. 1996. Isolation, identification and pathogenicity of Phytophthora species from declining oak stands. European Journal of Forest Pathology 26: 253–272.

Jung T, Blaschke M. 2004. Phytophthora root and collar rot of alders in Bavaria: distribution, modes of spread and possible management strategies. Plant Pathology 53: 197–208.

Jung T, Burgess TI. 2009. Re-evaluation of Phytophthora citricola isolates from multiple woody hosts in Europe and North America reveals a new species, Phytophthora plurivora sp. nov. Persoonia 22: 95–110.

Jung T, Chang TT, Bakonyi J, et al. 2016a. Diversity of Phytophthora species in natural ecosystems of Taiwan and association with disease symptoms. Plant Pathology: in press. doi: 10.1111/ppa.12564.

Jung T, Colquhoun IJ, Hardy GEStJ. 2013a. New insights into the survival strategy of the invasive soilborne pathogen Phytophthora cinnamomi in different natural ecosystems in Western Australia. Forest Pathology 43: 266–288.

Jung T, Hansen EM, Winton L, et al. 2002. Three new species of Phytophthora from European oak forests. Mycological Research 106: 397–411.

Jung T, Orlikowski L, Henricot B, et al. 2016b. Widespread Phytophthora infestations in European nurseries put forest, semi-natural and horticultural ecosystems at high risk of Phytophthora diseases. Forest Pathology 46: 134–163.

Jung T, Stukely MJC, Hardy GEStJ, et al. 2011. Multiple new Phytophthora species from ITS Clade 6 associated with natural ecosystems in Australia: evolutionary and ecological implications. Persoonia 26: 13–39.

Jung T, Vettraino AM, Cech TL, et al. 2013b. The impact of invasive Phytophthora species on European forests. In: Lamour K (ed), Phytophthora: A global perspective: 146–158. CABI, Wallingford, UK.

Katoh K, Standley DM. 2013. MAFFT multiple sequence alignment software version 7: improvements in performance and usability. Molecular Biology and Evolution 30: 772–780.

Ko WH, Chang HS, Su HJ. 1978. Isolates from Phytophthora cinnamomi from Taiwan as evidence for an Asian origin of the species. Transactions of the British Mycological Society 71: 496–499.

Ko WH, Wang SY, Ann PJ. 2006. The possible origin and relation of Phytophthora katsurae and P. heveae, discovered in a protected natural forest in Taiwan. Botanical Studies 47: 273–277.

Kroon LPNM, Bakker FT, Van den Bosch GBM, et al. 2004. Phylogenetic analysis of Phytophthora species based on mitochondrial and nuclear DNA sequences. Fungal Genetics and Biology 41: 766–782.

Man in 't Veld WA. 2007. Gene flow analysis demonstrates that Phytophthora fragariae var. rubi constitutes a distinct species, Phytophthora rubi comb. nov. Mycologia 99: 222–226.

Man in 't Veld WA, Rosendahl KCHM, Hong C. 2012. Phytophthora x serendipita sp. nov. and P. x pelgrandis, two destructive pathogens generated by natural hybridization. Mycologia 104: 1390–1396.

Martin FN, Blair JE, Coffey MD. 2014. A combined mitochondrial and nuclear multilocus phylogeny of the genus Phytophthora. Fungal Genetics and Biology 66: 19–32.

Nagel JH, Gryzenhout M, Slippers B, et al. 2013. Characterization of Phytophthora hybrids from ITS clade 6 associated with riparian ecosystems in South Africa and Australia. Fungal Biology 117: 329–347.

Nagy LG, Kocsube S, Csana Z, et al. 2012. Re-mind the gap! insertion – deletion data reveal neglected phylogenetic potential of the nuclear ribosomal internal transcribed spacer (ITS) of fungi. PLoS ONE 7: e49794.

Nagy ZÁ, Bakonyi J, Érsek T. 2003. Standard and Swedish variant types of the hybrid alder Phytophthora attacking alder in Hungary. Pest Management Science 59: 484–492.

Nylander JA, Wilgenbusch JC, Warren DL, et al. 2008. AWTY (are we there yet?): a system for graphical exploration of MCMC convergence in Bayesian phylogenetics. Bioinformatics 24: 581–583.

Oh E, Gryzenhout M, Wingfield BD, et al. 2013. Surveys of soil and water reveal a goldmine of Phytophthora diversity in South African natural ecosystems. IMA Fungus 4, 1: 123–131.

Oliva R, Kroon L, Chacon G, et al. 2010. Phytophthora andina sp. nov. a newly identified heterothallic pathogen of solanaceous hosts in the Andean highlands. Plant Pathology 59: 613–625.

Oudemans P, Coffey MD. 1991. Isozyme comparison within and among worldwide sources of three morphologically distinct species of Phytophthora. Mycological Research 95: 19–30.

Pais M, Win J, Yoshida K, et al. 2013. From pathogen genomes to host plant processes: the power of plant parasitic oomycetes. Genome Biology 14: 211–212.

Petri L. 1917. Ricerche sulla morfologia e biologia della Blepharospora cambivora, parasitica del Castagno. Atti della Reale Accademia dei Lincei, Rendiconti della Classe di Scienze Fisiche, Matematica e Naturali. Serie 5. 26: 297–299.

Petri L. 1918. Studi sulla malattia del castagno detta 'dell' Inchiostro'. Annali del Regio Istituto Superiore Forestale Nazionale 3: 1–34.

Raffaele S, Kamoun S. 2012. Genome evolution in filamentous plant pathogens: why bigger can be better. Nature Reviews Microbiology 10: 417–430.

Rea AJ, Burgess TI, Hardy GEStJ, et al. 2011. Two novel and potentially endemic species of Phytophthora associated with episodic dieback of kwongan vegetation in the south-west of Western Australia. Plant Pathology 60: 1055–1068.

Reeser PW, Sutton W, Hansen EM, et al. 2011. Phytophthora species in forest streams in Oregon and Alaska. Mycologia 103: 22–35.

Rizzo DM, Garbelotto M, Davidson JM, et al. 2002. Phytophthora ramorum as the cause of extensive mortality of Quercus spp. and Lithocarpus densiflorus in California. Plant Disease 86: 205–214.

Ronquist F, Huelsenbeck JP. 2003. MrBayes 3: Bayesian phylogenetic inference under mixed models. Bioinformatics 19: 1572–1574.

Saavedra A, Hansen EM, Goheen DJ. 2007. Phytophthora cambivora in Oregon and its pathogenicity to Chrysolepis chrysophylla. Forest Pathology 37: 409–419.

Safaiefarahani B, Mostowfizadeh-Ghalamfarsa R, Hardy GEStJ, et al. 2016. Species from within the Phytophthora cryptogea complex and related species, P. erythroseptica and P. sansomeana, readily hybridize. Fungal Biology 120: 975–987. doi: 10.1016/j.funbio.2016.05.002.

Santini A, Ghelardini L, De Pace C, et al. 2013. Biogeographic patterns and determinants of invasion by alien forest pathogens in Europe. New Phytologist 197: 238–250.

Scanu B, Hunter GC, Linaldeddu BT, et al. 2014. A taxonomic re-evaluation reveals that Phytophthora cinnamomi and P. cinnamomi var. parvispora are separate species. Forest Pathology 44: 1–20.

Scanu B, Linaldeddu BT, Deidda A, et al. 2015. Diversity of Phytophthora species from declining Mediterranean maquis vegetation, including two new species, Phytophthora crassamura and P. ornamentata sp. nov. PLoS ONE 10, 12: e0143234.

Shearer BL, Tippett JT. 1989. Jarrah dieback: the dynamics and management of Phytophthora cinnamomi in the jarrah (Eucalyptus marginata) forest of South-western Australia. Research Bulletin No. 3. Department of Conservation and Land Management, Como, Western Australia.

Shrestha SK, Zhou Y, Lamour K. 2013. Oomycetes baited from streams in Tennessee 2010–2012. Mycologia 105: 1516–1523.

Silvestro D, Michalak I. 2012. raxmlGUI: a graphical front-end for RAxML. Organisms Diversity & Evolution 12: 335–337.

Solla A, Pérez-Sierra A, Corcobado T, et al. 2010. Phytophthora alni on Alnus glutinosa reported for the first time in Spain. Plant Pathology 59: 798.

Staden R, Beal KF, Bonfield JK. 2000. The Staden package 1998. Methods in Molecular Biology 132: 115–130.

Stamatakis A. 2014. RAxML version 8: a tool for phylogenetic analysis and post-analysis of large phylogenies. Bioinformatics 30: 1312–1313.

Suzui T, Hoshino Y. 1979. Collar rot of apple caused by Phytophthora cambivora (Petri) Buism. Annals of the Phytopathological Society of Japan 45: 344–352.

Tamura K, Stecher G, Peterson D, et al. 2013. MEGA6: Molecular Evolutionary Genetics Analysis Version 6.0. Molecular Biology and Evolution 30: 2725–2729.

Vettraino AM, Brasier CM, Brown AV, et al. 2011. Phytophthora himalsilva sp. nov. an unusually phenotypically variable species from a remote forest in Nepal. Fungal Biology 115: 275–287.

Wang J, Presser JW, Goss EM. 2016. Nuclear DNA content of the hybrid plant pathogen Phytophthora andina determined by flow cytometry. Mycologia: in press. doi: 10.3852/15-107.

Waterhouse GM, Waterston JM. 1966. Phytophthora cambivora. CMI Descriptions of Pathogenic Fungi and Bacteria 112: 1–2.

White TJ, Bruns T, Lee S, et al. 1990. Amplification and direct sequencing of fungal ribosomal RNA genes for phylogenetics. In: Innes MA, Gelfand DH, Sninsky JJ, et al. (eds), PCR Protocols: A guide to methods and applications. Academic Press, San Diego, California, USA: 315–322.

Wilcox WF, Scott PH, Hamm PB, et al. 1993. Identity of a Phytophthora species attacking raspberry in Europe and North America. Mycological Research 97: 817–831.

Wilson EO. 2001. The diversity of life. Penguin Books Ltd., London, UK.

Yang X, Richardson PA, Hong C. 2014. Phytophthora x stagnum nothosp. nov., a new hybrid from irrigation reservoirs at ornamental plant nurseries in Virginia. PLoS ONE 9: e103450.

Zeng H-C, Ho H-H, Zheng F-C. 2009. A survey of Phytophthora species on Hainan Island of South China. Journal of Phytopathology 157: 33–39.